

Francisco Amaral, Marc Toth and
Jonas Zdrzalek

March 2025

Spatial distribution of housing liquidity

Abstract

Francisco Amaral, Mark Toth and Jonas Zdrzalek*

1st Draft March 2025; 2nd Draft September 2025; This Draft January 2026

This paper examines the relationship between location, liquidity, and prices in housing markets. We construct spatial datasets for German and U.S. cities and show that liquidity and prices decline with distance to the city center. To rationalize these patterns, we develop a spatial model of housing search. Location preferences concentrate buyers in central areas, generating tighter markets that are more liquid and command higher prices. Counterfactuals show that increasing search efficiency raises welfare and prices, especially in peripheral areas. Our findings highlight the importance of demand-side preferences and market tightness for understanding liquidity and asset prices.

Keywords: liquidity, housing prices, cities, spatial equilibrium, housing demand, asset pricing

JELs: G12, G51, R21, R30

Authors

Francisco Amaral (corresponding author)

University of Zurich

Email: francisco.amaral@df.uzh.ch

www.uzh.ch

Mark Toth

University of Bonn

Email: mark-toth@uni-bonn.de

www.uni-bonn.de

Jonas Zdrzalek

Kiel Institute

Email: jonas.zdrzalek@kielinstitut.de

www.kielinstitut.de

*Amaral and Zdrzalek were part of the Young ECONtribute Program by the Cluster of Excellence ECONtribute, a joint initiative of the Universities Bonn and Cologne and therefore wish to acknowledge support from the Deutsche Forschungsgemeinschaft (DFG) under Germany's Excellence Strategy - EXC 2126/1 - 390838866. Toth acknowledges support from the Bonn Graduate School of Economics and the Deutsche Forschungsgemeinschaft (DFG) under the Research Training Group 2281 - The Macroeconomics of Inequality as well as the CRC TR 224 "Economic Perspectives on Societal Challenges". For helpful feedback, we thank Gabriel Ahlfeldt, Christian Bayer, Pierre Collin-Dufresne, Gilles Duranton, Peter Egger, Rüdiger Fahlenbrach, Andreas Fuster, James Graham, Alexander Haas, Janko Heineken, Christian Hilber, Thomas Hintermaier, Matthijs Korevaar, Martin Kornejew, Lorenz Kueng, Keith Kuester, Antoine Levy, Alexander Monge-Naranjo, Emily Moschini, Per Östberg, Andrii Parkhomenko, Kathleen Rauck, Farzad Saidi, Zacharias Sautner, Moritz Schularick, Maxence Valentin, Anthony Lee Zhang, and Tom Zimmermann. We also thank seminar and workshop participants at the 13th European Meeting of the Urban Economics Association at Aalborg University Copenhagen; the 3rd Workshop on Residential Housing Markets at WU Vienna; the University of Bonn Institute of Finance and Statistics Seminar; the University of Bonn Macro Internal Seminar; the 1st and 2nd Bonn-Frankfurt-Mannheim PhD Conference; the UNSW Macro Lunch, UNSW Sydney; the 2024 ECHOPPE Housing Conference in Toulouse; the 2024 Wisconsin Real Estate Conference at UW-Madison; the 17th Annual Meeting of The Portuguese Economic Journal in Faro; the CERF Seminar at the Judge Business School, Cambridge; the Financial Economics Workshop 2024 in St. Gallen; the CRED Workshop on Regional and Urban Economics 2025 in Bern; the Swiss Finance Institute Brown Bag Seminar; The Swiss Finance Institute Research Days 2025; the CEPR Publishing in Top Macro and Finance Journals Workshop; the Oxford Real Estate Research Conference, Saïd Business School; the AREUEA National Conference 2025 in Washington D.C.; and the CMR Macro and Public Economics Seminar, University of Cologne.

The responsibility for the contents of this publication rests with the authors, not the Institute. Since working papers are of a preliminary nature, it may be useful to contact the author of a particular issue about results or caveats before referring to, or quoting, a paper. Any comments should be sent directly to the authors.

1 Introduction

Transactions in real estate markets involve search and negotiation processes that often take months to complete, making real estate a notably illiquid asset class (Piazzesi, Schneider, and Stroebel, 2020). Because housing constitutes a large share of household balance sheets, housing liquidity has substantial aggregate economic consequences (Garriga and Hedlund, 2020). While the drivers and effects of the *temporal* variation in housing liquidity have been extensively documented (see, for example, Ngai and Tenreyro, 2014), we know little about the *spatial* variation. This paper documents new stylized facts about the spatial variation in housing liquidity and shows that it has important implications for housing prices and welfare.

Liquidity in housing markets refers to the ease of selling a property, typically measured by the time to sell or the spread between the asking and transaction price. Scarcity of data has so far limited our knowledge about the spatial variation in housing liquidity. We fill this gap by building spatial datasets on housing prices and liquidity for cities in Germany and the United States. We empirically show that with increasing distance to the city center, housing prices decline, time to sell rises, and the spread between asking and transaction prices widens – controlling for property characteristics and demographics. While the result that prices decrease with distance to the city center is established in the literature (see Duranton and Puga, 2015), we are the first to document that liquidity also decreases with distance to the city center. Moreover, using online search data, we show that the number of potential buyers per property decreases with distance to the city center, reflecting lower market tightness.

To rationalize our empirical results, we build a structural model of housing search

within a city. In our model, travel costs increase with distance to the city center, implying a common preference for central locations. This leads to higher buyer-side tightness, which raises the probability of successful matches in the center, where properties sell quickly and at small spreads, despite their higher prices. Quantitatively, our model reproduces the observed distribution of liquidity and prices with high precision for both Germany and the United States. Using our model, we quantify the welfare and price impacts of search frictions. Due to search frictions, welfare is reduced by 3% (equivalent to 1.5% of housing prices) on average across a city. Welfare losses are particularly stark in the outskirts and mostly attributable to vacancies. Moreover, the spatial price gradient is substantially underestimated in a model version without search – specifically, by a factor of 3 – because such a model ignores how location preferences affect market tightness. This illustrates that ignoring market tightness, as standard spatial housing models do, fails to fully capture the impact of location preferences on prices.

Taken together, our results show that spatial search is central to understanding both liquidity and prices in housing markets. They provide new insights into the role of search and matching in decentralized markets and their relevance in light of the recent “great rotation” toward illiquid, private assets (Koijen, Shah, and Van Nieuwerburgh, 2025).

Empirics. In our empirical analysis, we match the universe of real estate transactions from German cities (introduced in Amaral et al., 2023) to corresponding real estate advertisements assembled by a private company¹ using a nearest-neighbor algorithm. We obtain geocoded datasets on housing liquidity and prices from 2012 to 2024 for Hamburg, Munich, Cologne, Frankfurt, and Duesseldorf. For the United States, we use ZIP-Code-level data from Redfin on housing liquidity and prices from 2012 to 2023, combined with

¹We are very grateful to Sebastian Hein from *VALUE Marktdaten* for giving us access to the data and support throughout the process of writing the paper.

data on local housing characteristics and demographics from the American Community Survey and data on neighborhood quality from Chetty et al. (2025). With these datasets, we cover two large and fundamentally distinct housing markets: the German housing market has a low homeownership rate and low turnover, while the U.S. housing market has a high homeownership rate and high turnover.

Our primary measure of liquidity is the time that properties remain on the market as online listings, the standard measure in the literature (see Han and Strange, 2015). We find that within-city spatial differences in time on the market are substantial and systematic. Even after controlling for spatial variation in property characteristics, income, and demographics, time on the market increases markedly with distance to the city center. The spatial variation in time on the market is an order of magnitude larger than that associated with commonly used determinants of housing liquidity, such as property size or age.² This variation implies economically meaningful differences in the probability of sale: conditional on observables, the weekly probability of sale is approximately 20 percent higher in city centers than in the outskirts in both German and U.S. cities.

Similarly, the spread between asking and sales price becomes larger with distance to the city center. Furthermore, we measure market tightness using the number of buyer contact clicks per listing and show that this measure declines with distance to the city center, even though listings are far more numerous in central areas. Accounting for differences in time on the market, we find that otherwise similar properties attract roughly twice as many potential buyers per week in the city center as in the outskirts. In addition, we find that rental yields increase with distance to the city center, consistent with illiquidity in peripheral markets being priced in.

²We review the existing papers on the determinants of time on the market in Internet Appendix C.4, noting that none of these papers has examined the role of distance to the city center.

Our empirical results hold in an extensive series of robustness checks. Among these, a time series analysis shows that the liquidity gradient flattens during the COVID-19 pandemic, but starts to recover thereafter. This finding is in line with the flattening of the price gradient during the COVID-19 pandemic as a consequence of the shift to working from home (see, for example, Gupta et al., 2022). Moreover, using data on job accessibility across U.S. ZIP Codes from Delventhal and Parkhomenko (2024), we show that our findings extend beyond traditional city centers to other locations that attract a large enough number of commuters.³

Model. In our theoretical analysis, we build a housing search model, in line with recent prominent papers on housing markets, such as Piazzesi, Schneider, and Stroebel (2020) and Guren and McQuade (2020), to analyze endogenous patterns in housing liquidity across space. We assume that households want to minimize their distance to a central location due to travel costs, given their idiosyncratic valuations for individual properties which they can observe by searching.⁴ Our model therefore captures the interaction of location preferences and search.

We show that as the cost of travel increases with distance to the city center, market tightness, defined as the number of potential buyers per seller, decreases. This is reflected in a lower probability of sale and therefore a longer time on the market outside of the city center. Sellers act as price setters for spatially differentiated goods and, consistent with the lower probability of sale, decrease their listing prices. Importantly, they trade off the listing price and the time to sell a housing unit (as emphasized in, for example, Guren, 2018). It is therefore not optimal for sellers to adjust prices downward so far

³We are very grateful to Andrii Parkhomenko for providing us access to the data.

⁴Conceptualizing location preferences via travel costs is in line with the canonical monocentric city model (Alonso, 1964; Mills, 1967; Muth, 1969). As an alternative interpretation of this travel cost, we also consider an opportunity cost of travel to the city center in terms of foregone wages.

that spatial liquidity differences disappear. In that sense, liquidity and prices are endogenously co-determined by travel costs which reflect fundamental demand-side location preferences. Consistent with our empirical findings on job accessibility centers, this mechanism applies beyond a single city center for multiple locations that attract sufficiently large pools of buyers.

We calibrate and estimate the parameters of our model for German and U.S. cities using the datasets from our empirical analysis. The resulting spatial liquidity and price distributions are quantitatively accurate. Using our model, we conduct a counterfactual analysis to quantify the effects of search frictions on welfare and housing prices. We compare our baseline model with (i) an efficient model that abstracts from search, and (ii) a constrained-efficient model that retains search but abstracts from sellers' price-setting behavior.

The efficient model corresponds to a standard spatial housing model, where spatial differences in housing prices merely reflect spatial differences in travel costs, but not in liquidity – all dwellings sell instantaneously. As such, the predicted price gradient is negative but the predicted liquidity gradient is flat, which is at odds with the empirical evidence. In contrast, our baseline model correctly matches both the empirical price and the liquidity gradient. In addition, the counterfactual analysis shows that the efficient model underestimates the price gradient by a factor of three when compared to our baseline model. As such, we show that a standard spatial housing model considerably underestimates the impact of location preferences on prices.

Moreover, when comparing our baseline model to the efficient model, we find that search frictions decrease welfare by 3% on average. These welfare losses are mostly driven by higher vacancies due to lower matching probabilities in the baseline model, especially

in peripheral locations. Hence, policies that shift housing demand to the periphery, for example, spatially targeted housing subsidies or transaction taxes, could reduce vacancies effectively. According to our constrained-efficient model, sellers' price-setting behavior does not notably distort welfare, leaving little room for policy.

In an extension of the model, we introduce a bargaining process which creates spreads between asking and sales prices that we can directly compare to our empirical price spread measure. We show that the time on the market and this spread are structurally interchangeable in the model. Finally, in an additional model experiment, we replicate the empirical flattening of liquidity and price gradients due to the shift to working from home induced by the COVID-19 pandemic. Overall, our model sheds light on how the interaction of location preferences and search accounts for the observed cross-sectional variation in housing liquidity and prices.

Related literature. We are the first to establish that housing liquidity decreases with distance to the city center. This adds to the well-known fact that housing prices decrease with distance to the city center (see, for example, Bruneel-Zupanc et al., 2025; Gupta et al., 2022; Albouy, Ehrlich, and Shin, 2018).

Our paper also contributes to the growing literature on the spatial variation in housing liquidity. Gerardi, Qian, and D. Zhang (2025), Jiang, Kotova, and A. L. Zhang (2024), and Vanhapelto and Magnac (2024) examine differences in housing liquidity across cities, rather than within cities as we do. Piazzesi, Schneider, and Stroebel (2020) show how segmented search behavior is important to understand the covariance of housing search and inventory across and within cities. We complement their work by quantifying how spatial search and the resulting variation in market tightness shape the distribution of prices and welfare within cities. This approach connects to the literature on search

frictions in OTC markets (see, for example, Lagos and Rocheteau, 2009; Duffie, Gârleanu, and Pedersen, 2005).

We also contribute to the literature on urban housing models (for an overview, see Duranton and Puga, 2015) by showing that incorporating search and market tightness substantially improves our theoretical understanding of urban spatial price gradients. Lastly, by integrating space into a framework with trading frictions, we contribute to, first, the well-established literature on housing market search (Badarinza, Balasubramanian, and Ramadorai, 2024; Han and Strange, 2015), second, the literature on how investor preferences shape real estate markets (Ghent, 2021; Badarinza and Ramadorai, 2018), and third, the emerging literature on urban finance which combines elements of structural urban and macro-finance models (see, for example, Koijen, Shah, and Van Nieuwerburgh, 2025; Favilukis, Mabille, and Van Nieuwerburgh, 2023).

The rest of this paper is organized as follows. Section 2 describes our data and our measurement of spatial variables and liquidity. Section 3 presents our empirical analysis. Section 4 describes our model framework and presents analytical and quantitative results. Section 5 presents our counterfactual analysis. Section 6 concludes.

2 Data and measurement

To study the spatial distribution of housing liquidity and prices, we construct two new spatial datasets for large cities in Germany and the United States. For Germany, we use property-level data covering Hamburg, Munich, Cologne, Frankfurt, and Duesseldorf. For the United States, we use ZIP-Code-level data covering the 30 largest MSAs.

2.1 Data for German cities

We combine administrative records on the universe of housing transactions in our sampled cities with a comprehensive dataset on housing advertisements. Our transaction dataset covers the universe of residential housing transactions over several decades. This dataset, introduced in Amaral et al. (2023), is based on data from local real estate committees (*Gutachterausschüsse*). Collecting information on all real estate transactions from notaries, these committees register information on sales prices, contract dates, addresses, and an extensive list of property characteristics which we document in Internet Appendix A.1.

We obtain data on apartment advertisements via *VALUE Marktdaten* who scrape and process real estate advertisements from online platforms and real estate agencies. The company's algorithm ensures that ads with both shorter and longer durations are scraped, preventing potential bias from user-influenced advertisement ordering. If an advertisement is posted multiple times across different platforms or within the same platform, this is taken into account when assigning identifiers to advertisements. We observe the dates on which ads were posted and removed, addresses (if available), further information on location such as ZIP Code or neighborhood, asking prices, and property characteristics. The dataset covers the period between 2012 and 2024, which, in combination with the longer time span covered by the transaction data, limits our sample to this period.

We match the two datasets using a nearest-neighbor algorithm based on location, contract and listing dates, asking and sales prices, apartment sizes, and building year of properties. We focus our analysis on apartments, which allows us to examine the role of location consistently within a city, since other types of housing are typically scarce

in German city centers. In a robustness analysis, we show that our results also hold for single-family homes. As we do not observe the addresses of all listings, we match only about one-third of the transactions with corresponding listings. Our final dataset consists of more than 80 thousand observations. In Internet Appendix A.1, we provide further details on the matching process and show that the matched sample is representative of the universe of transactions.

2.2 Data for U.S. cities

For the United States, we gather ZIP-Code-level data on median time on the market and median sales prices from Redfin.⁵ Our dataset covers the 30 largest MSAs from 2012 to 2023 at a monthly frequency. To obtain control variables for our empirical analysis, we gather ZIP-Code-level data on average housing size, average building year, income composition, and racial composition from the American Community Survey (U.S. Census Bureau, 2012–2023a; U.S. Census Bureau, 2012–2023b; U.S. Census Bureau, 2012–2023c) as well as ZIP-Code-level data on neighborhood quality from Chetty et al. (2025). We focus our analysis on single-family homes, the most common housing type in U.S. cities. In a robustness analysis, we show that our results also hold for condominiums, multi-family houses, and townhouses. Internet Appendix A.2 describes our data preparation procedure in further detail.

⁵Redfin is a real estate brokerage company that obtains its data directly from local listing services, especially those based in the largest MSAs (see: <https://www.redfin.com/news/data-center/>). We do not use data from Zillow, the most popular provider of U.S. real estate data, as Zillow does not provide access to data on time on the market at a more granular level than MSA. However, as we show in Internet Appendix A.2, the differences in coverage between Zillow and Redfin for the 30 largest MSAs are very small and should not affect our results. Moreover, we show that our results are robust to using data from Realtor.com, another online listing platform (<https://www.realtor.com/research/data/>).

2.3 Measurement of spatial variables

We measure spatial variation in our data using the distance to the city center, a standard measure in the urban economics literature (see Duranton and Puga, 2015). For Germany, we choose historic city centers for our baseline analysis.⁶ In a robustness check, we show that selecting the centroid of the business district with the highest land value (via the *Bodenrichtwerte* land value measurements from the *Gutachterausschusse* real estate committees)⁷ yields nearly identical city centers as the ones we choose by hand. We calculate kilometer distances between city centers and locations of apartments transacted within the corresponding city boundaries. For the United States, we define the center of an MSA as the location of its city hall (as done in, for example, Gupta et al., 2022). We calculate kilometer distances between MSA centers and ZIP Code centroids located within the corresponding MSA boundaries.⁸ In our main analysis, we exclude observations with a distance larger than 70km. Internet Appendix D.4 documents that our results are robust to using different cutoffs. Furthermore, we create a job access index using data from Delventhal and Parkhomenko (2024), which we use to find locations with high job access as alternative focal points beyond city centers.

As an alternative spatial measure, we use travel time estimates. The spatial structure of cities can feature rivers or other factors that influence local transportation. Such features could be more accurately represented via the travel time rather than the kilometer distance to the city center. Via openrouteservice,⁹ we request the typical travel time to

⁶We choose the following historic city centers: Hamburg: *Alsterhaus*, Munich: *Marienplatz*, Cologne: *Koelner Dom*, Frankfurt: *Konstablerwache*, Duesseldorf: *Marktplatz*.

⁷Retrieved from the *BORIS-D* database (<https://www.bodenrichtwerte-boris.de/>).

⁸Population-weighted ZIP Code centroids were retrieved from <https://catalog.data.gov/dataset/zip-code-population-weighted-centroids>. MSA boundaries were retrieved from <https://www2.census.gov/geo/tiger/TIGER2021/CBSA/>.

⁹<https://openrouteservice.org/>.

the city center by car. For robustness, we also request car and public transport travel times via the Google Maps Directions API.¹⁰ In addition, we show that our results remain robust when using actual commute times reported in the American Community Survey (U.S. Census Bureau, 2012–2023d).

2.4 Measurement of liquidity

Our main measure of housing liquidity is the time on the market, the standard measure in the literature (see Han and Strange, 2015). For the German dataset, we define this time as the period between the start and the end of an advertisement and report the number of weeks a property has been advertised if it sells on day T of being advertised, that is, $T/7$ weeks. For the U.S. dataset, we directly obtain the time on the market via Redfin. This time refers to the median number of advertised days for housing units sold within a ZIP Code area in a month. As an alternative liquidity measure, we also calculate the relative spread between the asking price and the sales price, akin to the bid-ask spread in financial markets. We call this measure the *asking price discount*.

Table 1: Summary statistics for both datasets (Germany and U.S.)

Dataset	Time on the market in weeks				Sales price in 1,000 € or \$				N
	Mean	SD	P25	P75	Mean	SD	P25	P75	
Germany	13.51	16.71	2.40	17.80	374	274	189	478	84,292
U.S.	7.60	7.87	3.50	9.64	446	502	205	530	682,100

Notes: This table provides summary statistics for the matched and cleaned datasets. N is the number of transactions for the German dataset. For the U.S. dataset, it represents the number of ZIP-Code-year-month pairs.

Table 1 presents summary statistics of the time on the market and prices for the German and U.S. datasets. Overall, we observe that the German market is substantially less liquid than the U.S. market. In Internet Appendices B.1 and B.2 we present these

¹⁰<https://developers.google.com/maps/documentation/directions>.

summary statistics by city, and in Internet Appendix B.3 we present summary statistics for the asking price discount.

3 Empirical analysis

In this section, we document new stylized facts on the spatial variation in housing liquidity within German and U.S. cities and replicate established stylized facts on the spatial variation in housing prices.

3.1 Spatial variation in liquidity and prices

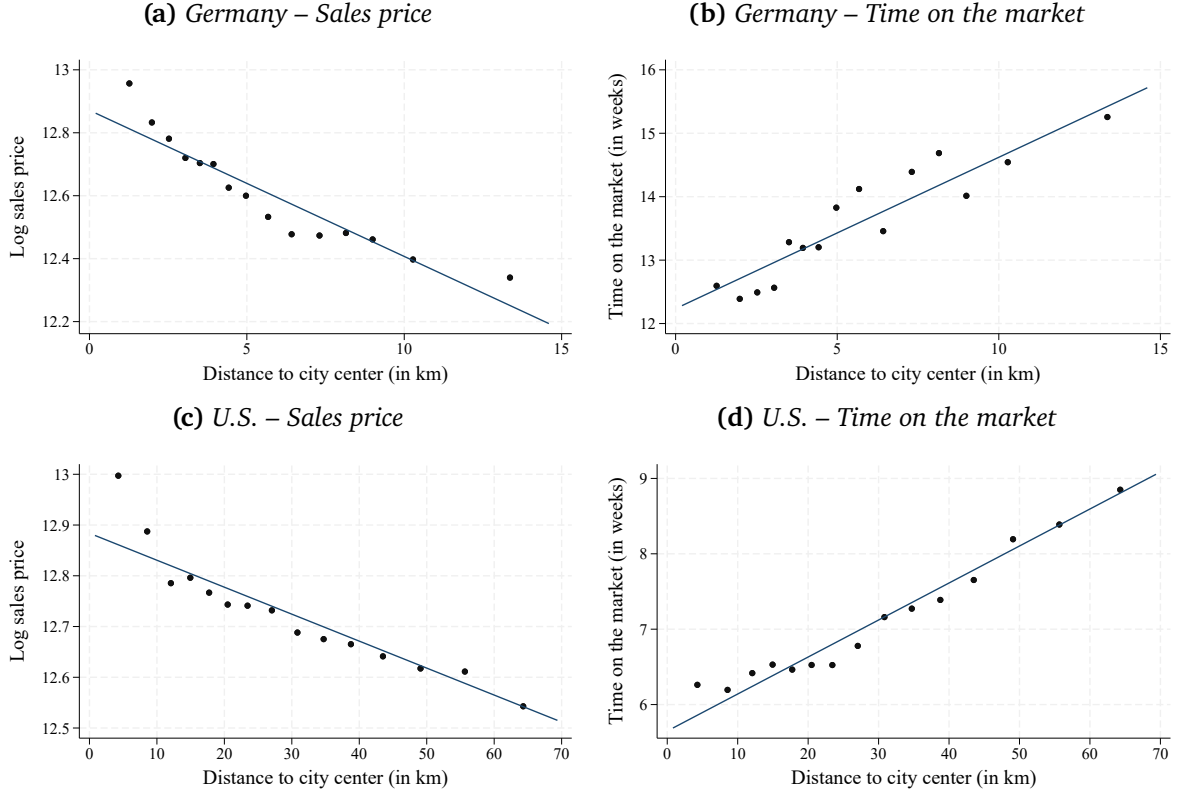
Regression framework. In our baseline analysis, we use hedonic regressions. This approach allows us to rule out that spatial liquidity or price differences are driven by systematic spatial variation in housing characteristics or demographics. We estimate

$$y_I = \alpha \times \text{distance}_I + \beta \times X_I + f_{ct} + \varepsilon_I, \quad (1)$$

where for the German dataset, I indexes transactions, with every transaction I being assigned to a city c and a calendar quarter t , while for the U.S. dataset, $I = it$ includes an index i for ZIP Codes, with every ZIP Code i being assigned to an MSA c , and an index t for time measured in months. The dependent variable y_I refers to the time on the market, the asking price discount, or sales prices. The explanatory variable distance_I is the distance to the city center, measured as a kilometer distance in the baseline specification and as a travel time in alternative specifications. X_I is a control vector, f_{ct} captures city-time fixed effects to account for common time trends in liquidity or prices within a city, and ε_I denotes the error term. To address spatial correlation in the error terms, we cluster standard errors at the city-year level. Note that by considering within-city variation, we

rule out bias due to confounding across-city variation in unobserved variables.

Figure 1: Liquidity and price gradients for Germany (2012–2024) and the U.S. (2012–2023)



Notes: These binned scatter plots display the results of Regression (1) with log sales price and time on the market as the outcome variables, using 15 equally-sized distance bins. The binned scatter plots are based on the complete regression specification, as shown in columns two and five of Tables 2 and 3. The binned scatter plots are produced following Cattaneo *et al.* (2024).

For regressions using the German dataset, the control vector X_I includes an extensive set of property characteristics, such as size, building year, number of bathrooms, or type of heating. We also consider borough (*Stadtbezirk*) fixed effects to capture demographic characteristics. For regressions using the U.S. dataset, X_I includes the median square footage of transacted properties and its square; the share of 1-room, 2–3-room, 4–5-room, 6–7-room, and 8-or-more-room dwellings; the share of housing units built after 2010, in 2000–2009, 1980–1999, 1960–1979, 1940–1959, and in 1939 or earlier; median household income; the share of households with annual income above \$150,000; the homeownership rate; and the share of Black households. These control variables are

observed annually, and the yearly values are assigned to all months within the corresponding year. In addition, we control for spatial differences in neighborhood quality from Chetty et al. (2025), measured by the fraction of children born between 1978 and 1983 in a given ZIP Code area who were incarcerated by April 1, 2010. For U.S. regressions with liquidity as the left-hand-side variable, we also control for the price level in 2011 to capture unobserved housing characteristics.

Results. In Figure 1, we present binned scatter plots based on Regression (1). The left-hand panels display a clear negative relationship between sales prices and distance to the city center. The negative price gradient has been documented in the literature for cities in the United States (Harris, 2024) and across the globe (Liotta, Viguié, and Lepetit, 2022), which we replicate here. The right-hand panels display a clear positive relationship between time on the market and distance to the city center, which constitutes our novel finding of a *negative liquidity gradient*. By showing the results for both German and U.S. cities, we demonstrate that these stylized facts hold for very different housing markets as well as city structures.¹¹

Next, we quantify the relation between time on the market and distance to the city center using several alternative specifications of Regression (1). Tables 2 and 3 present the results for Germany and the U.S. across model specifications, ranging from the most parsimonious model, which only includes city-time fixed effects, to the most comprehensive model, which features the full set of control variables. The coefficient on kilometer distance or travel time is consistently significant at the 1% level for both German and U.S. cities across all specifications. The coefficients remain significant when property characteristics are included as controls and when focusing solely on within-borough variation

¹¹U.S. cities are typically more sprawled than European cities (see Nechyba and Walsh, 2004). We therefore restrict the U.S. sample in the baseline analysis to transactions within 70 km of the city center. Appendix D.4 shows that the results are robust to including observations beyond this radius.

in German cities or controlling for demographics of U.S. cities. In terms of magnitude, properties located in the outskirts take approximately 18 percent longer to sell than comparable properties in city centers in Germany and about 27 percent longer in the United States.¹² This translates into a substantially lower probability that a property sells in a given week in the outskirts relative to the city center. As shown in Internet Appendix C.3, using both measures of the expected probability of sale and the probability that a listing sells within two weeks of being listed, an otherwise similar property in the outskirts is approximately 23 percent less likely to sell in Germany and 17 percent less likely to sell in the United States than a comparable property in the city center. As we show later in our structural model, this variation has substantial implications for prices and welfare.

Table 2: Time on the market and distance to the city center, Germany (2012–2024)

	(1) TOM	(2) TOM	(3) TOM	(4) TOM	(5) TOM	(6) TOM
Distance to center (in km)	0.34*** (0.04)	0.24*** (0.03)	0.20*** (0.03)			
Travel time to center (in min)				0.15*** (0.02)	0.10*** (0.01)	0.08*** (0.01)
City × Year-quarter FE	✓	✓	✓	✓	✓	✓
Property characteristics		✓	✓		✓	✓
Borough FE			✓			✓
<i>N</i>	84,292	84,292	84,292	84,292	84,292	84,292
Adj. <i>R</i> ²	0.04	0.13	0.13	0.04	0.13	0.13
Mean(TOM)	13.51	13.51	13.51	13.51	13.51	13.51

Notes: This table displays the output of Regression (1) on time on the market (TOM), measured in weeks. The first three columns show the results for distance to the city center measured in kilometers, while the last three columns show the results for car travel time to the city center measured in minutes. The list of property characteristics is available in Internet Appendix A.1. Regressions are based on the matched sample for all cities covering the period between 2012 and 2024. Standard errors (in parentheses) are clustered at the city-year level. * : $p < 0.1$; ** : $p < 0.05$; *** : $p < 0.01$.

¹²In German cities, this amounts to approximately two and a half weeks, while in U.S. cities, this corresponds to about two weeks. These results are based on a specification of Regression (1) in which we control for property characteristics and the “city center” is defined as all observations within a 3 km radius of the city center in Germany and a 10 km radius in the U.S., while the “outskirts” are defined as areas beyond 13 km for German cities and beyond 50 km for U.S. cities.

Table 3: Time on the market and distance to the city center, U.S. (2012–2023)

	(1) TOM	(2) TOM	(3) TOM	(4) TOM	(5) TOM	(6) TOM
Distance to center (in km)	0.02*** (0.006)	0.05*** (0.005)	0.03*** (0.005)			
Travel time to center (in min)				0.03*** (0.006)	0.06*** (0.005)	0.04*** (0.006)
MSA × Year-month FE	✓	✓	✓	✓	✓	✓
State FE	✓	✓	✓	✓	✓	✓
Property characteristics		✓	✓		✓	✓
Demographic controls			✓			✓
<i>N</i>	609,020	607,445	607,445	609,020	607,445	607,445
ZIP Codes	4,464	4,463	4,463	4,464	4,463	4,463
Adj. <i>R</i> ²	0.46	0.49	0.51	0.46	0.49	0.51
Mean(TOM)	7.13	7.11	7.11	7.13	7.11	7.11

Notes: This table displays the output of Regression (1) on time on the market (TOM), measured in weeks. The first three columns show the results for distance to the city center measured in kilometers, while the last three columns show the results for car travel time to the city center measured in minutes. The regressions are based on data for single-family homes located within a 70-kilometer radius of the centers of the 30 largest MSAs, covering the period from 2012 to 2023. Standard errors (in parentheses) are clustered at the MSA-year level.
*: $p < 0.1$; **: $p < 0.05$; ***: $p < 0.01$.

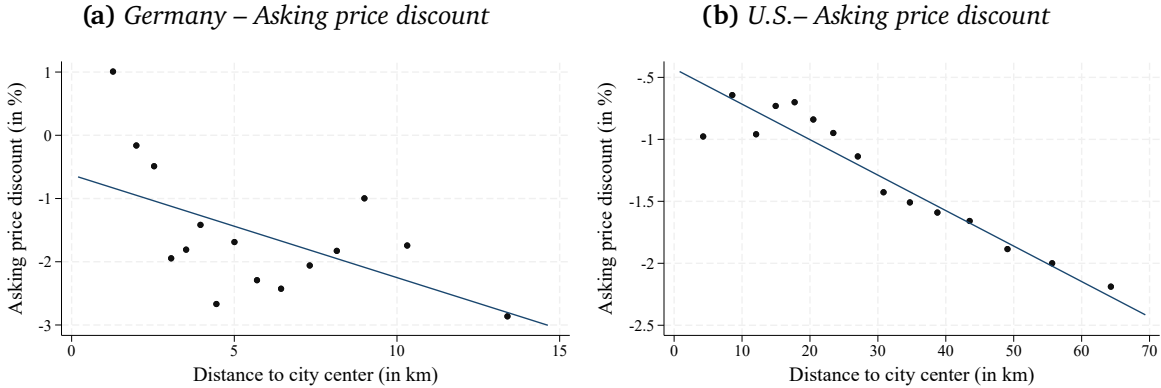
In Internet Appendix C.4, we show that distance to the city center is more strongly associated with time on the market than are other property characteristics such as size or building year.¹³ Moreover, as we demonstrate in Internet Appendix C.5, the spatial variation in time on the market for the U.S. is as large as the cyclical variation, where the latter has been shown to have important implications for business cycle dynamics (Garriga and Hedlund, 2020). Lastly, foreshadowing the result from our structural model that liquidity is priced in across space, we find that rental yields increase with distance

¹³Note that even though we estimate a strong and significant relationship between distance to the city center and time on the market, our results for Germany yield low R-squared values. This is consistent with prior studies summarized in Internet Appendix C.4. The limited explanatory power largely reflects unobserved bargaining dynamics between buyers and sellers, which, however, does not bias our estimated relationships as long as these unobservables are not systematically correlated with distance to the city center. Supporting evidence comes from the substantially higher R-squared in our U.S. analyses which are aggregated at the ZIP code level, suggesting that much of the idiosyncratic heterogeneity averages out once data are aggregated locally.

to the city center (see Internet Appendix C.8).

Asking price discount. Confirming the spatial liquidity patterns with our alternative measure, Figure 2 shows that the asking price discount becomes more negative with increasing distance to the city center in both German and U.S. cities. Sellers in peripheral areas therefore face larger markdowns relative to their asking prices. Additional results reported in Internet Appendix B.3 confirm that spatial differences in price discounts are highly statistically significant and robust to controlling for property characteristics and demographics.

Figure 2: Asking price discount for Germany (2012–2024) and the U.S. (2012–2023)



Notes: These binned scatter plots visualize the results of Regression (1) with asking price discount as the outcome variable and property characteristics controls, using 15 equally-sized distance bins. The binned scatter plots are produced following Cattaneo et al. (2024).

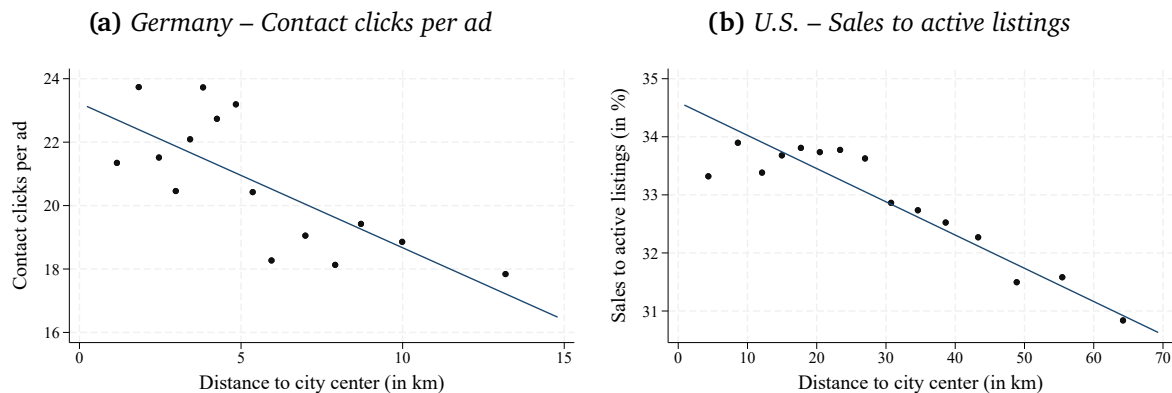
3.2 Spatial variation in market tightness

City centers not only have higher prices and liquidity, but also much denser housing supply. In Appendix C.6 we show that in both German and U.S. cities, housing supply, whether measured by listings or by residential built-up volume, is denser in central areas than in the outskirts. Yet, despite this denser supply, we find that market tightness is highest in central areas, implying that buyer demand is even more concentrated than supply. To obtain this pattern, we use the number of contact clicks per advertisement

(the number of times potential buyers contacted a seller). This variable directly captures search activity. It provides an indicator of local buyer concentration, and hence a natural link to observed liquidity and price differences, which we formalize in our structural model in the second part of the paper.

Figure 3 presents a binned scatter plot of contact clicks per ad against distance to the city center for German cities, see Panel (a). The number of contact clicks per ad declines sharply with distance to the city center: housing units located within 3 kilometers of the city center receive about 20 percent more buyer contacts than those located beyond 13 kilometers. Accounting for spatial differences in time on the market, this implies that, on a weekly basis, a centrally located listing receives roughly twice as many potential buyer contacts as a comparable listing in the outskirts.¹⁴ The coefficient on distance to the city center is negative and highly significant across all specifications (see Internet Appendix C.6).

Figure 3: Measures of market tightness for Germany (2012–2024) and the U.S. (2012–2023)



Notes: These binned scatter plots visualize the results of Regression (1) with contact clicks per ad (Germany) and the ratio of sales to active listings (U.S.) as the outcome variables and property characteristics controls, using 15 equally-sized distance bins. The binned scatter plots are produced following Cattaneo et al. (2024).

For the United States, where data on buyer contacts are not available via Redfin, we approximate market tightness using the ratio of homes sold to active listings in a

¹⁴This result is obtained by dividing the average number of contact clicks by the average weeks on the market, as reported in Figure 1.

given month, measured at the ZIP-Code level. This is a measure of market turnover rates. Markets in U.S. city centers exhibit substantially higher turnover rates than those in the outskirts. This pattern is robust across all specifications (see Internet Appendix C.6). Moreover, using ACS data on commute times, we provide both cross-sectional and time-series evidence that higher travel times to work are associated with lower market turnover (see Internet Appendix C.7).

3.3 Robustness analyses

Results for individual cities. In the previous sections, we have presented results for pooled samples of German and U.S. cities. Given that cities vary in size and other spatial characteristics, it is possible that our results are driven by a subsample of cities. As we show in Internet Appendix D.1, this is not the case. We find negative liquidity and price gradients for all cities in the German dataset and negative liquidity gradients for all cities as well as negative price gradients for most cities in the U.S. dataset. Our empirical analysis is not focused on heterogeneity in coefficients across cities, rather, it aims to detect systematic patterns across the cities in our sample. Our structural model in the second part of the paper then serves to explain these systematic patterns.

COVID. The COVID-19 pandemic and the subsequent shift to remote work significantly flattened the price gradient in the United States (Gupta et al., 2022). In contrast, the impact on the price gradient in Europe has been comparably muted (Biljanovska and Dell’Ariccia, 2024). We test whether remote work influenced liquidity gradients by splitting our samples into pre- and post-2020 periods. For both Germany and the U.S., the liquidity gradient flattened during the COVID-19 pandemic but started to recover thereafter, as documented in Internet Appendix D.2. The extent to which the flattening is

persistent depends on the future evolution of preferences to live near city centers.

Different housing types. In our baseline analysis, we focus on the most common housing types in German and U.S. cities: apartments and single-family houses, respectively. In this robustness check, documented in Internet Appendix D.3, we demonstrate that our results for German and U.S. cities remain robust when alternative housing types are considered (single-family homes for German cities and condominiums, multi-family homes, and townhouses for U.S. cities).

Alternative city boundary definitions. To ensure that our U.S. results are not specific to the definition of MSAs, we replicate our baseline analysis using functional urban area boundaries from Moreno-Monroy, Schiavina, and Veneri (2021), which define cities based on commuting flows. In Internet Appendix D.4, we show that our results hold when using functional urban area boundaries for U.S. cities. This robustness analysis is not possible for German cities, as we only have data available that refers to apartments transacted within administrative city boundaries.

Alternative city center definitions. In our baseline analysis, our definition of city center is based on historic locations for German cities and city halls for U.S. cities. We conduct a robustness analysis with alternative city centers. For Germany, we use the centroid of the business district with the highest land value in 2023, as given by the *Bodenrichtwerte* land values produced by the *Gutachterausschusse* real estate committees.¹⁵ For the United States, we do not have appraisal data available and therefore use the locations with the highest job access index as alternative city centers. The results, documented in Internet Appendix D.5, show practically unchanged gradients.

¹⁵For this analysis, we have to exclude Munich, as we do not have access to its local *Bodenrichtwerte* appraisals.

Alternative travel time estimates. Our results also hold with the alternative travel time estimates from the Google Maps Directions API and the ACS, as documented in Internet Appendices D.6 and C.7, except when using public transport travel times for U.S. cities. The latter finding is consistent with public transportation being rarely used in the United States (see, for example, Burrows, Burd, and McKenzie, 2021).

Non-parametric estimation. Although our main results are highly significant and robust to a multitude of controls and fixed effects, we still rely on the functional form of the OLS regression specified in Equation (1). To ensure that our results are not compromised by misspecification, we employ nonparametric methods. When applying these methods, we test whether liquidity and prices are on average lower in the outskirts than in the city center, where we match at the level of housing units based on observable characteristics. Accordingly, we can only produce these results for German cities.

Table 4: *Average differences between city center and outskirts, Germany (2012–2024)*

Method	Difference in TOM	Difference in log prices	N
OLS	1.89*** (0.227)	-0.40*** (0.004)	33,717
LASSO	2.11*** (0.378)	-0.43*** (0.006)	33,717
Propensity score	1.99*** (0.446)	-0.43*** (0.013)	33,717
Inverse probability	2.20*** (0.328)	-0.43*** (0.005)	33,717

Notes: This table shows the estimated average difference between city center and outskirts for time on the market (TOM), measured in weeks, and log sales prices for different non-parametric methods. The different methods are described in the main text. * : $p < 0.1$; ** : $p < 0.05$; *** : $p < 0.01$.

First, we use augmented inverse probability weighting to estimate the average difference in outcome variables between city center and outskirts, while using LASSO regression in the first stage to estimate the probability of treatment. Second, we use propensity score matching based on our full set of apartment characteristics. Third, we use inverse probability weights from a logistic regression to estimate average differences. The results are documented in Table 4, comparing the first 3 bins of the distance to the city center

with the 13th, 14th, and 15th (out of 15) bins. All non-parametric methods confirm our baseline OLS results both in terms of direction as well as in terms of magnitude. The relatively high number of observations and detailed information on properties explain the similar magnitudes across methods.

Properties that do not get sold. Our baseline results could be biased if the number of advertisements that did not result in a sale varies systematically across space. To assess this, we run an algorithm to identify such advertisements in the German data. Internet Appendix D.7 shows that the percentage of ads that did not result in a sale is small and increases slightly with distance to the city center. In addition, we conduct a survival analysis that includes ads which did not result in a sale, and find that the probability of sale decreases with distance to the city center.

Systematic overvaluation. A potential alternative explanation for lower liquidity in the outskirts is the presence of less-informed sellers, possibly due to an older population that is less engaged with housing markets. Specifically, if sellers in peripheral areas systematically overvalue their properties by setting unrealistically high asking prices, this may lead to longer marketing durations and a wider gap between asking and transaction prices in these areas. As demonstrated in Internet Appendix D.8, the spatial gradient for time on the market remains practically unchanged when controlling for the asking price discount, and vice versa.

3.4 Discussion of external validity

Our empirical analysis shows that liquidity and prices decrease with distance to the city center. In this section, we discuss to which extent these results can be generalized to other settings, considering alternative focal points beyond the city center and the rental

market in addition to the owner-occupied housing market.

Table 5: Liquidity and price gradients in the rental market, Germany (2012–2024)

	(1) TOM	(2) TOM	(3) TOM	(4) Net rent	(5) Net rent	(6) Net rent
Distance to center (in km)	0.17*** (0.02)	0.17*** (0.02)	0.21*** (0.08)	-0.02*** (0.00)	-0.03*** (0.00)	-0.02*** (0.00)
City \times Year-quarter FE	✓	✓	✓	✓	✓	✓
Property characteristics		✓	✓		✓	✓
ZIP Code FE			✓			✓
<i>N</i>	957,249	957,249	957,249	957,249	957,249	957,249
Adj. <i>R</i> ²	0.23	0.26	0.27	0.40	0.90	0.91
Mean(dependent variable)	6.72	6.72	6.72	6.52	6.52	6.52

Notes: This table displays the output of Regression (1) on time on the market (TOM) and log net rental value (net rent). All columns show the results for distance to the city center measured in kilometers. The list of property characteristics is available in Internet Appendix A.1. Regressions are based on the cleaned sample of rental listings from ValueAG for all cities covering the period between 2012 and 2024. Standard errors (in parentheses) are clustered at the city-year level. * : $p < 0.1$; ** : $p < 0.05$; *** : $p < 0.01$.

So far, we have implicitly assumed that the cities in our sample exhibit a monocentric structure. However, the mechanism we propose in the theoretical part of the paper extends beyond the monocentric structure. In particular, our theoretical mechanism only requires the existence of focal points that attract sufficiently large numbers of commuters. We test whether our empirical results hold when considering alternative focal points. Using data on commuting distances and the number of employees across ZIP Codes from Delventhal and Parkhomenko (2024), we construct an index of job accessibility at the ZIP-Code level as an inverse-distance-weighted average of accessible jobs. We identify the ZIP Codes with the highest job accessibility within a given MSA, which we refer to as *focal ZIP Codes*, and calculate the distance from each ZIP Code centroid to the nearest focal ZIP Code centroid. We then test whether we also find liquidity and price gradients in this alternative setting. The results, presented in Internet Appendix D.9, confirm that both gradients are also present when measuring distances to nearest focal ZIP Codes.

This finding is robust to varying the number of focal ZIP Codes per MSA.

Second, we test whether our results also hold beyond the owner-occupied housing market. If the observed liquidity and price gradients are driven by differences in local market tightness, as suggested by our results in Section 3.1, we should expect to observe similar patterns in the rental market. To test this, we use German rental listings data from *Value Marktdaten* for the same cities and time period as in our baseline analysis. The results, calculated using the baseline specification of Regression (1), are presented in Table 5. We find that the time on the market for rental housing units increases with distance to the city center, while net rents (defined as monthly rental prices excluding utilities) decrease. Note that due to the high number of observations for rentals, we are able to use more granular location fixed effects.

4 Rationalizing the empirical observations

We give structure to the empirical observations documented in the previous sections by building a spatial search model of a city's housing market. We start from a frictional search market for housing (see, for example, Ngai and Tenreyro, 2014; Piazzesi, Schneider, and Stroebel, 2020; Guren and McQuade, 2020), using the established basic setup from Krainer (2001). We incorporate location preferences following the monocentric city model,¹⁶ assuming that agents prefer to live closer to the city center. Such preferences increase the concentration of potential buyers in the city center, thereby generating tighter markets and raising liquidity.

This mechanism is consistent with our empirical findings: market tightness is higher in locations with lower travel time. Supplementary Appendix C.7 provides complementary time-series evidence that increases in travel time to work reduce market tightness, thereby

¹⁶See Alonso (1964), Mills (1967), and Muth (1969).

providing further support for a causal link between travel costs and market tightness.

4.1 Structural framework

Model environment. Time is discrete and measured in days. A large number N of infinitely-lived agents live in a monocentric city. The agents are risk-neutral,¹⁷ financially unconstrained, and discount with factor $\beta \in (0, 1)$. All agents travel to the city center for work and leisure activities. The daily travel cost $\tau(d)$ is associated with a distance to the city center $d \in \mathcal{D} = [\underline{d}, \bar{d}]$, where $\partial\tau/\partial d > 0$.

Housing. The housing stock is exogenous and consists of N housing units with given distances to the city center. Before deciding whether to purchase a housing unit, an agent draws an idiosyncratic valuation ε , referred to as *housing dividend* in the following. The housing dividend is a random variable with cumulative distribution function F and probability density function f . Having decided to purchase a property, the agent receives the corresponding dividend in every period until they are unmatched. The dividend is independently and identically distributed across agents, space, and time. An agent can only occupy one housing unit at a time, can only search for new housing units after they have been unmatched, and cannot rent out their property.

Search process. We focus on a stationary search equilibrium and omit time indices. In the first model period, every agent is endowed with a housing unit. In every following period, a match between an agent and a housing unit persists with probability π . With probability $1 - \pi$, an agent is unmatched, which can be interpreted as a moving shock. In this case, the agent puts their property up for sale and searches for a new one. Agents

¹⁷Risk neutrality is standard in housing search models, analogously to labor market search models (see, for example, Rogerson, Shimer, and Wright, 2005).

are therefore sellers and buyers simultaneously.¹⁸

In a given model period, first, sellers post prices, and second, buyers randomly visit housing units that are on the market. When visiting a housing unit, a buyer observes their dividend draw, the property's distance to the city center, and the posted price. The buyer either agrees on the price and moves into the property in the next period or does not agree on the price and continues to search. In Internet Appendix G, we extend the search process with a bargaining process, following Carrillo (2012).

Seller's problem. Risk neutrality allows us to analyze buyer and seller decisions separately due to linear additivity of agents' value functions. A seller chooses a posted price $p(d)$ to maximize their present value

$$\Pi(d) = \gamma(d)p(d) + (1 - \gamma(d))\beta\Pi(d). \quad (2)$$

With probability of sale $\gamma(d)$, the seller receives $p(d)$. With probability $1 - \gamma(d)$, they try to sell the housing unit again in the next period, obtaining a discounted continuation value $\beta\Pi(d)$. The probability of sale $\gamma(d)$ reflects expected demand, or market tightness, given $p(d)$. Sellers take into account the effect of posted prices on local market tightness. They act as local price setters.¹⁹

Buyer's problem. A matched buyer, that is, a buyer who has purchased a property and is either currently occupying the housing unit or will occupy the housing unit in the next

¹⁸An agent can only occupy one housing unit at a time, but can have multiple housing units on the market as a seller. Such a scenario occurs if an agent is unmatched, finds a new property, is unmatched again, but has not yet sold their old property/properties. Due to the large number of agents, the probability of a single agent accumulating all housing units is approximately zero.

¹⁹This assumption, which we take over from the original Krainer (2001) model, serves as the basis for one of our counterfactual exercises in Section 5. The assumption is not required to generate our key theoretical result, which is that buyer reservation dividends increase with distance to the city center. Specifically, a model version in Section 5 in which sellers do not set prices and buyers simply search for their preferred housing units also yields reservation dividends that increase with distance to the city center.

period, obtains the value

$$V(d, \varepsilon) = \beta \left(\varepsilon - \tau(d) + \pi V(d, \varepsilon) + (1 - \pi) (\Pi(d) + W) \right), \quad (3)$$

where W denotes the value of search. With a delay of one period, the buyer receives the dividend ε and incurs the travel cost $\tau(d)$. With probability π , the buyer keeps on living in the housing unit for another period and receives the discounted continuation value $\beta V(d, \varepsilon)$. With probability $1 - \pi$, the buyer becomes unmatched and receives the discounted resale value $\beta \Pi(d)$ and the discounted value of search

$$\beta W = \beta \mathbb{E}_{d, \varepsilon} [\max [V(d, \varepsilon) - p(d), \beta W]], \quad (4)$$

where a buyer either accepts a posted price and receives a discounted net value of $\beta(V(d, \varepsilon) - p(d))$, or continues to search and receives $\beta^2 W$.

4.2 Equilibrium

Seller's optimization. Rearranging the seller profit expression (2), we have that

$$\Pi(d) = \tilde{\gamma}(d)p(d), \quad (5)$$

where $\tilde{\gamma}(d) = \gamma(d)/(1 - \beta(1 - \gamma(d)))$ is the discount-factor-adjusted probability that a seller can sell their property in the current period or in any future period. It reflects the expected demand that is relevant for the seller from the perspective of the current period. The first-order condition for profit maximization is then similar to that of a typical price

setter, but with a probabilistic sale of a single good and without production costs:

$$\tilde{\gamma}(d) + p(d) \frac{\partial \tilde{\gamma}}{\partial p(d)|_d} = 0, \quad (6)$$

where the derivative $\partial \tilde{\gamma}(d)/\partial p(d)|_d$ is a reformulation of the derivative $\partial \gamma(d)/\partial p(d)|_d$.²⁰

It captures the tradeoff between price and probability of sale that the seller faces: if the seller changes their price, the probability of sale also changes. We show in Internet Appendix E that a seller's first-order condition provides a local maximum for their profit.

Buyer's optimization. Via the definition of the value of search (4), a buyer has to be indifferent between buying a property and continuing to search at some reservation dividend $\varepsilon^*(d)$:

$$V(d, \varepsilon^*(d)) - p(d) = \beta W. \quad (8)$$

The solution of this equation for a given distance to the city center characterizes the corresponding reservation dividend. The optimality condition (8) defines a cutoff rule for a stochastic event. Individual buyers can draw higher housing dividends than $\varepsilon^*(d)$, in which case they accept the equilibrium price $p(d)$ and obtain a net utility above βW .

The buyers' optimality condition (8) implies reservation dividends with which buyers are indifferent between purchases at all distances to the city center, as the discounted

²⁰Specifically, this derivative reads

$$\frac{\partial \tilde{\gamma}}{\partial p(d)|_d} = \frac{\partial \gamma}{\partial p(d)|_d} \left(\frac{1 - \frac{\beta \gamma(d)}{1 - \beta(1 - \gamma(d))}}{1 - \beta(1 - \gamma(d))} \right), \quad (7)$$

where the denominator reflects that if the seller marginally changes their posting price, the probability of sale changes in the current period, but also in the next period with probability $1 - \gamma(d)$ which is discounted with factor β , and so forth, ad infinitum. The numerator adjusts for the fact that the probability $1 - \gamma(d)$ with which the probability of sale changes in the next period, changes as well.

value of search βW does not vary across space. The buyer indifference condition is hence also a spatial equilibrium condition. Note that precisely because equilibrium expected net buyer utility is constant, required dividend draws have to offset travel costs. Hence, this spatial equilibrium condition is also to be interpreted as a spatial no-arbitrage condition for housing (see, for example, Glaeser and Gyourko, 2008).

Next, note that the equilibrium probability of sale at some distance to the city center is equal to the probability that a buyer's idiosyncratic dividend draw is above the reservation dividend at this distance:

$$\gamma(d) = \text{Prob}(\varepsilon \geq \varepsilon^*(d)) = 1 - F(\varepsilon^*(d)). \quad (9)$$

Thus, for the derivative in the seller's optimality condition (6) we have that²¹

$$\frac{\partial \gamma}{\partial p(d)|_d} = -f(\varepsilon^*(d)) \frac{\partial \varepsilon^*}{\partial p(d)|_d} = -f(\varepsilon^*(d)) \frac{1 - \pi\beta}{\beta}. \quad (12)$$

Now, we have all required information to define an equilibrium of the model.

Equilibrium definition. A *stationary spatial search equilibrium* consists of value functions $\{V, \Pi\}$, a value of search W , a posting price function p , a reservation dividend function ε^* , and a sale probability function γ that satisfy equations (2), (4), (6), (8), (9) for all distances to the city center $d \in \mathcal{D}$, given parameters $\{\beta, \pi, \underline{d}, \bar{d}\}$, a cumulative

²¹We can rearrange the buyer's value (3) and obtain the linear expression

$$V(d, \varepsilon) = \frac{\beta}{1 - \pi\beta} \left(\varepsilon - \tau(d) + (1 - \pi)(\Pi(d) + W) \right). \quad (10)$$

Using the indifference condition (8), we can isolate the reservation dividend:

$$\varepsilon^*(d) = \frac{1 - \pi\beta}{\beta} p(d) + \tau(d) - (1 - \pi)\Pi(d) + (\pi - \pi\beta)W. \quad (11)$$

Note that $\partial\Pi/\partial p(d)|_d = 0$ due to the envelope theorem.

distribution function for idiosyncratic dividends F with probability density function f , and a travel cost function τ .

4.3 Analytical results

Before calibrating and estimating the model's structural parameters, we first derive analytical results that rationalize our findings from the empirical part of the paper as general properties of our model. We show that the equilibrium expected time on the market increases with distance to the city center, while the equilibrium sales price decreases.

We derive these results here for uniformly distributed dividends $\varepsilon \sim U[\underline{\varepsilon}, \bar{\varepsilon}]$ which we later employ in our quantitative exercise. In Internet Appendix F, we show that these results hold with more general assumptions about the dividend distribution, and with the exponential distribution as a specific example of an alternative dividend distribution. In Internet Appendix G, we show that the expected time on the market is interchangeable with the asking price discount as an alternative concept of liquidity within the extended version of our model with bargaining. In Internet Appendix H, we provide proofs of the equilibrium's existence and uniqueness for our extended model with bargaining and our baseline model as a nested case of the extended model.

4.3.1 Reservation dividends across space

First, as an auxiliary result, we derive that buyer reservation dividends $\varepsilon^*(d)$ increase with distance to the city center. This result is auxiliary in the sense that it is essential to understand the spatial patterns in liquidity and prices, our main results. We show that buyers need higher draws of the dividend to make a purchase the farther a housing unit they visit is away from the city center, due to a higher travel cost $\tau(d)$. To obtain

that $\partial \varepsilon^* / \partial d > 0$, we reformulate $p(d)$ and $\Pi(d)$ in terms of $\varepsilon^*(d)$.²² Differentiating with respect to the distance to the city center, we have that:

$$\frac{\partial \varepsilon^*}{\partial d} \underbrace{\left(2 + 2 \frac{\pi \beta}{1 - \pi \beta} \frac{\bar{\varepsilon} - \varepsilon^*(d)}{\bar{\varepsilon} - \underline{\varepsilon}} \right)}_{>0} = \frac{\partial \tau}{\partial d} > 0, \quad (16)$$

and hence, $\partial \varepsilon^* / \partial d > 0$. Intuitively, buyers want to be compensated for higher travel costs with higher idiosyncratic housing dividends, taking into account spatial differences in prices and profits (encoded in the bracket). In other words, buyers are less willing to accept offers in the outskirts, which translates into lower market tightness. This auxiliary result provides the starting point for our description of the spatial variation in liquidity and prices.

4.3.2 Liquidity and prices across space

Liquidity. In line with the measurement of time on the market in the empirical part of the paper, we define that a property has been on the market for T days if it sells on day number T of being advertised. Via the expected value of the geometric distribution that results from the multiplication of sale probabilities over time, the expected time on the

²²First, we use the seller optimality condition characterized by (6) to express the equilibrium price as a function of the probability of sale:

$$p(d) = \frac{-1}{\partial \gamma(d) / \partial p(d)|_d} \left(\gamma(d) + \frac{\beta}{1 - \beta} (\gamma(d))^2 \right), \quad (13)$$

where $\gamma(d) = (\bar{\varepsilon} - \varepsilon^*(d)) / (\bar{\varepsilon} - \underline{\varepsilon})$ due to equilibrium relation (9) between probabilities of sale and reservation dividends. Then, together with the closed-form relation (12) for the derivative $\partial \gamma(d) / \partial p(d)|_d$,

$$p(d) = \frac{\beta(\bar{\varepsilon} - \varepsilon^*(d))}{1 - \pi \beta} + \frac{\beta^2(\bar{\varepsilon} - \varepsilon^*(d))^2}{(1 - \beta)(1 - \pi \beta)(\bar{\varepsilon} - \underline{\varepsilon})} \quad (14)$$

$$\Pi(d) = \frac{\beta(\bar{\varepsilon} - \varepsilon^*(d))^2}{(1 - \beta)(1 - \pi \beta)(\bar{\varepsilon} - \underline{\varepsilon})}. \quad (15)$$

We then plug these expressions into the equation for the isolated reservation dividend (11).

market in days at a given distance to the city center is

$$\mathbb{E}[TOM(d)] = \frac{1}{\gamma(d)} = \frac{\bar{\varepsilon} - \underline{\varepsilon}}{\bar{\varepsilon} - \varepsilon^*(d)} \quad (17)$$

$$\Rightarrow \frac{\partial \mathbb{E}[TOM]}{\partial d} = \underbrace{(\bar{\varepsilon} - \underline{\varepsilon})(\bar{\varepsilon} - \varepsilon^*(d))^{-2}}_{>0} \frac{\partial \varepsilon^*}{\partial d} > 0. \quad (18)$$

Reservation dividends increase with distance to the city center, which reflects compensation for higher travel costs. With a higher cutoff value for dividend draws, the market becomes less tight, and probability of sale decreases with distance to the city center. A lower probability of sale implies a higher expected time on the market.

Prices. Via (14),

$$\frac{\partial p}{\partial d} = \underbrace{\left(\frac{\beta}{1 - \pi\beta} + \frac{2\beta^2(\bar{\varepsilon} - \varepsilon^*(d))}{(1 - \beta)(1 - \pi\beta)(\bar{\varepsilon} - \underline{\varepsilon})} \right)}_{>0} \left(-\frac{\partial \varepsilon^*}{\partial d} \right) < 0. \quad (19)$$

Sellers expect to sell housing units with a higher probability in the city center, as reservation dividends are lower. Being local price setters, they optimally post higher prices, since they are more likely to meet a searcher that is willing to buy.

Further remarks. As additional results, we show that the variance of time on the market increases with distance to the city center (see Internet Appendix J.1) and that the model predicts the price gradient to be larger than the liquidity gradient in relative terms (see Internet Appendix J.2). We confirm both of these results empirically.

Next, note that our mechanism does not require a single city center, or any city center whatsoever to function. Whenever there is a location for which homebuyers share a common preference to live nearby, generating spatial patterns in market tightness, our mechanism applies. City centers provide established examples for such focal points, and

as such a special case of our mechanism.

Moreover, note that we assume all agents to be identical. In principle, different buyer clienteles in the city center and the outskirts could also generate spatial variation in liquidity and prices. However, in our empirical analysis, we condition on apartment size and on borough fixed effects for German cities, both of which should capture some dimension of buyer heterogeneity, and for U.S. cities, we control for ZIP-Code-level demographic characteristics. It is therefore consistent with the empirical analysis to abstract from buyer heterogeneity in the model.

Next, note that we assume that buyers randomly visit housing units and observe their idiosyncratic dividends during these visits. If buyers were more likely to visit properties in the city center, this would also affect the time on the market. More search flowing toward the center would increase the probability of sale, just as in our mechanism. Hence, under the alternative mechanism of spatial differences in search intensity rather than reservation dividends, the driving force behind spatial differences in liquidity would equally consist of spatial differences in market tightness.

Furthermore, note that if housing units are more heterogeneous in the outskirts and this causes higher search effort, buyers are also less likely to buy properties in the outskirts. This is a complementary interpretation of our mechanism.

Lastly, even though we assume risk-neutral agents, risk-averse agents would discount uncertainty about liquidity more in the outskirts than in the city center, which would reinforce spatial price differences.

4.4 Calibration and estimation of model parameters

Now, we turn to our quantitative model analysis and first calibrate and estimate the structural parameters of our model. Since our equilibrium conditions gives us a set of non-linear equations, we solve the model numerically. Internet Appendix I describes our numerical model solution method.

We discretize the set of distances to the city center: $\mathcal{D}^\Delta = \{d_1^\Delta, \dots, d_z^\Delta\}$, where $\underline{d} = d_1^\Delta$ and $\bar{d} = d_z^\Delta$. To obtain the discretized distances \mathcal{D}^Δ , we group the distances to the city center from the pooled German and U.S. datasets into $z = 15$ bins, using the distance bins from the scatterplots in Figure 1. Since the bins are constructed with equal numbers of observations per bin, the implied number of housing units in the model is equal for all 15 distance bins. This does not mean that housing supply is uniform across space. There are more bins in the city center and fewer bins in the outskirts, hence also more model housing units in the center and fewer model housing units in the outskirts. Moreover, we do not implicitly assume any city shape here. We represent the spatial distribution of housing in a city in the form of binned distances to the city center. Focusing on a stationary equilibrium, we calculate expectations using the whole set of distances \mathcal{D} . In other words, we calculate expectations for buyers expecting all distances to the city center being available on the market in the next period.

We obtain empirical travel time estimates as explained in Section 2.3 and convert them into travel cost estimates, assuming that $\tau(d^\Delta) = \mu \tilde{\tau}(d^\Delta)$, where $\tilde{\tau}(d^\Delta)$ is the travel time to the city center in minutes. This conversion of travel time into travel costs follows established approaches (see, for example, Ahlfeldt et al., 2015).²³ The scaling parameter

²³Note that our linear travel cost enters net utility additively, while the typical implementation in Ahlfeldt et al. (2015)-type models assumes an exponential travel cost that enters net utility multiplicatively. For small numbers (which applies for the modeled daily travel cost), these two approaches are approximately

μ measures the cost in model units of traveling 2 minutes by car, as agents travel from their property to the city center and back every day. We follow the canonical monocentric city model and calibrate the travel cost as a physical cost of travel, but also provide an alternative calculation in Internet Appendix J.3 in which we think of the travel cost as an opportunity cost due to lost time and thus foregone wages. We convert between model units and euros or dollars via the average sales price.

Calibrated parameters. We set $\beta = \sqrt[365]{0.95} \approx 0.9999$ such that the annual discount factor is 0.95. For German cities, the housing match persistence is given by $\pi = 1 - (1/(30 \times 122)) \approx 0.9997$, as the average holding period in the data is 122 months. This value is based on observations from January 1990 to 2024 to capture the full length of holding periods as well as possible. For Hamburg, we do not have data on holding periods available, thus the calibrated housing match persistence is based on information from Munich, Cologne, Frankfurt, and Duesseldorf. For the U.S., we use a holding period of 120 months as a typical value for large MSAs, based on the Redfin data.

Table 6: Estimated parameters, German and U.S. cities

Parameter	Value	95% CI	Value	95% CI
<i>Germany</i>				
μ	0.00619	[0.00618, 0.00630]	0.00403	[0.00400, 0.00407]
$\underline{\varepsilon}$	-0.437	[-0.443, -0.426]	0.300	[0.299, 0.301]
$\bar{\varepsilon}$	0.533	[0.527, 0.541]	0.713	[0.709, 0.728]

Notes: This table documents results from the parameter estimation using the method of simulated moments; for details see the main text. “95% CI” denotes bootstrapped 95% confidence intervals.

Estimated parameters. We estimate the travel cost scaling parameter μ and the uniform distribution bounds $\underline{\varepsilon}$ and $\bar{\varepsilon}$ with the method of simulated moments, using an identity weighting matrix for our three parameters. We match the average time on the equivalent via a first-order Taylor expansion of the exponential function.

market in the pooled German city and the pooled U.S. city. The estimation results are displayed in Table 6. We obtain 95% confidence intervals by drawing 1,000 bootstrapped replications of data inputs sized 1/3 of the entire sample with replacement, estimating the model for each draw, and using the 0.025 quantiles and 0.975 quantiles of the resulting parameter distributions as confidence bounds. Note that the estimated lower bound of the housing dividend distribution is negative for Germany, but positive for the United States. This stems from the level difference in time on the market between the two countries, as the U.S. housing market is substantially more liquid than the German housing market.

4.5 Model results

Table 7: Model results, German and U.S. cities

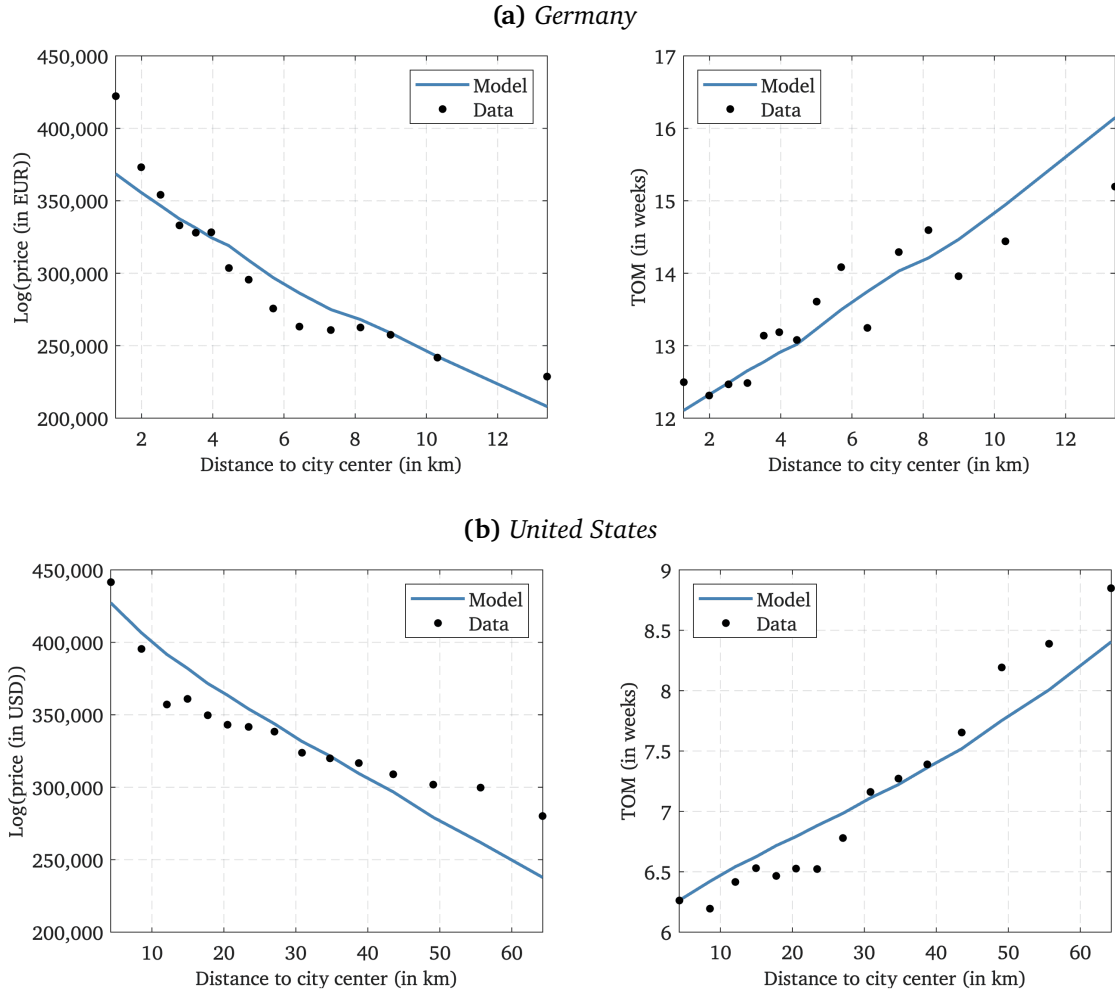
Object	Model	Data	Model	Data	Targeted
	<i>Germany</i>		<i>U.S.</i>		
Average price (in 1,000 € or \$)	302	302	339	339	Yes
Spatial price gradient (in 1,000 € or \$ per km)	-13.3	-14.5	-3.1	-2.1	No
Average TOM (in weeks)	13.5	13.5	7.1	7.1	Yes
Spatial TOM gradient (in weeks per km)	0.326	0.244	0.034	0.046	No
Average daily travel cost (in € or \$)	16.5	15	17.3	25	No

Notes: This table documents results from the calibrated and estimated model. “TOM” refers to the (expected) time on the market. The data values refer to averages over distance bins, where binned values are calculated using the main specification of Regression (1).

Table 7 shows the main model results. We match the average sales price by construction, as we convert between model units and euros or dollars via the average sales price. We also match the average time on the market, which directly results from the parameter estimation. More importantly, our model results exhibit spatial variation that closely aligns with the data. The untargeted spatial price and time on the market gradients are

matched with high accuracy. These gradients refer to the slopes of regression lines that fit the binned data points and the corresponding model values. As such, we argue for travel costs to be a quantitatively relevant spatial fundamental that generates within-city spatial variation in both housing liquidity and prices. Figure 4 provides a visual overview of the relevant spatial distributions from the model and the data.

Figure 4: Spatial distributions of liquidity and prices: model vs. data



Notes: This figure shows the main model results for individual bins of distances to the city center. “TOM” refers to the (expected) time on the market. The data points are calculated using the main specification of Regression (1), as displayed in Figure 1.

The estimated values of μ imply an average daily travel cost for the German cities of €16.5, which is in the range of average daily car operating costs in Germany of around €15 (see Andor et al., 2020). For the United States, the average daily travel cost in the

model is \$17.3 which is in the range of daily car operating costs in the U.S. of around \$25 (see Moody et al., 2021). The cited empirical travel cost estimates are rough calculations. It is furthermore not entirely clear that the car operating cost per se captures the full travel costs or is the only suitable measure. Hence, Internet Appendix J.5 provides an alternative measure of travel costs, using an opportunity cost calculation in terms of foregone wages due to travel time. Lastly, as an additional test of the ability of our model to generate realistic spatial patterns, we replicate the flattened liquidity and price gradient during and after the COVID-19 pandemic discussed in the empirical robustness analysis. This additional exercise is documented in Internet Appendix J.6 and relies on estimates from Gupta et al. (2022).

5 Housing liquidity, welfare, and spatial asset pricing

So far, we have established that spatial variation in travel costs leads to spatial variation in market tightness, which in turn creates spatial variation in housing liquidity. However, we also know from the literature on search markets that asset liquidity affects welfare and prices (see, for example, Duffie, Gârleanu, and Pedersen, 2005). Therefore, we now investigate to which extent housing liquidity affects welfare and housing prices across space. To do so, we conduct a counterfactual analysis, comparing our baseline model with two alternatives: a frictionless model without search, referred to as the *efficient model*, and a *constrained-efficient model*. Note that in our counterfactual analysis, we use the estimated structural parameters from the baseline model. By doing so, we assume that our baseline model, which matches the data on liquidity and prices with high precision, provides us with a reliable starting point.

Constrained-efficient model. First, following Krainer and LeRoy (2002), we implement a counterfactual constrained-efficient version of our model which is characterized by optimal buyer search behavior, but no strategic internalization of this search behavior in the price posting of sellers. We calculate reservation dividends $\varepsilon^{\text{CE}}(d^\Delta)$ that maximize steady-state welfare $\mathbb{W}(d^\Delta)$ at every distance $d^\Delta \in \mathcal{D}^\Delta$ defined as

$$\mathbb{W}(d^\Delta) = m(d^\Delta) \left(\mathbb{E}_\varepsilon \left[\varepsilon \mid \varepsilon \geq \varepsilon^{\text{CE}}(d^\Delta) \right] - \tau(d^\Delta) \right), \quad (20)$$

where $m(d^\Delta)$ denotes the probability of being matched.²⁴ The expected idiosyncratic dividend at distance d^Δ is $(\varepsilon^{\text{CE}}(d^\Delta) + \bar{\varepsilon})/2$, while the travel cost is $\tau(d^\Delta) = \mu \tilde{\tau}(d^\Delta)$. Agents transition from being unmatched to being matched with probability $(\bar{\varepsilon} - \varepsilon^{\text{CE}}(d^\Delta)) / (\bar{\varepsilon} - \underline{\varepsilon})$ and keep a housing unit with probability π . Therefore,

$$m(d^\Delta) = \pi m(d^\Delta) + \pi(1 - m(d^\Delta)) \frac{\bar{\varepsilon} - \varepsilon^{\text{CE}}(d^\Delta)}{\bar{\varepsilon} - \underline{\varepsilon}}, \quad (21)$$

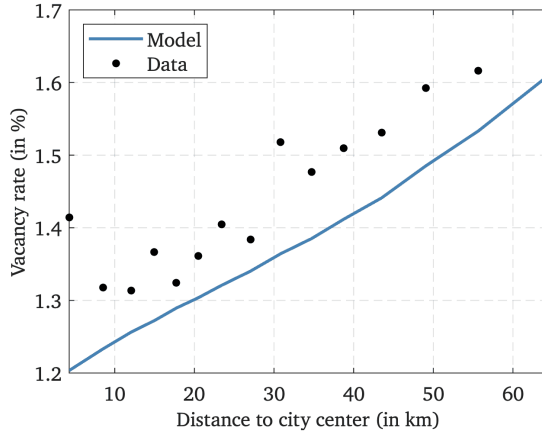
which allows us to calculate welfare in the constrained-efficient model as

$$\max_{\varepsilon^{\text{CE}}(d^\Delta)} \left(\frac{\pi \frac{\bar{\varepsilon} - \varepsilon^{\text{CE}}(d^\Delta)}{\bar{\varepsilon} - \underline{\varepsilon}}}{1 - \pi + \pi \frac{\bar{\varepsilon} - \varepsilon^{\text{CE}}(d^\Delta)}{\bar{\varepsilon} - \underline{\varepsilon}}} \right) \left(\frac{\varepsilon^{\text{CE}}(d^\Delta) + \bar{\varepsilon}}{2} - \mu \tilde{\tau}(d^\Delta) \right). \quad (22)$$

Search frictions imply a tradeoff: if the reservation dividend is high, the probability of being matched is low. The constrained-efficient reservation dividends are below $\bar{\varepsilon}$, since otherwise $m(d^\Delta) = 0$. Constrained-efficient illiquidity is hence larger than zero, which is analogous to a natural unemployment rate.

²⁴Note that we do not differentiate in notation between the German sample and the U.S. sample.

Figure 5: Spatial distribution of homeowner vacancy rate, U.S.: model vs. data



Notes: This figure shows the distribution of the homeowner vacancy rate, that is, the vacancy rate in the owner-occupied housing market, across distances to the city center from our baseline model and from the data. The model vacancy rates are calculated as defined via the probability of being matched, defined in (21). The data points are calculated using the ZIP-Code level yearly American Community Survey data from 2012–2023 introduced in Internet Appendix A.2, using the main specification of Regression (1).

The counterpart of $m(d^\Delta)$ is the steady-state vacancy rate $1 - m(d^\Delta)$. Our baseline model correctly predicts the level as well as the spatial variation in vacancy rates (none of which were targeted) for the United States, which we demonstrate in Figure 5.

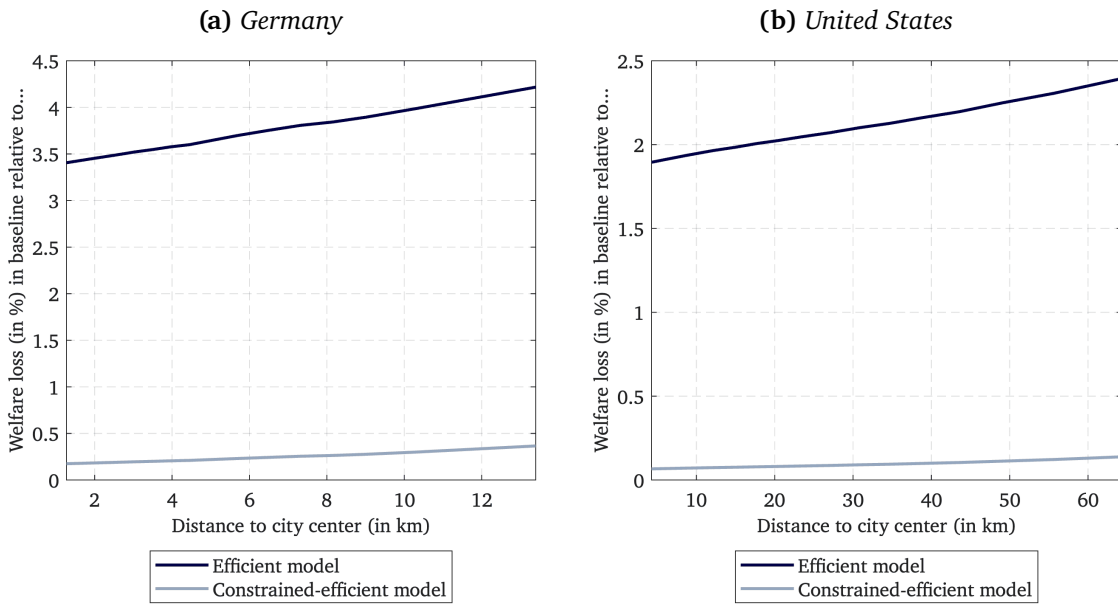
Efficient model. In a fully efficient version of the model, matches happen instantaneously and the time on the market is zero everywhere. This translates to $m(d^\Delta) = 1$ at every distance to the city center, such that there are no vacancies. Similarly, every agent can move directly into the housing unit they prefer best. Hence, with the definition from (20), welfare in the efficient model version at distance d^Δ is given by $\bar{\varepsilon} - \mu \tilde{\tau}(d^\Delta)$.

Welfare comparison. We calculate the spatial distributions of welfare, as defined in (20), in the two counterfactual model versions and compare them to the one in the baseline model in Figure 6. First, notice that search frictions cause large welfare losses.

Compared to the *efficient* model which abstracts from search frictions entirely, welfare losses in the baseline model are on average 3.7% in Germany and 2.1% in the United States, hence 3% on average across the two countries. In Internet Appendix J.3, we

document that the average welfare loss measured relative to housing prices amounts to 2% in Germany and to 1% in the United States, hence 1.5% on average across the two countries. These results are comparable to estimated welfare losses due to frictional illiquidity in other search markets, such as municipal bond markets (see Hugonnier, Lester, and Weill, 2019). The smaller average welfare loss in the U.S. arises due to a more liquid housing market, which implies that the baseline model is closer to the efficient model. The welfare loss relative to the *constrained-efficient* model is rather small, reaching up to 0.4% in Germany and 0.3% in the United States. The difference in the baseline model compared to the constrained-efficient model lies in the price posting of sellers. Hence, according to our findings, the interaction of pricing power and search frictions in the housing market causes small welfare losses.

Figure 6: Spatial welfare loss distributions



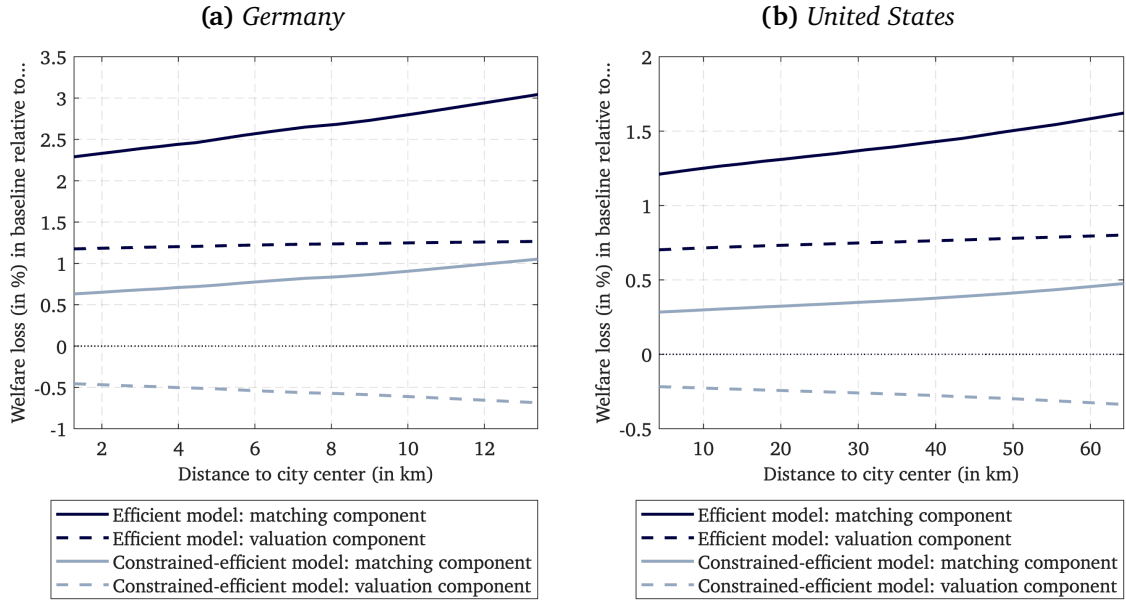
Notes: This figure shows our calculated welfare losses in the baseline model relative to the efficient model and the constrained-efficient model, for each distance to the city center. Welfare is calculated as defined in (20).

Next, we examine spatial patterns in welfare losses. As shown in Figure 6, welfare losses increase with distance to the city center. In Germany, agents in the city center

lose 3.4%, whereas agents in the outskirts lose 4.2% in the baseline model relative to the efficient model. The difference between these welfare losses amounts to one-fifth of the average welfare loss at 3.7%. In the United States, spatial differences in welfare losses are slightly larger (1.9% in the center and 2.4% in the outskirts) and amount to one-quarter of the average welfare loss at 2.1%. A welfare calculation that does not take into account these spatial differences would miss a fundamental and large factor.

Welfare decomposition. We further decompose welfare losses into those from lower probability of being matched (which we refer to as the “matching component”) and those from lower average dividends (which we refer to as the “valuation component”). This decomposition is shown in Figure 7. The matching component is dominant – our welfare results are hence mostly driven by vacancies. Particularly low matching probabilities in the outskirts imply particularly large welfare losses.

Figure 7: Spatial welfare loss distributions: decomposition



Notes: This figure shows our calculated welfare losses in the baseline model relative to the efficient model and the constrained-efficient model, for each distance to the city center. Welfare is calculated as defined in (20) and decomposed into the percentage change in the first factor $m(d^\Delta)$ (“matching component”) and the second factor $\mathbb{E}_\varepsilon [\varepsilon | \varepsilon \geq \varepsilon^{CE}(d^\Delta)] - \tau(d^\Delta)$ (“valuation component”).

In the efficient model, all agents obtain their maximum idiosyncratic dividend with zero search. However, in the constrained-efficient model, lower vacancies come at the cost of lower idiosyncratic valuations. In this model, to achieve a lower vacancy rate, agents have to accept lower idiosyncratic dividends. Hence, the valuation component is *negative*. It becomes more negative with distance to the city center, as vacancies are more strongly reduced.

Sensitivity analysis. We provide a sensitivity analysis for these results in Internet Appendix J.4. We find that, first, bootstrapped 95% confidence intervals for welfare losses are quite narrow and second, the welfare loss estimates are robust to alternative choices for the housing match persistence and the discount factor. As we would expect, when we decrease the match persistence, welfare losses become somewhat larger, since agents have to go into the search process more often. Choosing a different discount factor has a negligible effect on the welfare loss estimates.

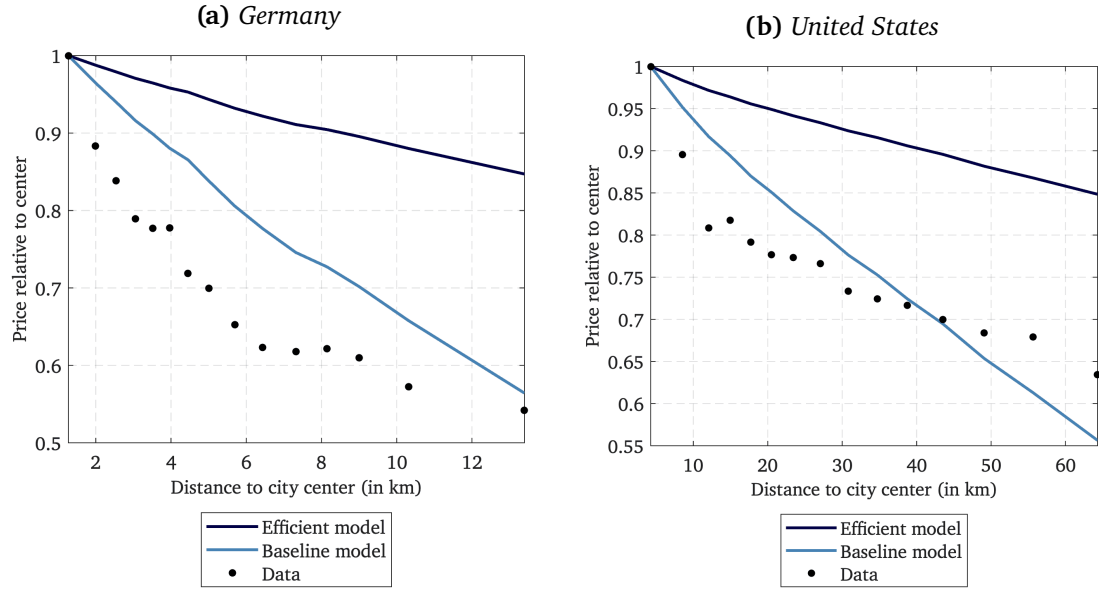
Spatial price gradient comparison. Next, we examine the impact of frictional illiquidity on housing prices. Our constrained-efficient model does not involve prices and thus does not allow for such an analysis. Our efficient counterfactual model describes a frictionless market in which the spatial price gradient merely reflects travel costs.

We scale up the daily travel cost $\tau(d^\Delta) = \mu \tilde{\tau}(d^\Delta)$ to an expected lifetime travel cost (where “lifetime” refers to the lifetime of a match) with factor $\beta/(1 - \pi\beta)$, assuming that when an agent becomes unmatched, they immediately find a new match. Then, we have that for the i -th distance to the city center with $i \geq 2$,

$$p^E(d_i^\Delta) - p^E(d_{i-1}^\Delta) = -\frac{\beta}{1 - \pi\beta} (\mu \tilde{\tau}(d_i^\Delta) - \mu \tilde{\tau}(d_{i-1}^\Delta)), \quad (23)$$

where $p^E(d^\Delta)$ is the price in the efficient model at distance d^Δ . This equation only considers spatial price differences, not levels. For comparison to the baseline model prices, we set the price in the city center to 1 and scale the spatial differences in (23) by the price in the distance bin closest to the city center from the baseline model.

Figure 8: Comparison of spatial price gradients



Notes: This figure shows housing prices in the baseline model, the efficient model, and the data, for each distance to the city center. For the data points and the baseline model, all prices are normalized by the price in the first distance bin. For the efficient model, the price in the first distance bin is set to 1 and the spatial differences in prices thereafter, as defined in (23), are normalized by the price in the first distance bin from the baseline model. The data points are calculated using the main specification of Regression (1), as displayed in Figure 1.

We plot the resulting normalized spatial price distributions in Figure 8. U.S. housing prices decrease by 0.71% per kilometer in the baseline model, but only by 0.24% per kilometer in the efficient model. For Germany, prices decrease by 3.61% per kilometer in the baseline model, but only by 1.27% per kilometer in the efficient model. Spatial price distortions due to inefficient illiquidity are therefore sizable. For both Germany and the United States, our model implies that the spatial gradient becomes about 3 times as large due to search frictions and the associated spatial differences in housing liquidity.

6 Conclusion

In this paper, we build novel spatial datasets from Germany and the United States to demonstrate that housing market liquidity declines with distance to the city center. We develop a spatial search model of the housing market and show that higher travel costs to the city center lead to lower market tightness, which in turn reduces liquidity and depresses sales prices. Moreover, we structurally estimate the extent to which search frictions shape the spatial distribution of welfare and housing prices. We conclude that accounting for search frictions and their impact on housing prices is essential for a more realistic perspective on housing markets. Our findings can also inform research on the link between liquidity and the valuation of real assets. In particular, given the recent “great rotation” (Koijen, Shah, and Van Nieuwerburgh, 2025) toward infrequently traded, heterogeneous private and real assets, our results can help future research identify systematic variation in the pricing of such assets.

References

Ahlfeldt, Gabriel M., Stephen J. Redding, Daniel M. Sturm, and Nikolaus Wolf (2015). “The economics of density: Evidence from the Berlin Wall”. In: *Econometrica* 83(6), pp. 2127–2189.

Albouy, David, Gabriel Ehrlich, and Minchul Shin (2018). “Metropolitan land values”. In: *Review of Economics and Statistics* 100(3), pp. 454–466.

Alonso, William (1964). *Location and land use: Toward a general theory of land rent*. Harvard University Press.

Amaral, Francisco, Martin Dohmen, Moritz Schularick, and Jonas Zdrzalek (2023). “German Real Estate Index (GREIX)”. ECONtribute Discussion Paper No. 231.

Andor, Mark A., Andreas Gerster, Kenneth T. Gillingham, and Marco Horvath (2020). “Running a car costs much more than people think: Stalling the uptake of green travel”. In: *Nature* 580, pp. 453–455.

Badarinza, Cristian, Vimal Balasubramaniam, and Tarun Ramadorai (2024). “In search of the matching function in the housing market”. Working paper.

Badarinza, Cristian and Tarun Ramadorai (2018). “Home away from home? Foreign demand and London house prices”. In: *Journal of Financial Economics* 130(3), pp. 532–555.

Biljanovska, Nina and Giovanni Dell’Ariccia (2024). “Flattening the curve and the flight of the rich: Pandemic-induced shifts in US and European housing markets”. CEPR Discussion Paper No. 18824.

Bruneel-Zupanc, Christophe, Guillaume Chapelle, Jean-Benoît Eyméoud, and Etienne Wasmer (2025). “Housing prices propagation: A theory of spatial interactions”. In: *European Economic Review* 184:105252.

Burrows, Michael, Charlynn Burd, and Brian McKenzie (2021). “Commuting by public transportation in the United States: 2019”. American Community Survey Report No. ACS-48.

Carrillo, Paul E. (2012). “An empirical stationary equilibrium search model of the housing market”. In: *International Economic Review* 53(1), pp. 203–234.

Cattaneo, Matias D., Richard K. Crump, Max H. Farrell, and Yingjie Feng (2024). “On binscatter”. In: *American Economic Review* 114(5), pp. 1488–1514.

Chetty, Raj, John N. Friedman, Nathaniel Hendren, Maggie R. Jones, and Sonya R. Porter (2025). “The Opportunity Atlas: Mapping the childhood roots of social mobility”. In: *American Economic Review* 116(1), pp. 1–51.

Delventhal, Matthew J. and Andrii Parkhomenko (2024). “Spatial implications of telecommuting”. Working paper.

Duffie, Darrell, Nicolae Gârleanu, and Lasse H. Pedersen (2005). “Over-the-counter markets”. In: *Econometrica* 73(6), pp. 1815–1847.

Duranton, Gilles and Diego Puga (2015). “Chapter 8 - Urban land use”. In: *Handbook of Regional and Urban Economics*. Ed. by Gilles Duranton, J. Vernon Henderson, and William C. Strange. Vol. 5. Elsevier, pp. 467–560.

Favilukis, Jack, Pierre Mabille, and Stijn Van Nieuwerburgh (2023). "Affordable housing and city welfare". In: *The Review of Economic Studies* 90(1), pp. 293–330.

Garriga, Carlos and Aaron Hedlund (2020). "Mortgage debt, consumption, and illiquid housing markets in the Great Recession". In: *American Economic Review* 110(6), pp. 1603–1634.

Gerardi, Kristopher, Franklin Qian, and David Zhang (2025). "Mortgage lock-in, lifecycle migration, and the welfare effects of housing market liquidity". Working paper.

Ghent, Andra C (2021). "What's wrong with Pittsburgh? Delegated investors and liquidity concentration". In: *Journal of Financial Economics* 139(2), pp. 337–358.

Glaeser, Edward L. and Joseph Gyourko (2008). "Arbitrage in housing markets". Harvard Institute of Economic Research Discussion Paper No. 2151.

Gupta, Arpit, Vrinda Mittal, Jonas Peeters, and Stijn Van Nieuwerburgh (2022). "Flattening the curve: Pandemic-induced revaluation of urban real estate". In: *Journal of Financial Economics* 146(2), pp. 594–636.

Guren, Adam M. (2018). "House price momentum and strategic complementarity". In: *Journal of Political Economy* 126(3), pp. 1172–1218.

Guren, Adam M. and Timothy J. McQuade (2020). "How do foreclosures exacerbate housing downturns?" In: *The Review of Economic Studies* 87(3), pp. 1331–1364.

Han, Lu and William C. Strange (2015). "Chapter 13 - The microstructure of housing markets: Search, bargaining, and brokerage". In: *Handbook of Regional and Urban Economics*. Ed. by Gilles Duranton, J. Vernon Henderson, and William C. Strange. Vol. 5. Elsevier, pp. 813–886.

Harris, Nathaniel (2024). "Measuring aggregate land values using individual city land value gradients". In: *Regional Science and Urban Economics* 106:103995.

Hugonnier, Julien, Benjamin Lester, and Pierre-Olivier Weill (2019). "Frictional intermediation in over-the-counter markets". In: *The Review of Economic Studies* 87(3), pp. 1432–1469.

Jiang, Erica Xuewei, Nadia Kotova, and Anthony Lee Zhang (2024). "Liquidity in residential real estate markets". Working paper.

Koijen, Ralph, Neel Shah, and Stijn Van Nieuwerburgh (2025). "The commercial real estate ecosystem". CEPR Discussion Paper No. 20053.

Krainer, John (2001). "A theory of liquidity in residential real estate markets". In: *Journal of Urban Economics* 49(1), pp. 32–53.

Krainer, John and Stephen F. LeRoy (2002). "Equilibrium valuation of illiquid assets". In: *Economic Theory* 19(2), pp. 223–242.

Lagos, Ricardo and Guillaume Rocheteau (2009). "Liquidity in asset markets with search frictions". In: *Econometrica* 77(2), pp. 403–426.

Liotta, Charlotte, Vincent Viguié, and Quentin Lepetit (2022). "Testing the monocentric standard urban model in a global sample of cities". In: *Regional Science and Urban Economics* 97:103832.

Mills, Edwin S. (1967). "An aggregative model of resource allocation in a metropolitan area". In: *The American Economic Review* 57(2), pp. 197–210.

Moody, Joanna, Elizabeth Farr, Marisa Papagelis, and David R. Keith (2021). "The value of car ownership and use in the United States". In: *Nature Sustainability* 4, pp. 769–774.

Moreno-Monroy, Ana I., Marcello Schiavina, and Paolo Veneri (2021). "Metropolitan areas in the world. Delineation and population trends". In: *Journal of Urban Economics* 125:103242.

Muth, Richard F. (1969). *Cities and housing – The spatial pattern of urban residential land use*. University of Chicago Press.

Nechyba, Thomas J. and Randall P. Walsh (2004). "Urban sprawl". In: *Journal of Economic Perspectives* 18(4), pp. 177–200.

Ngai, L. Rachel and Silvana Tenreyro (2014). "Hot and cold seasons in the housing market". In: *American Economic Review* 104(12), pp. 3991–4026.

Piazzesi, Monika, Martin Schneider, and Johannes Stroebel (2020). "Segmented housing search". In: *American Economic Review* 110(3), pp. 720–759.

Rogerson, Richard, Robert Shimer, and Randall Wright (2005). "Search-theoretic models of the labor market: A survey". In: *Journal of Economic Literature* 43(4), pp. 959–988.

U.S. Census Bureau (2012–2023a). "Median income in the past 12 months". 2012–2023 American Community Survey 5-year estimates.

U.S. Census Bureau (2012–2023b). "Physical housing characteristics for occupied housing units". 2012–2023 American Community Survey 5-year estimates.

U.S. Census Bureau (2012–2023c). “Selected housing characteristics”. 2012–2023 American Community Survey 5-year estimates.

U.S. Census Bureau (2012–2023d). “Travel time to work”. 2012–2023 American Community Survey 5-year and 1-year estimates.

Vanhapelto, Tuuli and Thierry Magnac (2024). “Housing search and liquidity in spatial equilibrium”. TSE Working Paper No. 24-1596.

Internet Appendix for

“Spatial Distribution of Housing Liquidity”

A Data sources and cleaning procedures

In this section, we present in detail the steps that we took to prepare the data for the empirical analysis.

A.1 German data

Matching algorithm. We start the algorithm by matching each transaction to potential ads based on location. This gives us a pool of potential matching ads for each transaction. We then follow a series of steps to eliminate those ads that are unrealistic matches. First, we exclude advertisements that were published after the contract date and ads that were removed more than one year before the contract date. The algorithm proceeds by matching observations with complete addresses, that is, addresses which include street names and house numbers. However, for apartments, having information on solely the street name and the house number is insufficient for a successful match, as there may be multiple apartment transactions related to the same building. If that is the case, the algorithm excludes ads based on property characteristics in the following order:

1. The living area differs by more than 10%.
2. The floor number differs by more than 2.
3. The building year differs by more than 5 years.

We choose these property characteristics since they have the lowest number of missing values from the set of variables that are covered by both datasets and select numeric

values for the criteria that give us reasonable buffers for measurement errors due to incorrect user inputs. If, after this process, we still have more than one potential listing for a particular transaction, we continue to eliminate listings in the following sequential steps until we have only one listing for a particular transaction:

1. We keep the ad(s) that minimize(s) the distance to the transaction in terms of living area.
2. We keep the ad(s) that minimize(s) the distance in terms of floor number.
3. We keep the ad(s) that minimize(s) the spread between the listing price and the sales price.
4. We eliminate listings that were taken out more than three months prior to the actual transaction.

If we still have multiple matches after these steps, we drop them because we have no way of identifying the correct match.

Next, we check if we have assigned an ad to multiple transactions. If this is the case, we keep only the most likely match following the steps described above. When we match based on the building's exact address, we do not exclude matches with different building years. Matching by address is sufficient to identify a building, and typically the building year is the same for all flats within a building. When this is not the case, we attribute the different building years to measurement error, that is, incorrect user-specified information on the advertisement websites. We match the transactions which do not have entries with complete addresses via the same process as for those with complete addresses, but condition sequentially on the following geographical objects: street name, ZIP Code, and neighborhood (*Stadtteil*), until we have a unique match. If there is no unique match, we drop the observation.

On average, we match about 30% of the transactions across cities. The relatively low proportion of transactions that are matched is largely due to overmatching, that is, the fact that in many cases we end up with more than one potential advertisement for a given transaction after the algorithm has applied all criteria. In Table A1, we provide further information on the matched observations by city.

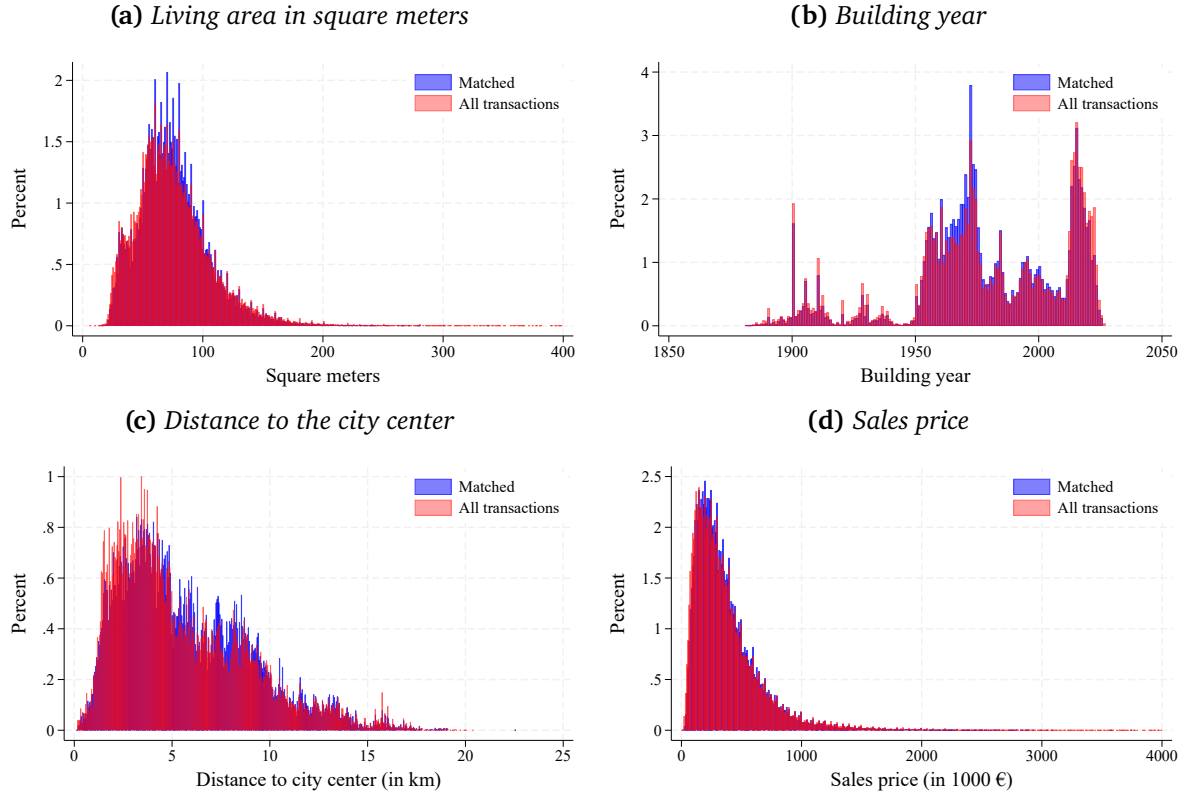
Table A1: *Summary statistics: matched dataset*

City	# Transactions	# Ads	# Matched	Avg. sales price (€)	Avg. asking price (€)
Hamburg	80,157	78,342	20,418	356,541	358,604
Munich	57,629	112,135	25,966	493,312	495,710
Cologne	41,338	46,349	14,273	237,462	254,164
Frankfurt	35,493	39,083	12,035	388,445	405,843
Duesseldorf	35,581	34,669	11,611	288,863	303,802

Notes: This table reports summary statistics about the matched transaction and advertisement data for the period 2012–2024.

We show that the matched sample is not biased along several important characteristics of the transacted properties in Figure A1. We plot the distributions from the matched sample and the universe of transactions, with all cities pooled together, of the variables living area, building year, distance to the city center, and sales price. For each of these variables, the two distributions mostly overlap, which indicates that the matched sample is representative of the universe of transactions.

Figure A1: Matched sample and universe of transactions, all German cities pooled



Notes: These plots show histograms of different variables in the matched sample and the universe of transactions. The y-axis measures the frequency in percent of a given value on the x-axis in the respective sample.

Data preparation. We transform several variables to prepare them for regression analysis. We control for the following variables: living area in m^2 , living area squared, number of rooms, year of construction, “Altbau” or not, “Neubau” or not, physical condition of the building, whether the apartment is in the upper floor of the house or not, whether the apartment is rented out or not, type of heating, source of heating, whether the apartment has a fitted kitchen or not, whether the apartment has an open kitchen or not, whether the bathroom has a shower, whether the bathroom has a bathtub, whether the apartment has a terrace or balcony, whether the apartment has a basement, whether the apartment has a garden, and the number of parking spaces. These control variables are identical for the regressions with rental housing.

We control for the age of the properties by creating a categorical variable that di-

vides the observations into different construction periods. We follow the commonly used categories introduced by the official German appraisers. In particular, we construct the following categories: pre-1950, 1950–1977, 1978–1990, 1990–2005, and post-2005. We use a categorical variable rather than a continuous variable for the building year of the property because the relationship between age and price or liquidity is highly non-linear in the case of the German housing market, as shown in Amaral et al. (2023). In addition, we also include a category for properties that are being occupied for the first time and another category that identifies properties where construction is not yet complete. We divide the heating type of each home into four different categories. We define “brown” dwellings as those that consume energy produced by oil or coal, or use space heating and tile stove heating. We define “standard” dwellings as those that consume energy produced by gas and use central heating. We define “green” properties as those where the energy comes from solar, heat pumps or pellets, or use district heating or CHP. We also use an “other” category, taken directly from the dataset, which includes other energy sources. We use a categorical variable to consider the quality of the furnishings and interiors of the property and a categorical variable to categorize the quality of the construction of the building, both of which are provided directly in the dataset. We create a categorical variable to control for the number of rooms in the property. The variable has four categories: 1 room, 2 rooms, 3 rooms, and 4 or more rooms. We also control for the number of floors on which the apartment is located and the total number of floors in the building where the apartment is located.

A.2 U.S. data

Redfin is both a real estate brokerage and an online platform. Redfin typically has direct access to data from local multiple listing services (MLS) and adds those listings to the platform. However, unlike the well-known Zillow platform (which we cannot use due to a lack of data availability for liquidity variables at the ZIP-Code level), Redfin has a low coverage of for-sale-by-owner (FSBO) listings because Redfin does not allow sellers to post listings themselves. Since FSBOs account for only about 6% of all home sales in the U.S. (see: National Association of Realtors), by including the majority of MLS listings, Redfin covers most of the market. We clean the data by dropping all ZIP Codes for which the time on the market estimates are, on average, based on less than 10 observations and there is one month with less than 5 observations. For a robustness analysis, we collect data on time on the market from another online platform, Realtor.com, which covers most local MLS in the United States, and compare these results to our baseline results. We estimate the time on the market gradient using both datasets. Because the Realtor.com platform only provides data for an “all residential” category, we cannot perform the comparison for different segments separately. Moreover, the dataset from Realtor.com only starts in 2016, so we limit our analysis to the period between 2016 and 2023. In Table A2, we provide outputs for regressions of time on the market on distance to the city center using both the Redfin and Realtor.com data, with very similar results.

For our U.S. control variables on housing characteristics and demographic composition, we use yearly data from the American Community Survey 5-year estimates at the ZIP-Code level from 2012 to 2023. The variables are listed in Section 3.1. Lastly, for the measure of U.S. neighborhood quality, we use data from Chetty et al. (2025).

We calculate ZIP-Code-level averages of the fraction of children born between 1978 and 1983 who were incarcerated on April 1st, 2010 (*jail_pooled_pooled_mean*).

Table A2: *Time on the market and distance to the city center in the U.S. (2016–2023)*

	(1) Redfin	(2) Realtor.com	(3) Redfin	(4) Realtor.com
Distance to center (in km)	0.01** (0.005)	0.02*** (0.002)	0.03*** (0.004)	0.03*** (0.002)
MSA × Year-Month FE	✓	✓	✓	✓
State FE	✓	✓	✓	✓
Property characteristics			✓	✓
<i>N</i>	503,101	503,101	503,101	503,101
ZIP Codes	5,666	5,666	5,666	5,666
Adj. <i>R</i> ²	0.37	0.34	0.42	0.37
Mean(TOM)	6.36	7.32	6.36	7.32

Notes: This table shows results for regressions of time on the market on the distance to the city center as specified in Regression (1). Time on the market is measured in weeks. Standard errors (in parentheses) are clustered at the MSA-year level. Median income and property characteristics are control variables. The underlying data bundles all residential housing types into one category. * : $p < 0.1$; ** : $p < 0.05$; *** : $p < 0.01$.

B Additional summary statistics

B.1 German cities

Table B1: Summary statistics: time on the market and prices in German cities (2012–2024)

City	Time on the market in weeks				Sales price in €1,000				N
	Mean	SD	P25	P75	Mean	SD	P25	P75	
Hamburg	15.13	17.59	3.10	20.40	357	267	188	437	20,418
Munich	12.34	15.53	2.30	16.30	493	308	285	611	25,966
Cologne	12.42	16.19	2.30	16.20	237	153	130	300	14,273
Frankfurt	15.04	18.23	2.60	20.20	388	253	210	499	12,035
Duesseldorf	12.99	16.28	2.30	17.00	289	225	137	365	11,611

Notes: This table reports summary statistics of time on the market and sales prices by city for the period 2012–2024. All estimates are based on the matched dataset. N is the total number of transactions in the respective matched dataset.

B.2 U.S. cities

Table B2: Summary statistics: time on the market and prices in U.S. cities (2012–2023)

MSA	Time on the market in weeks				Sales price in \$1000				Nr. ZIP Codes	N
	Mean	SD	P25	P75	Mean	SD	P25	P75		
Atlanta-Sandy Springs-Alpharetta, GA	6.12	3.53	3.57	8.00	293	197	161	368	156	22,125
Austin-Round Rock-Georgetown, TX	5.71	4.39	2.86	7.43	415	264	240	505	68	9,790
Baltimore-Columbia-Towson, MD	7.26	5.61	3.64	9.43	404	177	280	495	117	16,547
Boston-Cambridge-Newton, MA-NH	6.90	6.32	2.57	10.71	609	373	372	705	211	25,239
Charlotte-Concord-Gastonia, NC-SC	10.36	6.25	6.29	12.86	266	178	156	324	94	12,173
Chicago-Naperville-Elgin, IL-IN-WI	7.87	4.77	4.86	9.86	311	243	170	374	285	24,336
Cincinnati, OH-KY-IN	10.47	7.11	6.57	13.43	193	104	122	240	115	16,287
Dallas-Fort Worth-Arlington, TX	5.36	3.06	3.29	6.57	291	207	169	352	208	16,691
Denver-Aurora-Lakewood, CO	3.22	3.09	1.14	4.14	461	197	320	565	98	14,056
Detroit-Warren-Dearborn, MI	4.66	3.36	2.36	6.00	225	130	129	300	174	13,375
Houston-The Woodlands-Sugar Land, TX	5.80	4.01	3.00	7.57	270	208	155	310	182	26,188
Las Vegas-Henderson-Paradise, NV	8.59	3.89	5.93	10.86	293	128	200	366	57	8,208
Los Angeles-Long Beach-Anaheim, CA	5.72	3.19	3.86	6.86	851	529	505	999	315	29,210
Miami-Fort Lauderdale-Pompano Beach, FL	9.31	5.00	6.43	10.43	509	402	284	575	126	7,633
Minneapolis-St. Paul-Bloomington, MN-WI	6.09	4.58	3.00	7.86	320	147	222	385	168	24,188
New York-Newark-Jersey City, NY-NJ-PA	10.55	8.07	5.29	13.57	613	374	378	728	613	21,050
Orlando-Kissimmee-Sanford, FL	7.25	5.87	3.14	10.07	281	142	180	350	77	10,799
Philadelphia-Camden-Wilmington, PA-NJ-DE-MD	7.89	5.85	4.00	10.29	323	188	190	402	256	10,865
Phoenix-Mesa-Chandler, AZ	6.48	2.76	4.79	7.57	344	220	211	418	123	17,691
Pittsburgh, PA	13.53	7.12	8.57	16.43	177	109	104	222	146	20,752
Portland-Vancouver-Hillsboro, OR-WA	4.75	5.00	1.57	6.07	431	184	300	528	103	14,540
Riverside-San Bernardino-Ontario, CA	6.19	3.44	4.00	7.57	390	180	260	488	92	13,156
Sacramento-Roseville-Folsom, CA	3.57	2.72	1.71	4.57	424	181	295	526	74	10,654
San Antonio-New Braunfels, TX	7.77	4.86	4.71	9.50	234	122	150	300	84	12,084
San Diego-Chula Vista-Carlsbad, CA	4.27	4.15	2.14	5.07	783	446	490	906	79	11,279
San Francisco-Oakland-Berkeley, CA	2.71	1.56	1.86	3.14	1,111	585	672	1,450	128	8,344
Seattle-Tacoma-Bellevue, WA	3.19	3.18	1.00	4.29	591	374	335	726	136	11,382
St. Louis, MO-IL	9.20	7.64	4.93	11.57	200	142	111	245	167	19,190
Tampa-St. Petersburg-Clearwater, FL	6.21	4.48	2.64	9.00	292	218	168	357	12	1,728

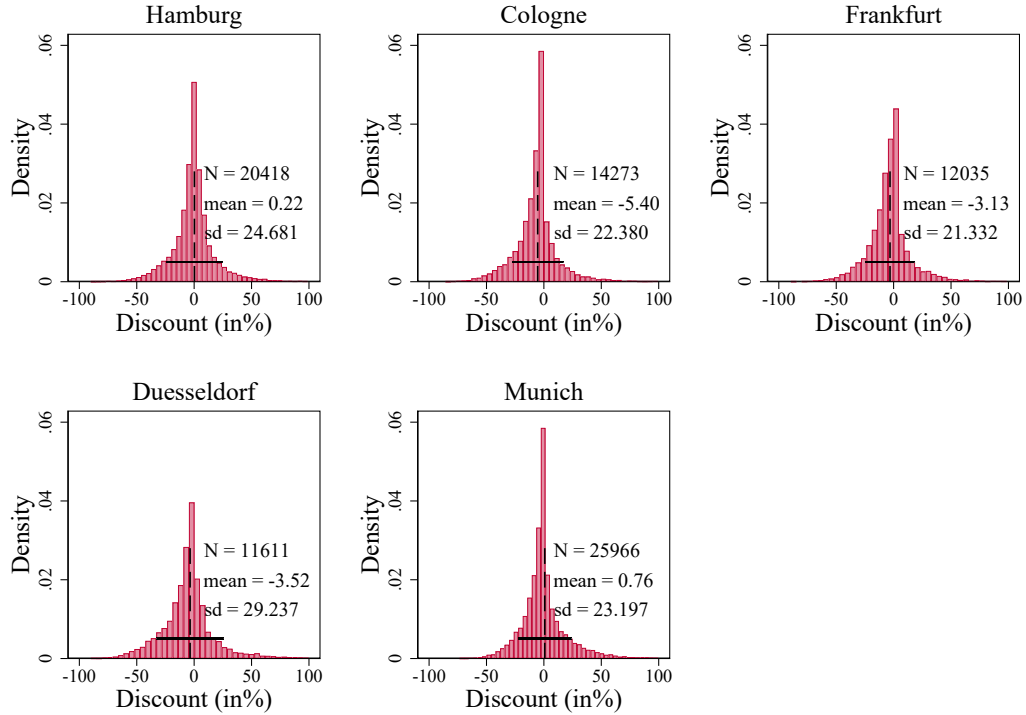
Notes: This table reports summary statistics of time on the market and sales prices by MSA for the period 2012–2023. N is the number of ZIP-Code-year-month observations in the respective subset of data.

B.3 Asking price discount

In Figure B1, we plot a histogram of the asking price discount for our matched German sample by city. The majority of transactions exhibit a negative discount, that is, properties typically sell below their asking prices. The distribution resembles a normal distribution but has a more positive skew and thinner tails. On average, a property is transacted at a sales price below its asking price. There is a clear bunching at an asking price discount of 0%. This finding has been documented for other countries and reflects that the asking price is a relevant anchor for the bargaining process in housing markets, as it is a partial

commitment for the seller (Han and Strange, 2016). In Table B3, we present results for regressions of the asking price discount on distance to the city center. For all specifications, there is a negative and highly significant coefficient on the distance to the city center.

Figure B1: Histograms of asking price discount (2012–2024)



Notes: These plots show histograms for the asking price discount in our matched data set.

Table B3: Asking price discount and distance to the city center, Germany (2012–2024)

	(1) APD	(2) APD	(3) APD	(4) APD	(5) APD	(6) APD
Distance to center (in km)	-0.15*** (0.04)	-0.16*** (0.03)	-0.11** (0.05)			
Travel time to center (in min)				-0.07*** (0.02)	-0.07*** (0.01)	-0.03 (0.03)
City \times Year-quarter FE	✓	✓	✓	✓	✓	✓
Property characteristics		✓	✓		✓	✓
Borough FE			✓			✓
<i>N</i>	84,292	84,292	84,292	84,292	84,292	84,292
Adj. <i>R</i> ²	0.02	0.05	0.05	0.02	0.05	0.05
Mean(APD)	-1.56	-1.56	-1.56	-1.56	-1.56	-1.56

Notes: This table shows results for regressions of the asking price discount on the distance to the city center as specified in Regression (1). “APD” refers to the asking price discount in percent. Standard errors (in parentheses) are clustered at the city-year level. The list of property characteristics controls is available in Internet Appendix A.1. * : $p < 0.1$; ** : $p < 0.05$; *** : $p < 0.01$.

Table B4: Asking price discount and distance to the city center, U.S. (2012–2023)

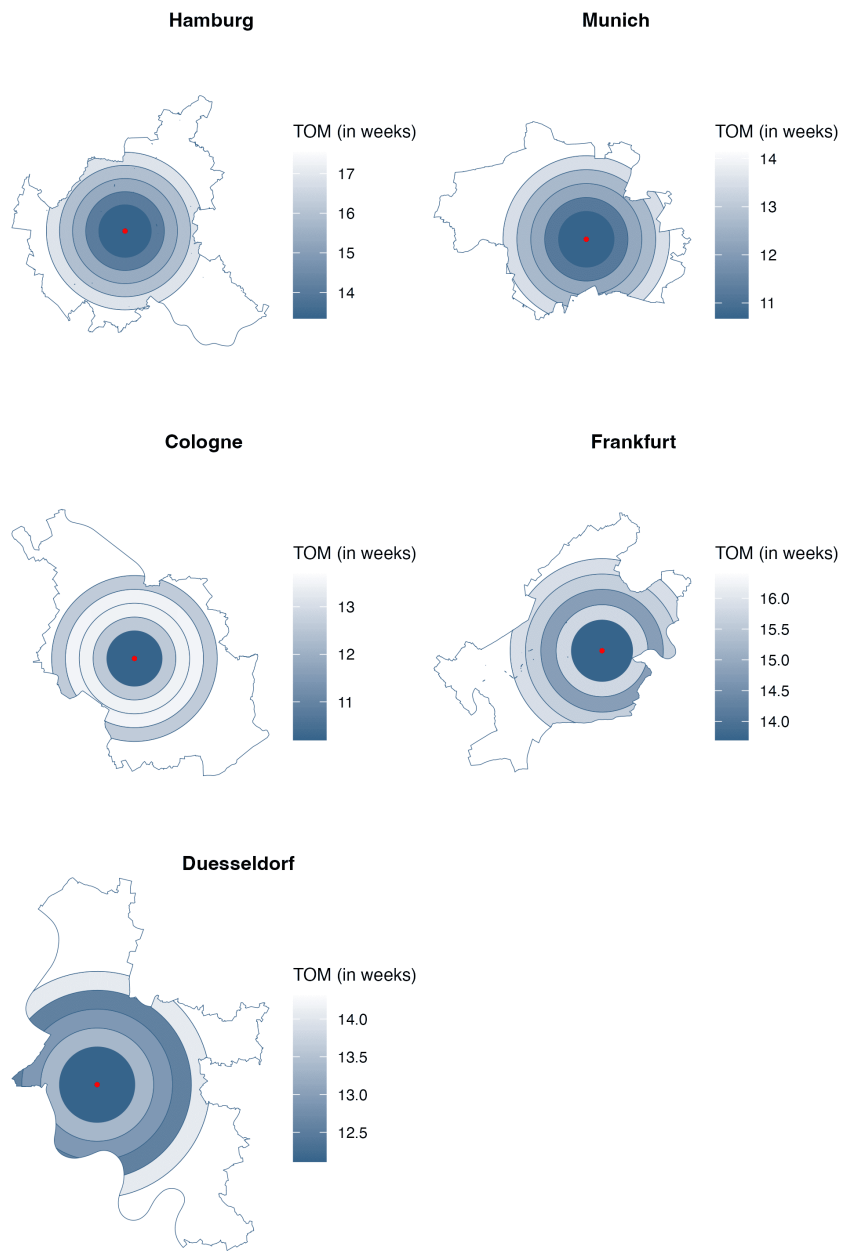
	(1) APD	(2) APD	(3) APD	(4) APD	(5) APD	(6) APD
Distance to center (in km)	-0.01*** (0.002)	-0.03*** (0.002)	-0.02*** (0.003)			
Travel time to center (in min)				-0.01*** (0.002)	-0.03*** (0.002)	-0.02*** (0.003)
MSA \times Year-month FE	✓	✓	✓	✓	✓	✓
State FE	✓	✓	✓	✓	✓	✓
Property characteristics		✓	✓		✓	✓
Demographic controls			✓			✓
<i>N</i>	608,986	607,411	607,411	608,986	607,411	607,411
ZIP Codes	4,464	4,463	4,463	4,464	4,463	4,463
Adj. <i>R</i> ²	0.53	0.55	0.56	0.53	0.55	0.56
Mean(APD)	-1.29	-1.28	-1.28	-1.29	-1.28	-1.28

Notes: This table displays the output of Regression (1) on asking price discount (APD), measured in percent of the asking price. The regressions are based on data for single-family houses for the 30 largest MSAs in the U.S. in the period between 2012–2023. Standard errors (in parentheses) are clustered at the MSA-year level. * : $p < 0.1$; ** : $p < 0.05$; *** : $p < 0.01$.

C Additional empirical results

C.1 Spatial distribution of time on the market in German cities

Figure C1: Time on the market across space, Germany (2012–2024)



Notes: These maps display the spatial distribution of time on the market (TOM) by city from our matched German dataset, averaged within rings around city centers. Shapefile data sources:

Hamburg: <https://suche.transparenz.hamburg.de/dataset/stadtteil-profile-hamburg10>.

Munich: https://opendata.muenchen.de/dataset/vablock_stadtbezirke_opendata.

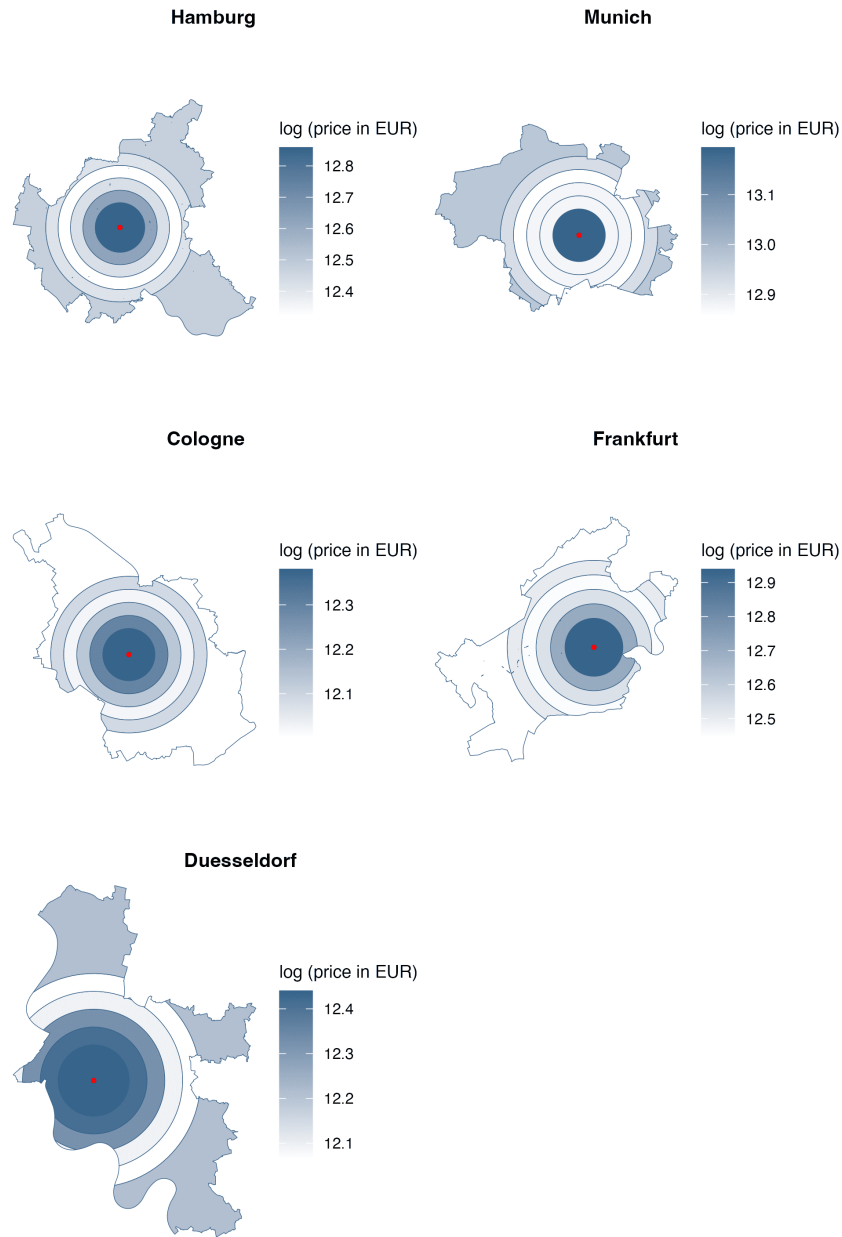
Cologne: <https://offenedaten-koeln.de/dataset/stadtbezirke-koeln>.

Frankfurt: https://geowebdienste.frankfurt.de/WFS_Stadtgebietsgliederung.

Düsseldorf: <https://opendata.duesseldorf.de/dataset/stadtteilgrenzen-duesseldorf-2025>.

C.2 Spatial distribution of sales prices in German cities

Figure C2: Sales prices across space, Germany (2012–2024)



Notes: These maps display the spatial distribution of sales prices by city from our matched German dataset, averaged within rings around city centers. Shapefile data sources:

Hamburg: <https://suche.transparenz.hamburg.de/dataset/stadtteil-profile-hamburg10>.

Munich: https://opendata.muenchen.de/dataset/vablock_stadtbezirke_opendata.

Cologne: <https://offenedaten-koeln.de/dataset/stadtbezirke-koln>.

Frankfurt: https://geowebdienste.frankfurt.de/WFS_Stadtgebietsgliederung.

Düsseldorf: <https://opendata.duesseldorf.de/dataset/stadtteilgrenzen-duesseldorf-2025>.

C.3 Probability of sale

In the main text, we document that time on the market increases with distance to the city center. In this appendix, we translate this duration pattern into the probability that a given listing is sold. Because time on market is measured in weeks, we approximate the weekly probability of sale at location d using the reciprocal of the mean time on the market in that distance bin, $\hat{p}(d) = 1/\overline{\text{TOM}}(d)$. This mapping is motivated by a simple discrete-time sale process in which a listing sells each week with probability $p(d)$, implying an expected duration $E[T | d] = 1/p(d)$. In practice, the sample mean $\overline{\text{TOM}}(d)$ provides an empirical approximation to the expected duration $E[T | d]$ within each location bin, so its inverse yields a transparent, easily interpretable proxy for the probability of sale.

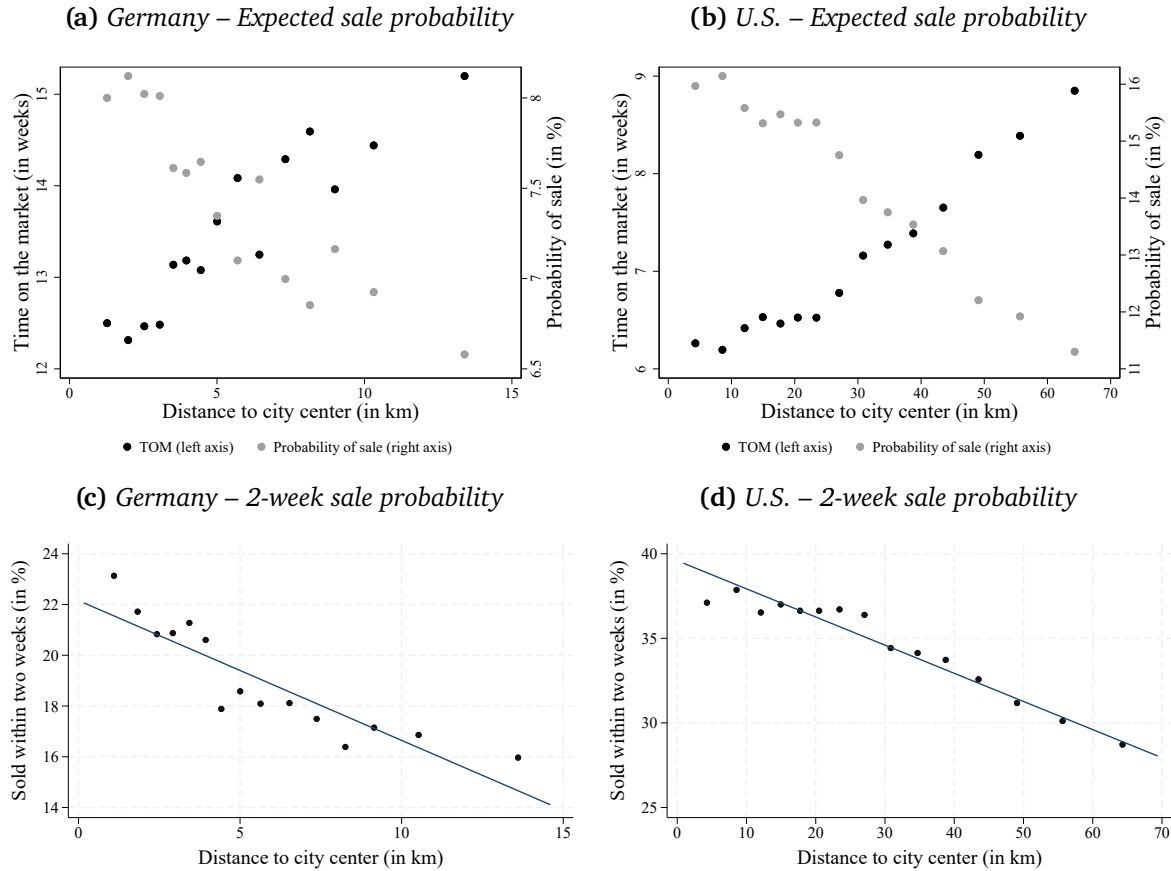
This approach implicitly assumes that all listings eventually sell, which is unlikely to hold exactly in the data. To show that this assumption does not drive our results, we additionally exploit a measure available from Redfin that reports the share of listings sold within two weeks of being listed. For Germany, we construct an analogous measure using listing-level data.²⁵

Figure C3 plots the relationship between distance to the city center and both the implied weekly probability of sale and the share of listings sold within two weeks. The resulting estimates indicate that the probability of sale declines sharply with distance to the city center, closely mirroring the increase in time on market. Listings located farther from the center are therefore less liquid in the sense that they face a lower probability of selling in the subsequent week. Comparing the city center to the outskirts, the implied weekly probability of sale decreases by approximately 20 percent in both Germany and the United States.

²⁵We classify listings that are removed from the platform within two weeks as successful sales.

These findings are corroborated by the two-week sale measure, which exhibits a similarly pronounced negative gradient with distance. Quantitatively, the probability of selling within two weeks is higher in the city center than in the outskirts by approximately 22 percent in Germany and 18 percent in the United States.

Figure C3: Time on the market and probability of sale gradients for Germany (2012–2024) and U.S. (2012–2023)



Notes: The binned scatter plots in the first row display the results of Regression (1) with time on the market as the outcome variable, using 15 equally sized distance bins. The probability of sale is calculated using the predicted time on the market from the regression. The binned scatter plots in the second row have the share of listings that get sold within two weeks as the outcome variable. The binned scatter plots are produced following Cattaneo et al. (2024) and based on the complete regression specification, as shown in columns two and five of Tables 2 and 3.

C.4 Additional determinants of housing liquidity in German cities

In our main analysis, we focus on how liquidity varies across space. Nevertheless, houses differ along several other dimensions that may also influence liquidity. In fact,

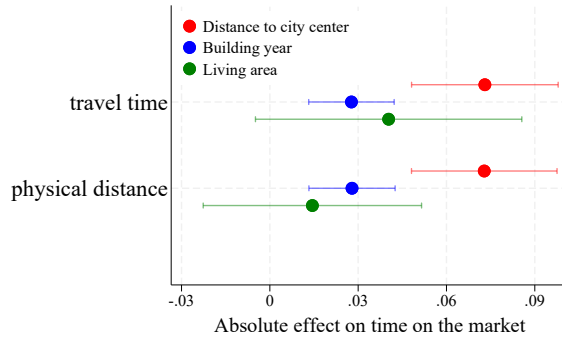
an extensive literature has investigated determinants of housing liquidity. Particularly expensive locations (“prime locations”) are associated with a shorter time on the market (Smith, 2009). By contrast, atypical properties experience both longer times on the market and higher listing prices, due to strong search frictions and thin buyer pools (Haurin et al., 2010). Dwelling size and age exhibit nonlinear effects: larger, appropriately priced homes tend to sell more quickly, while older or functionally obsolete properties often remain longer on the market (see Knight, 2002; Cirman, Pahor, and Verbic, 2015). In what follows, we compare the most important property characteristics – location, size, and age – in explaining variation in time on the market.

In Figure C4, we plot the coefficients for living area (in square meters), building year, and distance to the city center from Regression (1), standardized by their standard deviations and set into absolute values. As is evident from the plot, distance to the city center has the strongest impact on liquidity, whether measured as travel time or physical distance. Its coefficient is more than twice as large as that of building year. The coefficient for size is not significant.²⁶ Overall, this indicates that although liquidity varies with other physical characteristics of the property, location – measured by distance to the city center – is the most important factor. Unfortunately, due to data limitations, we cannot run similar regressions for the United States. However, Smith (2009) uses U.S. data to regress time on the market on property characteristics and shows that including the exact location, as given by the properties’ coordinates, strongly increases the predictive power of the regression – even when size and age are already included.

Other determinants of time on the market. A large body of empirical work has examined the determinants of time on the market (TOM) in residential real estate. In addition

²⁶The coefficient for size is negative and significant in the more parsimonious specification of the regression, but becomes insignificant once other property characteristics are included.

Figure C4: Determinants of time on the market, Germany (2012–2024)



Notes: This plots shows OLS regression coefficients for the combined German sample, as well as their respective 99% confidence intervals, based on regression (1). The coefficients are standardized across the displayed determinants using the respective sample standard deviation. Travel time is measured in car travel minutes from the city center. Physical distance is the kilometer distance to the city center.

to the property characteristics mentioned in the previous paragraph, U.S. studies highlight the role of pricing strategy and overpricing (Anglin, Rutherford, and Springer, 2003), seller motivation and urgency (Glower, Haurin, and Hendershott, 1998), and financial constraints such as low equity or high indebtedness (Genesove and Mayer, 1997) as key drivers of selling time. Despite these consistent patterns, the explanatory power of empirical TOM models remains limited. Studies typically report low R-squared values, often below 0.20, which reflects that a large share of variation in selling times is left unexplained. This issue has been widely acknowledged in the literature, with a meta-analysis in Sirmans, MacDonald, and Macpherson (2010) noting that TOM is inherently difficult to predict due to idiosyncratic buyer–seller interactions and unobserved heterogeneity. Even when controlling for pricing, seller characteristics, and credit conditions, much of the observed dispersion in TOM persists, suggesting that random shocks, local demand fluctuations, and negotiation dynamics play a central role. In our estimation, the uncertainty surrounding time on the market does not bias the estimated relationship, provided that unobserved determinants are not systematically correlated with location. Evidence for this is given by the substantially higher R-squared values we obtain in our more

aggregated U.S. analyses at the ZIP code level. This suggests that a considerable share of the unobserved heterogeneity averages out once observations are spatially aggregated.

C.5 Time series of housing liquidity and prices in the U.S.

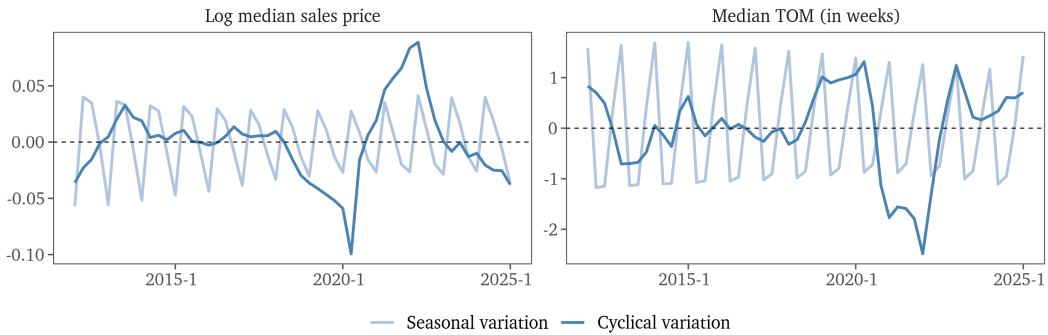
As we mention in the main text, our documented within-city spatial variation in housing liquidity and prices is comparable to the variation over time. Figure C5 displays Redfin time series of U.S.-level quarterly log median sales prices and time on the market, decomposed via a Hodrick–Prescott filter with standard penalty parameter $\lambda = 1,600$. The cyclical variation is obtained by isolating the cyclical component of a seasonally adjusted time series (provided by Redfin via X-13ARIMA-SEATS) from the Hodrick–Prescott filter. The seasonal variation is obtained by isolating the cyclical component of the unadjusted time series from the Hodrick–Prescott filter and subtracting the cyclical time series.

As becomes evident from the figure, the seasonal variation in prices amounts to about 10%, while the variation over the business cycle amounts to 10-15%. This is comparable to a spatial price difference in the U.S. over 20-30km (with prices changing by 0.5% per kilometer, see Table D7). For the time on the market, the seasonal variation amounts to about 2 weeks, while the the variation over the business cycle amounts to 2-3 weeks. This is comparable to a spatial time-on-the-market difference in the U.S. over 40-60km (with the time on the market changing by 0.05 weeks per kilometer, see Table D6).

C.6 Market tightness in German and U.S. cities

Germany. The data are from RWI - Leibniz-Institut für Wirtschaftsforschung and ImmobilienScout24 (2024). Since in this dataset we do not have the exact location of each

Figure C5: Variation in U.S. housing market variables around long-run trends



Notes: These plots display decomposed time series of U.S.-level quarterly log median sales prices and time on the market (TOM).

apartment, but only the ZIP Code, we calculate distances to the city center using the centroids of ZIP Code areas. For the same reason, we cannot present results with ZIP Code fixed effects. In addition to year-quarter- and city fixed effects, we control for the following property characteristics: size in square meters, number of rooms, bathrooms, kitchens, and balconies, floor number of the apartment, building year category, type of heating system, whether the building is a landmark, and whether the apartment is owner-occupied or rented. The results are documented in Table C1. The number of contact clicks per ad decreases significantly with distance to the city center, confirming the results from the binned scatterplot in the main text.

Table C1: Contact clicks and distance to the city center, Germany (2012–2024)

	(1)	(2)
	Clicks	Clicks
Distance to center (in km)	-0.49*** (0.11)	-0.46*** (0.11)
City \times Year-quarter FE	✓	✓
Property characteristics		✓
<i>N</i>	192,512	192,512
Adj. <i>R</i> ²	0.20	0.20
Mean(clicks)	20.72	20.72

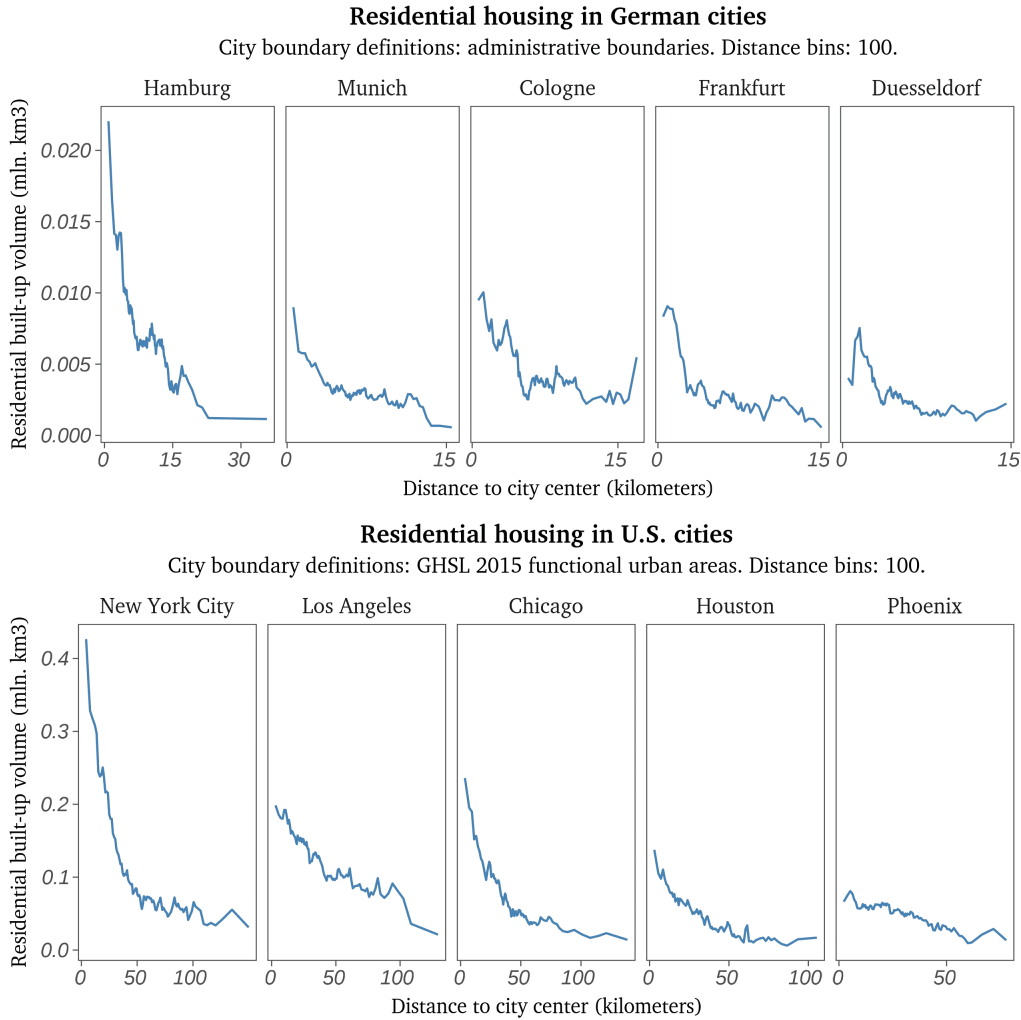
Notes: This table shows results for regressions of contact clicks per advertisement on the distance to the city center as specified in Regression (1). “Clicks” refers to the contact clicks per ad as defined in the text. Standard errors (in parentheses) are clustered at the city-year level. The list of property characteristics controls is available in Internet Appendix A.1. * : $p < 0.1$; ** : $p < 0.05$; *** : $p < 0.01$.

Moreover, as mentioned in the main text, these results on market tightness are unlikely to be driven by an increasing supply of housing with distance to the city center. In Figure C6, we plot the amount of residential built-up volume by distance to the city center in the German cities from our sample and the 5 largest U.S. cities, retrieved via the Global Human Settlement Layer Database (Pesaresi and Politis, 2023; Pesaresi et al., 2024). We observe that the amount of residential built-up volume in fact decreases with distance to the city center, generally speaking.

To get these measures, we first subtract the non-residential layer of built-up volume (*GHS-BUILT-V-NRES*) from the total layer of built-up volume (*GHS-BUILT-V-RES+NRES*) to obtain residential built-up volume across 100m \times 100m grid cells. We select all grid cells within the respective city boundary and calculate the distance to the city center for each grid cell (using the city centers defined in Section 2.3). Then, we create 100 distance bins for these grid cells and sum up the residential built-up volume by distance bin. We select the year 2015 to show results for the definition year of functional urban areas for U.S. cities (see Moreno-Monroy, Schiavina, and Veneri, 2021), also retrieved via the

GHSL database (*GHS-FUA*), which define cities based on commuting flows, following the EU-OECD definition from Dijkstra, Poelman, and Veneri (2019). For consistency, we also show built-up volume in 2015 for German cities, even though here we use administrative boundaries, as in the main empirical exercise.

Figure C6: Residential built-up volume by distance to city center (2015)



Notes: These plots display the amount of residential built-up volume by distance to the city center in the German cities from our sample and the 5 largest U.S. cities.

United States. For the U.S., we are not aware of publicly available data on contact applications to listings. We therefore approximate market tightness using a turnover-based measure. Specifically, for each ZIP-code-year-month combination, we compute the ratio of homes sold in a given month to the sum of end-of-month active listings, homes

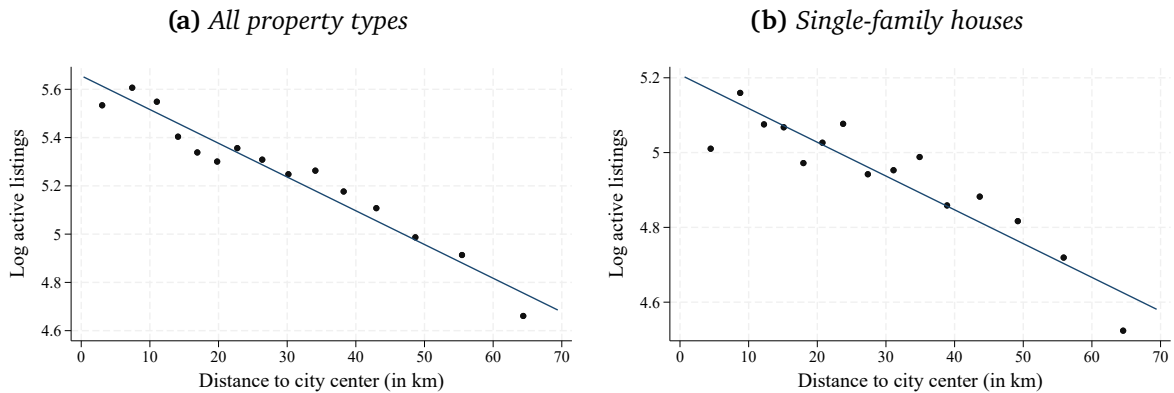
sold, and pending sales (which are not counted as active listings). We then regress this turnover measure on distance to the city center using our baseline Regression (1). The results, reported in Table C2, consistently show a negative and significant coefficient across all regression specifications. This shows that locations farther from the city center exhibit lower market turnover, which suggests lower market tightness. As in Germany, in U.S. housing markets demand is tighter closer to the city center, even though these areas contain more housing units. Figure C7 displays binned scatter plots to show the relation between the number of listings and distance to the city center controlling for differences in property characteristics and demographics. The figure shows that the number of active listings decreases with distance from the city center, both for single-family homes and for all property types combined. Housing supply is denser in central areas and becomes increasingly sparse toward the outskirts.

Table C2: *Sales to active listings and distance to the city center, U.S. (2012–2023)*

	(1)	(2)	(3)	(4)	(5)	(6)
	Turnover	Turnover	Turnover	Turnover	Turnover	Turnover
Distance to center (in km)	-0.02*** (0.006)	-0.06*** (0.006)	-0.04*** (0.005)			
Travel time to center (in min)				-0.03*** (0.006)	-0.07*** (0.006)	-0.05*** (0.006)
MSA × Year-month FE	✓	✓	✓	✓	✓	✓
State FE	✓	✓	✓	✓	✓	✓
Property characteristics		✓	✓		✓	✓
Demographic controls			✓			✓
<i>N</i>	569,099	568,235	568,235	569,099	568,235	568,235
ZIP Codes	4,200	4,199	4,199	4,200	4,199	4,199
Adj. <i>R</i> ²	0.50	0.53	0.56	0.51	0.53	0.56
Mean(TOM)	32.89	32.90	32.90	32.89	32.90	32.90

Notes: This table displays the output of Regression (1) on turnover, which we define as the ratio of sales to active listings within a given month. The regressions are based on data for single-family houses for the 30 largest MSAs in the U.S. in the period between 2012–2023. Standard errors (in parentheses) are clustered at the MSA-year level. * : $p < 0.1$; ** : $p < 0.05$; *** : $p < 0.01$.

Figure C7: Total listings by distance to city center, U.S. (2012–2023)



Notes: These binned scatter plots display the results of Regression (1) with log active listings as the outcome variable, using 15 equally-sized distance bins. Panel a shows the results for the sum of listings across all property types. Panel b shows the results for all listings of single-family houses. The binned scatter plots are based on the complete regression specification, as shown in columns three and six of Tables 2 and 3. The binned scatter plots are produced following Cattaneo et al. (2024).

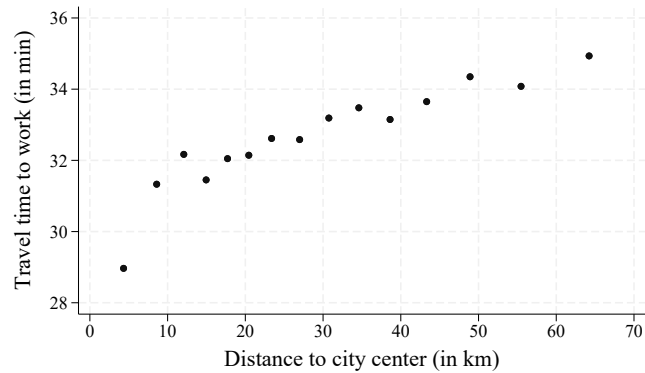
C.7 Travel time and market tightness

In Section 3, we document for both the U.S. and Germany that housing liquidity and market tightness decline with distance from the city center and other focal locations within a city. In this section, we show that actual travel costs, as measured in the data, are closely correlated with distance to these focal locations and are strongly associated with both market tightness and liquidity in cross-sectional and time-series variation.

To approximate actual travel costs, we use data from the American Community Survey (ACS), which asks respondents how many minutes they typically spend commuting to work each day. We obtain ZIP-code-level information from the five-year ACS samples and county-level information from the one-year samples.²⁷ The one-year samples provide a time-varying measure of travel time to work at an annual frequency and are therefore more suitable for time-series analyses. However, these one-year samples do not report data at the ZIP-code level.

²⁷Because the 2024 one-year sample is already available, we include it in our analysis. Note that no one-year sample was collected in 2020 due to the pandemic, so that year is omitted from the county-level analysis.

Figure C8: Time to work and distance to city center, U.S. (2012–2023)



Using the ACS commuting data, we first examine its correlation with our distance-to-city-center measure. As shown in Figure C8, the two measures are strongly positively correlated: households living closer to the city center report substantially shorter commute times than those living farther away. This provides direct evidence that our distance measure also captures differences in commuting costs.

Table C3: Cross-sectional evidence on turnover and travel time to work, U.S. (2012–2023)

	(1)	(2)	(3)	(4)	(5)	(6)
	TOM	TOM	TOM	Turnover	Turnover	Turnover
Travel time to work (in min)	0.07*** (0.010)	0.12*** (0.012)	0.07*** (0.011)	-0.14*** (0.011)	-0.21*** (0.013)	-0.12*** (0.012)
MSA × Year-month FE	✓	✓	✓	✓	✓	✓
State FE	✓	✓	✓	✓	✓	✓
Property characteristics		✓	✓		✓	✓
Demographic controls			✓			✓
<i>N</i>	569,099	568,235	568,235	569,099	568,235	568,235
ZIP Codes	4,200	4,199	4,199	4,200	4,199	4,199
Adj. <i>R</i> ²	0.45	0.48	0.50	0.51	0.53	0.56
Mean(dependent variable)	6.85	6.84	6.84	32.89	32.90	32.90

Notes: This table displays the output of Regression (1) on time on the market and turnover, which we define as the ratio of sales to active listings within a given month. The regressions are based on data for single-family houses for the 30 largest MSAs in the U.S. in the period between 2012–2023. Standard errors (in parentheses) are clustered at the MSA-year level. * : $p < 0.1$; ** : $p < 0.05$; *** : $p < 0.01$.

We then repeat our baseline analysis, replacing distance with actual commute time.

The first three columns of Table C3 show that longer commute times are significantly associated with longer time on the market, confirming our baseline findings. Running the same specification with turnover as the dependent variable yields consistent results: ZIP Codes with longer average commute times exhibit lower turnover. These findings are robust across alternative specifications, including those controlling for income and demographic characteristics.

Finally, we provide time-series evidence on the relationship between liquidity and commute time. We estimate county-level time-series regressions that include county fixed effects, thereby exploiting within-county variation over time and controlling for all time-invariant county characteristics. The results, reported in Table C4, corroborate the cross-sectional evidence: in periods with longer commute times, properties stay on the market longer and turnover is lower.

Table C4: Time-series evidence on turnover and travel time to work, U.S. (2012–2024)

	(1) Log TOM	(2) Log TOM	(3) Log TOM	(4) Log Turnover	(5) Log Turnover	(6) Log Turnover
Travel time to work (in min)	0.04*** (0.007)	0.04*** (0.007)	0.06*** (0.006)	-0.02*** (0.004)	-0.02*** (0.004)	-0.03*** (0.004)
County FE	✓	✓	✓	✓	✓	✓
Demographic controls		✓	✓		✓	✓
Property characteristics			✓			✓
<i>N</i>	4,876	4,876	4,876	4,876	4,876	4,876
Counties	431	431	431	431	431	431
Adj. <i>R</i> ²	0.61	0.62	0.65	0.58	0.58	0.65
Mean(dependent variable)	1.94	1.94	1.94	2.88	2.88	2.88

Notes: This table displays the output of Regression (1) on log turnover, which we define as the ratio of sales to actives listings within a given month, and log time on the market. The regressions are based on data for single-family houses for the 431 largest counties in the U.S. in the period between 2012–2024. The year of 2020 is omitted as the American Community Survey (ACS) did not collect data for that year. Standard errors (in parentheses) are clustered at the state level. * : $p < 0.1$; ** : $p < 0.05$; *** : $p < 0.01$.

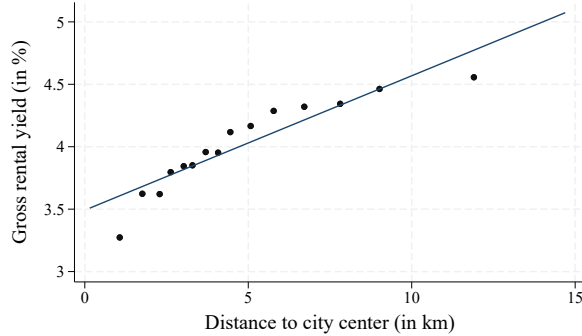
C.8 Spatial distribution of rental yields

In this section of the internet appendix, we present results on the spatial distribution of rental yields. We use listings data for investment properties, that is, properties advertised with both a rental income and a listing price, to construct property-level estimates of rental yields. These estimates reflect gross rental yields; however, as long as maintenance and utility costs do not vary systematically with distance to the city center, this does not affect our results.

Our dataset comprises approximately 51,000 observations across all cities in our German sample. We then estimate Regression (1), using gross rental yield as the dependent variable. In Figure C9, we plot the binned scatter results, and in Table C5 we report the regression estimates, including specifications in which the dependent variable is the logarithm of gross rental yield.

Across all specifications, our results are robust and show that rental yields increase significantly with distance to the city center. The differences between central and peripheral locations are sizable: properties on the outskirts exhibit rental yields more than 1 percentage point higher than those in the city center. Overall, these findings provide additional evidence that market liquidity is priced in across space.

Figure C9: Rental yields and distance to city center, Germany (2012–2024)



Notes: These binned scatter plots visualize the results of Regression (1) with gross rental yield as the outcome variable, using 15 equally-sized distance bins. The binned scatter plots are produced following Cattaneo et al. (2024)

Table C5: Rental yields and distance to city center, Germany (2012–2024)

	(1)	(2)	(3)	(4)
	Rental yield	Rental yield	Log rental yield	Log rental yield
Distance to center (in km)	0.10*** (0.01)	0.11*** (0.01)	0.03*** (0.00)	0.03*** (0.00)
City \times Year-quarter FE	✓	✓	✓	✓
Property characteristics		✓		✓
N	51,545	51,545	51,545	51,545
Adj. R^2	0.38	0.43	0.47	0.53
Mean(dependent variable)	4.02	4.02	1.31	1.31

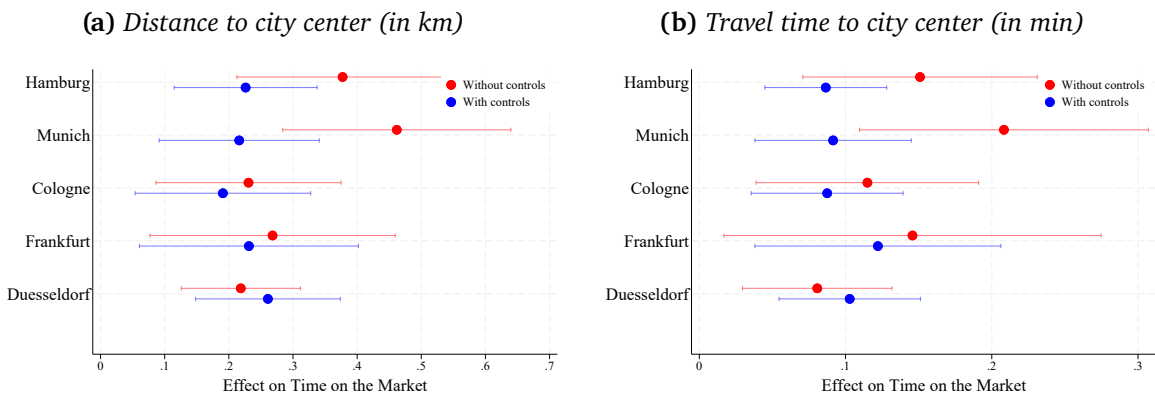
Notes: This table displays the output of Regression (1) on gross rental yield, measured as the ratio of annual gross rental income to listings price in percent. In columns 3 and 4, the left hand side variable is log gross rental yields. The regressions are based on data for apartments for the five large German cities in our sample between 2012 and 2024. The list of property characteristics controls is available in Internet Appendix A.1. The second and fourth columns additionally control for time on the market and the asking price discount, respectively. The regressions are based on the matched sample for all cities, covering the period from 2012 to 2024. Standard errors (in parentheses) are clustered at the ZIP Code level. * : $p < 0.1$; ** : $p < 0.05$; *** : $p < 0.01$.

D Robustness analysis

D.1 Results for individual cities

Germany. We run Regression (1) for each city separately and report the coefficients with the corresponding 95% confidence intervals by city bundled in Figure D1. For all cities, the coefficients for both kilometer distance and car travel time are positive and highly significant. The coefficient magnitudes are similar across cities, especially after including controls.

Figure D1: Time on the market and distance to city center by city (2012–2024)



Notes: These plots show the OLS regression coefficients of distance to the city center as specified in (1) with 95% confidence intervals with the standard errors clustered at the year level. All regressions include year-quarter fixed effects. See Internet Appendix A.1 for a full list of property characteristics controls.

United States. We also test whether we can find the time on the market gradient for individual MSAs. For all cities, we find a positive time on the market gradient with significance at the 1% level, with the exception of San Francisco-Oakland-Berkeley, CA. For San Francisco-Oakland-Berkeley, CA, the Realtor.com data show a larger inventory than the Redfin data, suggesting that the latter do not provide good coverage. In fact, with the Realtor.com data, we find a positive slope for San Francisco. Spatial price gradients are negative and significant at the 1% level for almost every MSA. For Sacramento-Roseville-

Folsom, CA and San Antonio-New Braunfels, TX, we find positive price gradients, which is due the fact that they have especially low prices in the city center. This has already been documented in Gupta et al. (2022).

Table D1: TOM and price gradient by MSA, 2012–2023

MSA	TOM gradient	Price gradient	P-value TOM	P-value Price	N
Atlanta-Sandy Springs-Alpharetta, GA	0.060	-0.003	0.00	0.00	27,135
Austin-Round Rock-Georgetown, TX	0.105	-0.010	0.00	0.00	10,509
Baltimore-Columbia-Towson, MD	0.116	0.001	0.00	0.00	17,409
Boston-Cambridge-Newton, MA-NH	0.063	-0.007	0.00	0.00	35,391
Charlotte-Concord-Gastonia, NC-SC	0.111	-0.009	0.00	0.00	13,472
Chicago-Naperville-Elgin, IL-IN-WI	0.041	-0.006	0.00	0.00	48,296
Cincinnati, OH-KY-IN	0.059	-0.006	0.00	0.00	17,386
Dallas-Fort Worth-Arlington, TX	0.058	-0.001	0.00	0.00	34,448
Denver-Aurora-Lakewood, CO	0.153	-0.002	0.00	0.00	15,441
Detroit-Warren-Dearborn, MI	0.037	-0.001	0.00	0.30	26,769
Houston-The Woodlands-Sugar Land, TX	0.075	0.002	0.00	0.00	29,352
Las Vegas-Henderson-Paradise, NV	0.060	-0.001	0.00	0.00	8,781
Los Angeles-Long Beach-Anaheim, CA	0.044	-0.001	0.00	0.00	47,218
Miami-Fort Lauderdale-Pompano Beach, FL	0.030	-0.000	0.00	0.03	22,828
Minneapolis-St. Paul-Bloomington, MN-WI	0.092	-0.004	0.00	0.00	28,338
New York-Newark-Jersey City, NY-NJ-PA	0.022	-0.003	0.01	0.00	85,145
Orlando-Kissimmee-Sanford, FL	0.136	-0.005	0.00	0.00	12,224
Philadelphia-Camden-Wilmington, PA-NJ-DE-MD	0.069	-0.002	0.00	0.00	38,652
Phoenix-Mesa-Chandler, AZ	0.060	-0.003	0.00	0.00	20,268
Pittsburgh, PA	0.077	-0.008	0.00	0.00	20,207
Portland-Vancouver-Hillsboro, OR-WA	0.145	-0.005	0.00	0.00	15,542
Riverside-San Bernardino-Ontario, CA	0.038	-0.005	0.00	0.00	17,789
Sacramento-Roseville-Folsom, CA	0.065	0.000	0.00	0.03	12,090
San Antonio-New Braunfels, TX	0.115	0.005	0.00	0.00	13,376
San Diego-Chula Vista-Carlsbad, CA	0.068	-0.007	0.00	0.00	11,999
San Francisco-Oakland-Berkeley, CA	-0.017	-0.011	0.00	0.00	18,091
Seattle-Tacoma-Bellevue, WA	0.067	-0.012	0.00	0.00	20,073
St. Louis, MO-IL	0.114	-0.002	0.00	0.00	23,567
Tampa-St. Petersburg-Clearwater, FL	0.122	-0.003	0.00	0.00	18,144
Washington-Arlington-Alexandria, DC-VA-MD-WV	0.071	-0.007	0.00	0.00	35,529

Notes: This table reports the output of regressions of time on the market in weeks on distance to the city center, median income, property characteristics, and year-quarter fixed effects by MSA. The underlying data is for single-family houses from Redfin. See the text for information on the data sources. Standard errors are clustered at the year level. N stands for the number of ZIP-Code-year-month observations.

D.2 COVID

This section of the internet appendix examines how the liquidity gradient shifted in Germany and the U.S. following the onset of COVID-19 and the widespread adoption of remote work. Tables D2 and D3 report the baseline regression results for the periods

before and after 2020. In both countries, the liquidity gradient became significantly flatter, consistent with the increase in working from home. Figures D2a and D2b show how the coefficient on distance to the city center evolved between 2018 and 2023. In both Germany and the U.S., the liquidity gradient nearly disappeared in 2021 and 2022, but began to rise again afterward.

Table D2: *TOM gradients before and after COVID, Germany (2012–2024)*

	(1)	(2)	(3)
	Full sample	Pre-2020	Post-2020
Distance to center (in km)	0.24*** (0.03)	0.26*** (0.03)	0.13*** (0.04)
City × Year-quarter FE	✓	✓	✓
Property characteristics	✓	✓	✓
<i>N</i>	84,292	60,377	23,914
Adj. <i>R</i> ²	0.13	0.14	0.29
Mean(TOM)	13.51	13.46	13.61

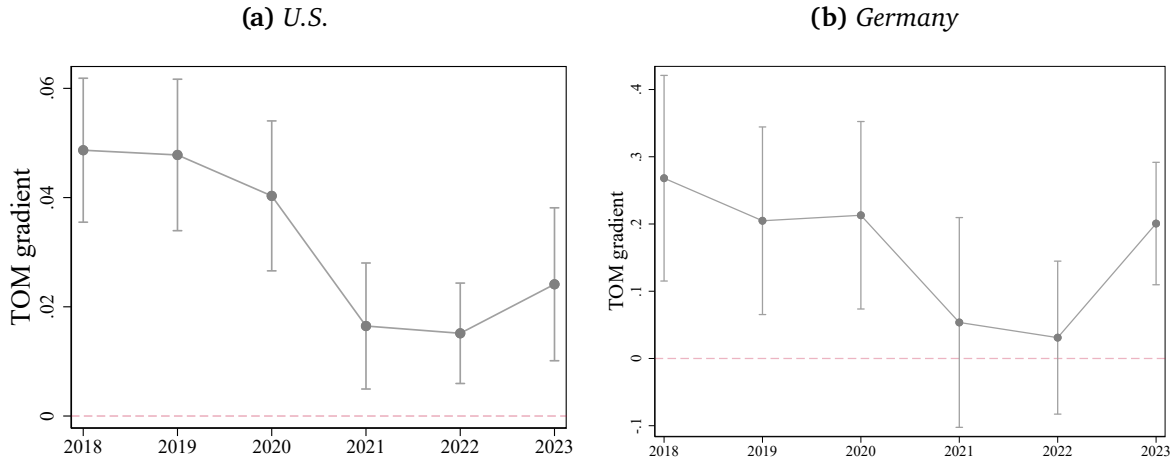
Notes: This table displays the output of Regression (1) on time on the market (TOM), measured in weeks. The list of property characteristics controls is available in Internet Appendix A.1. Regressions are based on the matched sample for all cities covering the period between 2012 and 2024. Standard errors (in parentheses) are clustered at the city-year level. * : $p < 0.1$; ** : $p < 0.05$; *** : $p < 0.01$.

Table D3: *TOM gradients before and after COVID, U.S. (2012–2023)*

	(1)	(2)	(3)
	Full sample	Pre-2020	Post-2020
Distance to center (in km)	0.06*** (0.003)	0.08*** (0.004)	0.02*** (0.004)
MSA × Year-month FE	✓	✓	✓
State FE	✓	✓	✓
Property characteristics	✓	✓	✓
<i>N</i>	745,469	487,556	257,913
Zip-codes	5,452	5,450	5,440
Adj. <i>R</i> ²	0.46	0.44	0.38
Mean(TOM)	7.48	8.70	5.18

Notes: This table displays the output of Regression (1) on time on the market (TOM), measured in weeks. Regressions are based on data for the 30 largest MSAs covering the period between 2012 and 2023. Standard errors (in parentheses) are clustered at the city-year level. * : $p < 0.1$; ** : $p < 0.05$; *** : $p < 0.01$.

Figure D2: Variation over time in the TOM gradient, U.S. and Germany (2018–2023)



Notes: These plots display outputs by year of Regression (1) on time on the market (TOM), measured in weeks. Regressions are based on data for the 30 largest MSAs for the U.S. and for the 5 German cities covered by our sample. 90% Confidence bands are constructed using standard errors clustered at the city-year level.

D.3 Different housing types

This section of the internet appendix presents the results for the liquidity gradient across different housing types. Table D4 reports the coefficient on distance to the city center from Regression (1), using time on the market as the dependent variable for our sample of five German cities: single-family houses (columns 1 and 2) and apartments (columns 3 and 4). To ensure comparability across housing types and due to data availability, we rely on listings data from RWI - Leibniz-Institut für Wirtschaftsforschung and ImmobilienScout24 (2024) for this analysis. The results closely mirror our baseline findings for Germany. Tables D5, D6, and D7 present the results for the 30 largest MSAs in the U.S. Table D5 reports the results for the pooled sample, which includes data on single-family houses, condos, townhouses, and multi-family houses. Table D6 reports the results for time on the market separately by housing type, and Table D7 does so for prices.

Table D4: Time on the market and distance to the city center by housing type, Germany (2012–2024)

	(1) Single-family	(2) Single-family	(3) Apartment	(4) Apartment
Distance to center (in km)	0.074*** (0.018)	0.066*** (0.018)	0.068*** (0.016)	0.059*** (0.019)
City × Year-quarter FE	✓	✓	✓	✓
Property characteristics		✓		✓
<i>N</i>	129,427	129,427	192,512	192,512
Adj. <i>R</i> ²	0.04	0.06	0.05	0.07
Mean(dependent variable)	4.87	4.87	4.80	4.80

Notes: This table displays the output of Regression (1) on time on the market (TOM), measured in weeks. Property characteristics controls are: living area, building year category, type of property, type of heating system and whether the house is under monument protection. Regressions are based on the full sample of listings from RWI - Leibniz-Institut für Wirtschaftsforschung and ImmobilienScout24 (2024) for all cities in our sample covering the period between 2012 and 2024. Standard errors (in parentheses) are clustered at the city-year level. * : $p < 0.1$; ** : $p < 0.05$; *** : $p < 0.01$.

Table D5: Time on the market and distance to city center, U.S.: all housing types (2012–2023)

	(1) TOM	(2) TOM	(3) TOM	(4) TOM	(5) TOM	(6) TOM
Distance to center (in km)	0.02*** (0.004)	0.04*** (0.003)	0.03*** (0.003)			
Travel time to center (in min)				0.02*** (0.006)	0.05*** (0.004)	0.04*** (0.004)
MSA × Year-month FE	✓	✓	✓	✓	✓	✓
Property type FE	✓	✓	✓	✓	✓	✓
State FE	✓	✓	✓	✓	✓	✓
Property characteristics		✓	✓		✓	✓
Demographic controls			✓			✓
<i>N</i>	1,331,457	1,325,016	1,325,016	1,331,457	1,325,016	1,325,016
ZIP Codes	5,124	5,107	5,107	5,124	5,107	5,107
Adj. <i>R</i> ²	0.35	0.38	0.39	0.35	0.38	0.39
Mean(TOM)	7.53	7.50	7.50	7.53	7.50	7.50

Notes: This table displays the output of Regression (1) on time on the market (TOM), measured in weeks. The first three columns show the results for distance to the city center measured in kilometers, while the last three columns show the results for the car travel time to the city center measured in minutes. Regressions are based on data for the 30 largest MSAs covering the period between 2012 and 2023. Standard errors (in parentheses) are clustered at the MSA-year level. * : $p < 0.1$; ** : $p < 0.05$; *** : $p < 0.01$.

Table D6: Time on the market and distance to the city center by property type, U.S. (2012–2023)

	(1) Single-family	(2) Condos	(3) Multi-family	(4) Townhouse
Distance to center (in km)	0.04*** (0.003)	0.02*** (0.004)	0.03*** (0.006)	0.03*** (0.003)
MSA × Year-month FE	✓	✓	✓	✓
State FE	✓	✓	✓	✓
Property characteristics	✓	✓	✓	✓
Demographic controls	✓	✓	✓	✓
<i>N</i>	673,308	317,842	89,909	243,822
ZIP Codes	4,941	2,420	908	1,842
Adj. <i>R</i> ²	0.49	0.40	0.26	0.33
Mean(TOM)	7.46	7.68	9.25	6.72

Notes: This table displays the output of Regression (1) on time on the market (TOM), measured in weeks. The four columns show the results for distance to the city center measured in kilometers. Regressions are based on data for each property type separately for the 30 largest MSAs covering the period between 2012 and 2023. Standard errors (in parentheses) are clustered at the MSA-year level. * : $p < 0.1$; ** : $p < 0.05$; *** : $p < 0.01$.

Table D7: Log sales prices and distance to the city center by property type, U.S. (2012–2023)

	(1) Single-family	(2) Condos	(3) Multi-family	(4) Townhouse
Distance to center (in km)	-0.002*** (0.000)	-0.001*** (0.000)	-0.004*** (0.000)	-0.001*** (0.000)
MSA × Year-month FE	✓	✓	✓	✓
State FE	✓	✓	✓	✓
Property characteristics	✓	✓	✓	✓
Demographic controls	✓	✓	✓	✓
<i>N</i>	673,308	317,842	89,909	243,822
ZIP Codes	4,941	2,420	908	1,842
Adj. <i>R</i> ²	0.91	0.83	0.90	0.90
Mean(Log price)	12.70	12.34	12.84	12.50

Notes: This table displays the output of Regression (1) on log sales prices. The four columns show the results for distance to the city center measured in kilometers. Regressions are based on data for each property type separately for the 30 largest MSAs covering the period between 2012 and 2023. Standard errors (in parentheses) are clustered at the MSA-year level. * : $p < 0.1$; ** : $p < 0.05$; *** : $p < 0.01$.

D.4 Alternative city boundary definitions

In this section of the internet appendix, we present the results based on the sample of the 30 largest FUAs (functional urban areas) for U.S. cities (see Moreno-Monroy, Schiavina, and Veneri, 2021), retrieved via the GHSL database (Schiavina et al., 2019), which define cities based on commuting flows, following the EU-OECD definition from Dijkstra, Poelman, and Veneri (2019). Columns 1 and 2 of Table D18 (further below) show the results using distance to the MSA city center definition, while columns 3 and 4 show the results using distance to the FUA city center definition, which measures the location with the highest residential built-up volume within the FUA.

Table D8: *Price and liquidity gradients for functional urban areas, U.S. (2012–2023)*

	(1) TOM	(2) Price	(3) TOM	(4) Price
Distance to MSA center (in km)	0.021*** (0.004)	-0.001*** (0.000)		
Distance to FUA center (in km)			0.023*** (0.003)	-0.001*** (0.000)
FUA × Year-month FE	✓	✓	✓	✓
State FE	✓	✓	✓	✓
Property characteristics	✓	✓	✓	✓
Demographic controls	✓	✓	✓	✓
<i>N</i>	647,770	647,770	647,770	647,770
ZIP Codes	4,735	4,735	4,735	4,735
Adj. <i>R</i> ²	0.52	0.92	0.52	0.92
Mean dependent variable	7.06	12.75	7.06	12.75

Notes: This table displays the output of Regression (1) on time on the market (TOM), measured in weeks, and log sales prices. The four columns show the results for distance to the city center measured in kilometers. In the first two columns, the distance is measured to the city hall of the respective MSA, while in the last two columns, the distance is measured to the location with the highest residential built-up volume within the functional urban area (FUA). The regressions are based on data for single-family dwellings in the 30 largest FUAs for the period 2012–2023. Standard errors (in parentheses) are clustered at the FUA-year level.
*: $p < 0.1$; **: $p < 0.05$; ***: $p < 0.01$.

In addition, we also compare the results across different cutoffs for the size of the MSAs. In the baseline analysis, we restrict the sample to observations within a 70 km radius of MSA city centers to avoid including very sparsely populated areas. To show that our results are not driven by this specific cutoff, we re-estimate equation (1) using alternative distance thresholds. The results are presented in Table D9 and show a clear consistency in the significance and magnitude of the coefficient on distance to center.

Table D9: Liquidity gradients with different city sizes, U.S. (2012–2023)

	(1) < 50km	(2) < 70km	(3) < 90km	(4) Full sample
Distance to center (in km)	0.04*** (0.006)	0.05*** (0.005)	0.06*** (0.004)	0.05*** (0.003)
MSA × Year-month FE	✓	✓	✓	✓
State FE	✓	✓	✓	✓
Property characteristics	✓	✓	✓	✓
<i>N</i>	513,276	607,445	649,795	673,308
ZIP Codes	3,773	4,463	4,770	4,941
Adj. <i>R</i> ²	0.51	0.49	0.48	0.47
Mean(TOM)	6.88	7.11	7.29	7.46

*Notes: This table displays the output of Regression (1) on time on the market (TOM), measured in weeks. The four columns show the results for distance to the city center measured in kilometers. The first column is based on the regression using only observations within 50km of the city center; the second only observations within 70km, the third only 90km and the fourth considers all observations. The regressions are based on data for single-family dwellings in the 30 largest FUAs for the period 2012–2023. Standard errors (in parentheses) are clustered at the MSA-year level. * : $p < 0.1$; ** : $p < 0.05$; *** : $p < 0.01$.*

D.5 Alternative city center definitions

In this section of the internet appendix, we present the results for the baseline Regression (1) using distance to alternative definitions of the city center. Table D10 (further below) shows the results for Germany. Table D18 shows the results for the U.S. in Columns 1 and 2, which we report together with our results on focal locations as multiple alternative city centers.

Table D10: Price and liquidity gradients using alternative city centers, Germany (2012–2024)

	(1) TOM	(2) TOM	(3) TOM	(4) Price	(5) Price	(6) Price
Distance to center (in km)	0.31*** (0.05)	0.25*** (0.03)	0.20*** (0.03)	-0.04*** (0.00)	-0.05*** (0.00)	-0.04*** (0.00)
City \times Year-quarter FE	✓	✓	✓	✓	✓	✓
Property characteristics		✓	✓		✓	✓
Borough FE			✓			✓
<i>N</i>	58,326	58,326	58,326	58,326	58,326	58,326
Adj. <i>R</i> ²	0.05	0.13	0.13	0.23	0.84	0.86
Mean(dep. variable)	14.03	14.03	14.03	12.45	12.45	12.45

Notes: This table displays the output of Regression (1) on time on the market (TOM), measured in weeks, and log sales prices. The six columns show the results for distance to the city center measured in kilometers. The distance is measured to the centroid of the business district with the highest land value (Bodenrichtwert) in the city. The list of property characteristics controls is available in Internet Appendix A.1. The regressions are based on data for apartments in Hamburg, Cologne, Frankfurt, and Dusseldorf for the period 2012–2024. Standard errors (in parentheses) are clustered at the city-year level. * : $p < 0.1$; ** : $p < 0.05$; *** : $p < 0.01$.

D.6 Alternative travel time estimates

In our main analysis, we use car travel times from openrouteservice. Here, we also present our regression results using travel times obtained from Google Maps. We retrieve car travel times and public transport travel times to the city center. In Tables D11 and D12, we present the results for Germany, using Google car travel times and public transport times, respectively. The results are both quantitatively and qualitatively similar to those in our baseline analysis.

We then perform the same analysis for the United States. The results are shown in Tables D13 and D14. For car travel times, we find that the results remain unchanged compared to the baseline. For public transport, however, we find that both time on the market and price gradients are considerably smaller. This is probably due to the fact that only a small part of the population uses public transport to commute in some U.S.

cities, meaning that it serves as a poor proxy for actual commuting costs. In the United States, only about 5% of the population uses public transport to commute to work daily (Burrows, Burd, and McKenzie, 2021).

Table D11: Liquidity and price gradients with Google car travel times, Germany (2012–2024)

	(1) TOM	(2) TOM	(3) TOM	(4) Price	(5) Price	(6) Price
Google travel time (in min)	0.15*** (0.02)	0.10*** (0.01)	0.08*** (0.02)	-0.02*** (0.00)	-0.02*** (0.00)	-0.02*** (0.00)
City × Year-quarter FE	✓	✓	✓	✓	✓	✓
Property characteristics		✓	✓		✓	✓
Borough FE			✓			✓
<i>N</i>	84,292	84,292	84,292	84,292	84,292	84,292
Adj. <i>R</i> ²	0.04	0.13	0.13	0.30	0.86	0.88
Mean(dependent variable)	13.51	13.51	13.51	12.60	12.60	12.60

Notes: This table displays the output of Regression (1) on time on the market (TOM), measured in weeks, and log sales prices using Google car travel times to measure commuting time to the city center. The list of property characteristics controls is available in Internet Appendix A.1. The regressions are based on data for apartments for the five cities in our sample in the period between 2012–2024. Standard errors (in parentheses) are clustered at the city-year level. * : $p < 0.1$; ** : $p < 0.05$; *** : $p < 0.01$.

Table D12: Liquidity and price gradients with public transport travel times, Germany (2012–2024)

	(1) TOM	(2) TOM	(3) TOM	(4) Price	(5) Price	(6) Price
Public transport travel time (in min)	0.09*** (0.01)	0.06*** (0.01)	0.04*** (0.01)	-0.01*** (0.00)	-0.01*** (0.00)	-0.01*** (0.00)
City × Year-quarter FE	✓	✓	✓	✓	✓	✓
Property characteristics		✓	✓		✓	✓
Borough FE			✓			✓
<i>N</i>	84,292	84,292	84,292	84,292	84,292	84,292
Adj. <i>R</i> ²	0.04	0.13	0.13	0.29	0.85	0.87
Mean(dependent variable)	13.51	13.51	13.51	12.60	12.60	12.60

Notes: This table displays the output of Regression (1) on time on the market (TOM), measured in weeks, and log sales prices using Google public transport travel times to measure commuting time to the city center. The list of property characteristics controls is available in Internet Appendix A.1. The regressions are based on data for apartments for the five cities in our sample in the period between 2012–2024. Standard errors (in parentheses) are clustered at the city-year level. * : $p < 0.1$; ** : $p < 0.05$; *** : $p < 0.01$.

Table D13: Liquidity and price gradients with Google car travel times, U.S. (2012–2023)

	(1) TOM	(2) TOM	(3) TOM	(4) Price	(5) Price	(6) Price
Google car travel time (in min)	0.034*** (0.0078)	0.069*** (0.0065)	0.049*** (0.0068)	-0.003*** (0.0005)	-0.003*** (0.0003)	-0.002*** (0.0003)
MSA × Year-month FE	✓	✓	✓	✓	✓	✓
State FE	✓	✓	✓	✓	✓	✓
Property characteristics		✓	✓		✓	✓
Demographic controls			✓			✓
<i>N</i>	609,020	607,445	607,445	609,020	607,445	607,445
ZIP codes	4,464	4,463	4,463	4,464	4,463	4,463
Adj. <i>R</i> ²	0.46	0.49	0.51	0.57	0.88	0.91
Mean(dependent variable)	7.13	7.11	7.11	12.73	12.73	12.73

Notes: This table displays the output of Regression (1) on time on the market (TOM), measured in weeks, and log sales prices using Google car transport travel times to measure commuting time to the city center. The regressions are based on data for single-family houses for the 30 largest MSAs in the U.S. in the period between 2012–2023. Standard errors (in parentheses) are clustered at the MSA-year level. * : $p < 0.1$; ** : $p < 0.05$; *** : $p < 0.01$.

Table D14: Liquidity and price gradients with public transport travel times, U.S. (2012–2023)

	(1) TOM	(2) TOM	(3) TOM	(4) Price	(5) Price	(6) Price
Public transport travel time (in min)	-0.001 (0.0016)	0.006*** (0.0009)	0.005*** (0.0008)	-0.001*** (0.0001)	-0.001*** (0.0001)	-0.001*** (0.0001)
MSA × Year-month FE	✓	✓	✓	✓	✓	✓
State FE	✓	✓	✓	✓	✓	✓
Property characteristics		✓	✓		✓	✓
Demographic controls			✓			✓
<i>N</i>	451,243	450,041	450,041	451,243	450,041	450,041
ZIP codes	3,335	3,334	3,334	3,335	3,334	3,334
Adj. <i>R</i> ²	0.48	0.52	0.52	0.58	0.89	0.92
Mean(dependent variable)	6.77	6.74	6.74	12.79	12.79	12.79

Notes: This table displays the output of Regression (1) on time on the market (TOM), measured in weeks, and log sales prices using Google public transport travel times to measure commuting time to the city center. The regressions are based on data for single-family houses for the 30 largest MSAs in the U.S. in the period between 2012–2023. Standard errors (in parentheses) are clustered at the MSA-year level. * : $p < 0.1$; ** : $p < 0.05$; *** : $p < 0.01$.

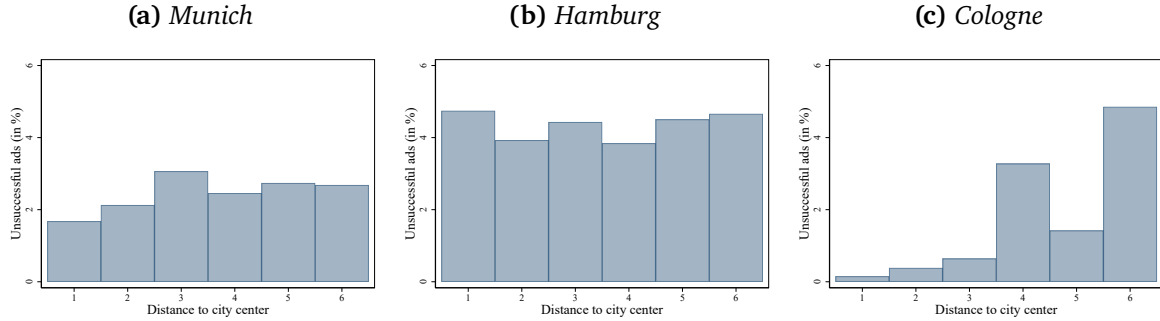
D.7 Properties that do not get sold

We identify listed properties that do not get sold via three steps. First, we match all ads with transactions that occurred within the same neighborhood (*Stadtteil*). Each ad is then associated with a set of potential transactions in the neighborhood. Out of these ads, we identify those as “unsuccessful” that are associated with transactions one year after or before the ad was published. Second, we identify ads as “unsuccessful” that are associated with transactions for which the living area of the matched apartment differs by more than 50%. Third, we identify ads as “unsuccessful” for which the remaining potential matches have a living area and building year that deviate by more than 10% and 10 years.

While this algorithm will identify listings that, with a very high probability, did not end up in a sale, it does not identify all listings that did not end up in a sale. As such, the algorithm presents a lower bound of “unsuccessful” ads. However, we do not have reasons to believe that this lower bound is systematically biased across space, which is the variation we want to explore. We focus only on the three largest cities in our German sample – Hamburg, Munich, and Cologne – because, for the other cities, the number of “unsuccessful” ads is too small to conduct a meaningful statistical analysis.

We first analyze the spatial distribution of unsuccessful ads, measured as the percentage of unsuccessful ads in terms of total ads at the city level, displayed in Figure D3. In all three cities, the relative number of unsuccessful ads is not larger in the city center. If anything, we see that this number slightly increases with distance to the city center.

Figure D3: Unsuccessful ads and distance to the city center, Germany (2012–2024)



Notes: These plots display the percentage of ads that do not result in a sale by distance to the city center with 6 equally-sized distance bins. The algorithm to identify the “unsuccessful” ads is described in the text.

To conduct a more formal assessment, we run a survival analysis on time on the market. In other words, we test for the relationship between expected time on the market and distance to the city center by estimating the following hazard function for time on the market:

$$h(TOM_{it}) = h_0(TOM) \times \exp [\gamma \times \text{distance}_i + \delta \times X_i + f_t + g_c + \varepsilon_{it}], \quad (D1)$$

where $h_0(TOM)$ is the baseline hazard rate which depends on the assumption on the functional form of the distribution of error terms ε_{it} . The hazard rate $h(TOM_{it})$ denotes the probability of property i being sold at time t , conditional on the seller listing the property in that point in time, the property characteristics are X_i , time fixed effects are f_t , and city fixed effects are g_c . We estimate the hazard rate using various error term distributions and present the results in Table D15. The first row of the table displays the effect of distance to the city center on the hazard rate of time on the market, given by its hazard ratio. Across all specifications, it is significantly larger than one, meaning that a greater distance to the city center is associated with a longer expected time on the market. In other words, an ad has a higher chance of “surviving” in the outskirts.

Table D15: Expected time on the market and distance to city center, Germany (2012–2024)

	Exponential	Weibull	Cox
Distance to center (in km)	1.013*** (0.0032)	1.012*** (0.0037)	1.014*** (0.0037)
City \times Year FEs	✓	✓	✓
Property characteristics	✓	✓	✓
<i>N</i>	56,279	56,279	56,279

Notes: This table displays the output of Regression (1) for three different duration models of time on the market, measured in weeks. The first row displays the estimated hazard ratio for the predicted distance to the city center. The regressions are based on data for apartments in Hamburg, Cologne and Munich. The list of property characteristics controls is available in Internet Appendix A.1. Standard errors are in parentheses.
*: $p < 0.1$; **: $p < 0.05$; ***: $p < 0.01$.

D.8 Systematic overvaluation

Table D16: Liquidity gradients, Germany (2012–2024)

	(1) TOM	(2) TOM	(3) APD	(4) APD
Distance to center (in km)	0.241*** (0.0260)	0.241*** (0.0261)	-0.162*** (0.0279)	-0.158*** (0.0275)
Asking price discount (in %)		-0.006 (0.0036)		
Time on the market (in weeks)				-0.014 (0.0084)
City \times Year-quarter FE	✓	✓	✓	✓
Property characteristics	✓	✓	✓	✓
<i>N</i>	84,292	84,292	84,292	84,292
Adj. R^2	0.13	0.13	0.05	0.05
Mean(dependent variable)	13.51	13.51	-1.56	-1.56

Notes: This table presents the results of Regression (1) on time on the market (TOM), measured in weeks, and asking price discount (APD), measured as a percentage of the asking price. The list of property characteristics controls is available in Internet Appendix A.1. The second and fourth columns additionally control for time on the market and the asking price discount, respectively. The regressions are based on the matched sample for all cities, covering the period from 2012 to 2024. Standard errors (in parentheses) are clustered at the city-year level. *: $p < 0.1$; **: $p < 0.05$; ***: $p < 0.01$.

In this section of the internet appendix, we present the regression results for the robustness analysis regarding systematic overvaluation of apartments in the outskirts. Tables D16 and D17 report the estimates from Regression (1) on time on the market and the asking price discount (the asking price) for Germany and the U.S. The first and third columns in both tables are based on the specification with the full set of controls used in our baseline analysis. Columns two and four additionally include controls for the asking price discount and the time on the market, respectively. As shown, the coefficients remain largely unchanged across all specifications for both Germany and the U.S.

Table D17: Liquidity gradients, U.S. (2012–2023)

	(1) TOM	(2) TOM	(3) APD	(4) APD
Distance to center (in km)	0.040*** (0.0032)	0.031*** (0.0028)	-0.022*** (0.0017)	-0.018*** (0.0014)
Asking price discount (in %)		-0.396*** (0.0201)		
Time on the market (in weeks)			-0.111*** (0.0082)	
MSA \times Year-month FE	✓	✓	✓	✓
State FE	✓	✓	✓	✓
Property characteristics	✓	✓	✓	✓
Demographic controls	✓	✓	✓	✓
<i>N</i>	673,264	673,264	673,264	673,264
ZIP Codes	4,941	4,941	4,941	4,941
Adj. <i>R</i> ²	0.49	0.51	0.55	0.57
Mean(dependent variable)	7.46	7.46	-1.45	-1.45

Notes: This table presents the results of Regression (1) on time on the market (TOM), measured in weeks, and asking price discount (APD), measured as a percentage of the asking price. The second and fourth columns additionally control for time on the market and the asking price discount, respectively. Regressions are based on data for single-family houses for the 30 largest MSAs covering the period between 2012 and 2023. Standard errors (in parentheses) are clustered at the city-year level. * : $p < 0.1$; ** : $p < 0.05$; *** : $p < 0.01$.

D.9 Focal ZIP Codes

Table D18: *Time on the market and distance to job centers, U.S. (2012–2023)*

	(1) TOM	(2) TOM	(3) TOM	(4) TOM	(5) TOM	(6) TOM
Distance to largest job center (in km)	0.02*** (0.004)	0.02*** (0.003)				
Distance to nearest job center (in km)			0.02*** (0.005)	0.02*** (0.003)		
Distance to nearest job center (in km)					0.02*** (0.006)	0.02*** (0.004)
MSA × Year-month FE	✓	✓	✓	✓	✓	✓
State FE	✓	✓	✓	✓	✓	✓
Property characteristics		✓		✓		✓
Demographic controls		✓		✓		✓
<i>N</i>	588,917	587,316	588,917	587,316	588,917	587,316
ZIP Codes	4,311	4,310	4,311	4,310	4,311	4,310
Adj. R^2	0.46	0.51	0.46	0.51	0.46	0.51
Mean(TOM)	7.19	7.16	7.19	7.16	7.19	7.16

Notes: This table displays the output of Regression (1) on time on the market (TOM), measured in weeks, using focal points from the job access index instead of the city center. Columns 3 and 4 assume 3 different focal ZIP Codes, while columns 5 and 6 assume 5 different focal ZIP Codes. The regressions are based on data for single-family dwellings in the 30 largest MSAs for the period 2012–2023. Standard errors (in parentheses) are clustered at the MSA-year level. * : $p < 0.1$; ** : $p < 0.05$; *** : $p < 0.01$.

In this section of the internet appendix, we present the results of Regression (1), allowing for multiple city centers within an MSA for the U.S. Columns 1 and 2 of Table D18 show the results when defining a single city center based on the job access index using data from Delventhal and Parkhomenko (2024). To obtain the job access index, we calculate the distance-weighted average of the number of jobs that can be accessed from a ZIP Code and normalize such that 1 represents the maximum available number of jobs across all ZIP Codes. Columns 3 and 4 show the results when defining 3 focal ZIP Codes per MSA as the three ZIP Codes with the highest job access index. Columns

5 and 6 display the results when defining 5 focal ZIP Codes. Our results hold for any definition of focal ZIP Codes.

D.10 Log time on the market

Lastly, we show that our baseline results are robust to using the log of time on the market as the left-hand-side variable (not mentioned in the main text). The results for Germany are reported in Table D19, and those for the U.S. in Table D20. Using the log of time on the market, which is less sensitive to potential outliers, does not change our main findings: we continue to find a positive and highly significant time-on-the-market gradient across all specifications.

Table D19: *Log time on the market and distance to city center, Germany (2012–2024)*

	(1) Log TOM	(2) Log TOM	(3) Log TOM	(4) Log TOM	(5) Log TOM	(6) Log TOM
Distance to center (in km)	0.04*** (0.00)	0.03*** (0.00)	0.03*** (0.00)			
Travel time to center (in min)				0.02*** (0.00)	0.01*** (0.00)	0.01*** (0.00)
City \times Year-quarter FE	✓	✓	✓	✓	✓	✓
Property characteristics		✓	✓		✓	✓
Borough FE			✓			✓
<i>N</i>	84,292	84,292	84,292	84,292	84,292	84,292
Adj. <i>R</i> ²	0.05	0.12	0.12	0.05	0.12	0.12
Mean(TOM)	1.77	1.77	1.77	1.77	1.77	1.77

Notes: This table displays the output of Regression (1) on log time on the market (TOM). The list of property characteristics controls is available in Internet Appendix A.1. The regressions are based on data for apartments for the five cities in our sample in the period between 2012–2024. Standard errors (in parentheses) are clustered at the ZIP Code level. * : $p < 0.1$; ** : $p < 0.05$; *** : $p < 0.01$.

Table D20: Log time on the market and distance to city center, U.S. (2012–2023)

	(1) Log TOM	(2) Log TOM	(3) Log TOM	(4) Log TOM	(5) Log TOM	(6) Log TOM
Distance to center (in km)	0.003*** (0.0007)	0.006*** (0.0006)	0.005*** (0.0006)			
Travel time to center (in min)				0.004*** (0.0007)	0.007*** (0.0007)	0.005*** (0.0007)
MSA × Year-month FE	✓	✓	✓	✓	✓	✓
State FE	✓	✓	✓	✓	✓	✓
Property characteristics		✓	✓		✓	✓
Demographic controls			✓			✓
<i>N</i>	609,020	607,445	607,445	609,020	607,445	607,445
ZIP Codes	4,464	4,463	4,463	4,464	4,463	4,463
Adj. <i>R</i> ²	0.63	0.65	0.67	0.63	0.66	0.67
Mean(TOM)	1.69	1.69	1.69	1.69	1.69	1.69

Notes: This table displays the output of Regression (1) on log time on the market (TOM). The regressions are based on data for single-family houses for the 30 largest MSAs in the U.S. in the period between 2012–2023. Standard errors (in parentheses) are clustered at the city-year level. * : $p < 0.1$; ** : $p < 0.05$; *** : $p < 0.01$.

E Local maximum in the seller's optimization problem

To save on notation, we show that the first-order condition of the seller's profit maximization problem provides a local maximum via

$$\frac{\partial \Pi}{\partial p(d)|_d} = \gamma(d) + p(d) \frac{\partial \gamma}{\partial p(d)|_d} - \beta \Pi(d) \frac{\partial \gamma}{\partial p(d)|_d} = 0 \quad (\text{E1})$$

rather than the reformulated expression (6) in the main text. The second-order condition for a local maximum is

$$\frac{\partial^2 \Pi}{\partial p^2(d)|_d} = 2 \frac{\partial \gamma}{\partial p(d)|_d} + \frac{\partial^2 \gamma}{\partial p^2(d)|_d} (p(d) - \beta \Pi(d)) < 0. \quad (\text{E2})$$

From (12), we know that

$$\frac{\partial \gamma}{\partial p(d)|_d} = -f(\varepsilon^*(d)) \frac{1-\pi\beta}{\beta} \leq 0 \quad (\text{E3})$$

and therefore

$$\frac{\partial^2 \gamma}{\partial p^2(d)|_d} = -f'(\varepsilon^*(d)) \frac{1-\pi\beta}{\beta} \frac{\partial \varepsilon^*}{\partial p(d)|_d} = -f'(\varepsilon^*(d)) \left(\frac{1-\pi\beta}{\beta} \right)^2. \quad (\text{E4})$$

Hence, for (E2) to hold, we need that

$$-2f(\varepsilon^*(d)) \frac{1-\pi\beta}{\beta} - f'(\varepsilon^*(d)) \left(\frac{1-\pi\beta}{\beta} \right)^2 (p(d) - \beta \Pi(d)) < 0 \quad (\text{E5})$$

or equivalently

$$f'(\varepsilon^*(d)) > \frac{-2 f(\varepsilon^*(d)) \frac{1-\pi\beta}{\beta}}{\left(\frac{1-\pi\beta}{\beta}\right)^2 (p(d) - \beta\Pi(d))}, \quad (\text{E6})$$

where $p(d) - \beta\Pi(d) > 0$ follows immediately from (6) and (12). In particular, for $\varepsilon \sim U[\underline{\varepsilon}, \bar{\varepsilon}]$,

$$f'(\varepsilon^*(d)) = 0 > \frac{-2 \frac{1}{\bar{\varepsilon} - \underline{\varepsilon}} \frac{1-\pi\beta}{\beta}}{\left(\frac{1-\pi\beta}{\beta}\right)^2 (p(d) - \beta\Pi(d))}. \quad (\text{E7})$$

F Analytical results with more general dividend distributions

In this section, we show that the buyer reservation dividend $\varepsilon^*(d)$ increases with distance to the city center d with more general assumptions on the cumulative distribution function of buyer dividends F than with the uniform distribution applied in the main text. As in Section 4.3, we start from the expression for the equilibrium price (F1):

$$p(d) = \frac{-1}{\partial \gamma(d)/\partial p(d)|_d} \left(\gamma(d) + \frac{\beta}{1-\beta} (\gamma(d))^2 \right),$$

Plugging in the equilibrium relations between probabilities of sale and reservation dividends (9) and (12), we have that

$$p(d) = \frac{\beta}{1-\pi\beta} \frac{1-F(\varepsilon^*(d))}{f(\varepsilon^*(d))} + \frac{\beta^2}{(1-\beta)(1-\pi\beta)} \frac{(1-F(\varepsilon^*(d)))^2}{f(\varepsilon^*(d))}. \quad (\text{F1})$$

and, via the seller optimality condition (6),

$$\Pi(d) = \frac{\beta}{(1-\beta)(1-\pi\beta)} \frac{(1-F(\varepsilon^*(d)))^2}{f(\varepsilon^*(d))}. \quad (\text{F2})$$

Plugging these results into the linear expression for buyer dividends (11) yields

$$\begin{aligned} \varepsilon^*(d) = & \frac{1-F(\varepsilon^*(d))}{f(\varepsilon^*(d))} + \frac{\beta}{1-\beta} \frac{(1-F(\varepsilon^*(d)))^2}{f(\varepsilon^*(d))} - \frac{(1-\pi)\beta}{(1-\beta)(1-\pi\beta)} \frac{(1-F(\varepsilon^*(d)))^2}{f(\varepsilon^*(d))} \\ & + \tau(d) + (\pi - \pi\beta)W. \end{aligned} \quad (\text{F3})$$

Taking the derivative with respect to d gives us

$$\frac{\partial \varepsilon^*}{\partial d} \left(1 + \frac{(f(\varepsilon^*(d)))^2 + f'(\varepsilon^*(d))(1 - F(\varepsilon^*(d)))}{(f(\varepsilon^*(d)))^2} \right. \\ \left. + \frac{2(1 - F(\varepsilon^*(d)))(f(\varepsilon^*(d)))^2 + f'(\varepsilon^*(d))(1 - F(\varepsilon^*(d)))^2}{(f(\varepsilon^*(d)))^2} \right) = \frac{\partial \tau}{\partial d} > 0. \quad (\text{F4})$$

Hence, for $\partial \varepsilon^* / \partial d > 0$, we need

$$f'(\varepsilon^*(d)) > \frac{-(f(\varepsilon^*(d)))^2 (2 + 2(1 - F(\varepsilon^*(d))))}{(1 - F(\varepsilon^*(d))) + (1 - F(\varepsilon^*(d)))^2}, \quad (\text{F5})$$

that is, $f'(\varepsilon^*(d))$ may be negative, but not too negative. For the uniform distribution in the main text, this holds immediately with $f'(\varepsilon^*(d)) = 0$. Another distribution commonly used in housing search models is the exponential distribution (see, for example, Guren and McQuade, 2020). With an exponential distribution with rate parameter $\lambda > 0$,

$$f'(\varepsilon^*(d)) = -\lambda^2 \exp(-\lambda \varepsilon^*(d)) \quad (\text{F6})$$

and

$$\frac{-(f(\varepsilon^*(d)))^2 (2 + 2(1 - F(\varepsilon^*(d))))}{(1 - F(\varepsilon^*(d))) + (1 - F(\varepsilon^*(d)))^2} = \frac{-2\lambda^2 \exp(-2\lambda \varepsilon^*(d)) - 2\lambda^2 \exp(-3\lambda \varepsilon^*(d))}{\exp(-\lambda \varepsilon^*(d)) + \exp(-2\lambda \varepsilon^*(d))}. \quad (\text{F7})$$

Hence, noting that

$$(1 - F(\varepsilon^*(d))) + (1 - F(\varepsilon^*(d)))^2 = \exp(-\lambda \varepsilon^*(d)) + \exp(-2\lambda \varepsilon^*(d)) > 0, \quad (\text{F8})$$

we have that

$$\begin{aligned}
& f'(\varepsilon^*(d)) \left((1 - F(\varepsilon^*(d))) + (1 - F(\varepsilon^*(d)))^2 \right) \\
&= -\lambda^2 \exp(-2\lambda\varepsilon^*(d)) - \lambda^2 \exp(-3\lambda\varepsilon^*(d)) \\
&= -\lambda^2 \left(\exp(-2\lambda\varepsilon^*(d)) + \exp(-3\lambda\varepsilon^*(d)) \right) < 0,
\end{aligned} \tag{F9}$$

while in the numerator of (F7),

$$\begin{aligned}
& - (f(\varepsilon^*(d)))^2 \left(2 + 2(1 - F(\varepsilon^*(d))) \right) \\
&= -2\lambda^2 \left(\exp(-2\lambda\varepsilon^*(d)) + \exp(-3\lambda\varepsilon^*(d)) \right) < 0.
\end{aligned} \tag{F10}$$

Therefore,

$$\begin{aligned}
& f'(\varepsilon^*(d)) \left((1 - F(\varepsilon^*(d))) + (1 - F(\varepsilon^*(d)))^2 \right) \\
& > (f(\varepsilon^*(d)))^2 \left(2 + 2(1 - F(\varepsilon^*(d))) \right)
\end{aligned} \tag{F11}$$

as $2 > 1$ and both sides are negative, such that

$$f'(\varepsilon^*(d)) > -\frac{(f(\varepsilon^*(d)))^2 \left(2 + 2(1 - F(\varepsilon^*(d))) \right)}{(1 - F(\varepsilon^*(d))) + (1 - F(\varepsilon^*(d)))^2} \tag{F12}$$

as desired. Even though the exponential distribution's probability density function has a negative slope, it is not too negative, such that our key result that reservation dividends increase with distance to the city center still holds. The results that liquidity and prices decrease with distance to the city center follow from this result, as shown in the main text.

G Extended model with bargaining

We extend our model with a bargaining process, following Carrillo (2012). With this addition, the model features asking prices and sales prices, which allows us to form a model notion of an asking price discount (APD), as in the internet empirical results. In this model, the asking price discount will always be weakly negative. In the data, it can reach positive values, however, in most cases, it is indeed weakly negative.

The search process changes as follows. When a buyer visits a housing unit, the buyer and the seller may or may not bargain, which is determined stochastically. With probability θ , the seller does not accept counteroffers, and $p(d)$ is a take-it-or-leave-it offer (“no-counteroffer scenario”, subscript n). The buyer accepts or rejects the offer. If the buyer accepts, the seller receives $p(d)$, and the buyer receives their first housing dividend ε and incurs their first commuting cost $\tau(d)$ in the following period. If the buyer rejects, the seller relists the property, and the buyer visits a new housing unit in the following period. With probability $1 - \theta$, the buyer can bargain by making a take-it-or-leave-it counteroffer $o(d)$ to the seller (“counteroffer scenario”, subscript c). If the buyer makes a counteroffer, the seller accepts or rejects the offer. The outcomes of accepting or rejecting the offer are analogous to those in the no-counteroffer scenario.

Changes in the seller’s problem. The seller maximizes their expected profit $\Pi(d)$ over an asking price $p(d)$ and a reservation value $r(d)$. We assume that buyers have perfect information about sellers’ decision problems. Hence, in the counteroffer scenario, the offer $o(d)$ is equal to the seller’s reservation value $r(d)$, as this offer corresponds to the lowest price the seller is willing to accept. In the following, we denote by $\gamma_n(d)$ the probability that a buyer is willing to buy in the no-counteroffer scenario. The analogous

probability in the counteroffer scenario is $\gamma_c(d)$. The expected profit is

$$\begin{aligned}\Pi(d) = & \theta \left(\gamma_n(d)p(d) + (1 - \gamma_n(d))\beta\Pi(d) \right) \\ & + (1 - \theta) \left(\gamma_c(d) \max [r(d), \beta\Pi(d)] + (1 - \gamma_c(d))\beta\Pi(d) \right).\end{aligned}\quad (\text{G1})$$

Changes in the buyer's problem. The buyer's search value is given by

$$W = E_{d,\varepsilon} [\theta V_n(d, \varepsilon) + (1 - \theta) V_c(d, \varepsilon)]. \quad (\text{G2})$$

The buyer's value in the no-counteroffer scenario is given by

$$V_n(d, \varepsilon) = \max [V(d, \varepsilon) - p(d), \beta W]. \quad (\text{G3})$$

The buyer's value in the counteroffer scenario is given by

$$V_c(d, \varepsilon) = \max [\delta(d)(V(d, \varepsilon) - o(d)) + (1 - \delta(d))(\beta W), \beta W], \quad (\text{G4})$$

where $\delta(d)$ denotes the probability that the seller accepts the buyer's counteroffer. The seller always accepts the optimal counteroffer $o(d) = r(d)$. Hence, $\delta(d) = 1$ at all distances to the city center in equilibrium.

G.1 Equilibrium in the extended model

Seller's optimization. Since the counteroffer $o(d) = r(d)$ is the lowest price that the seller is willing to accept, the seller's reservation value $r(d) = \beta\Pi(d)$. The expression for

the expected profit (G1) then simplifies to

$$\Pi(d) = \theta \gamma_n(d) p(d) + (1 - \theta \gamma_n(d)) r(d). \quad (G5)$$

Optimizing with regard to the asking price $p(d)$ yields

$$p(d) = r(d) - \frac{\gamma_n(d)}{\partial \gamma_n / \partial p(d)|_d}, \quad (G6)$$

and plugging the condition $r(d) = \beta \Pi(d)$ into (G5) yields

$$r(d) = \frac{\beta \theta \gamma_n(d) p(d)}{1 - \beta (1 - \theta \gamma_n(d))}. \quad (G7)$$

The pair of the optimal asking price and reservation value for a given distance to the city center solves equations (G6) and (G7) simultaneously.

Buyer's optimization. Via the buyer value function in the no-counteroffer scenario (G3), we define a reservation dividend $\varepsilon_n^*(d)$ such that a buyer is indifferent between buying a housing unit and continuing to search:

$$V(d, \varepsilon_n^*(d)) - p(d) = \beta W. \quad (G8)$$

Analogously, via the buyer value function in the counteroffer scenario (G4), we define a reservation dividend $\varepsilon_c^*(d)$ such that

$$V(d, \varepsilon_c^*(d)) - r(d) = \beta W. \quad (G9)$$

Probability of sale. The probability of sale conditional on a bargaining scenario is equal to the probability that the buyer's idiosyncratic dividend is above their respective reservation dividend. Hence, in the no-counteroffer scenario,

$$\gamma_n(d) = 1 - F(\varepsilon_n^*(d)) \quad (G10)$$

and in the counteroffer scenario,

$$\gamma_c(d) = 1 - F(\varepsilon_c^*(d)). \quad (G11)$$

Thus, for the derivative in the seller optimality condition (G6) we have that

$$\frac{\partial \gamma_n}{\partial p(d)|_d} = -f(\varepsilon_n^*(d)) \frac{\partial \varepsilon_n^*}{\partial p(d)|_d}. \quad (G12)$$

By proceeding as in the main text, we get

$$\varepsilon_n^*(d) = \frac{1 - \pi\beta}{\beta} p(d) + \tau(d) - (1 - \pi)\Pi(d) + (\pi - \pi\beta)W \quad (G13)$$

and

$$\frac{\partial \gamma_n}{\partial p(d)|_d} = -f(\varepsilon_n^*(d)) \frac{1 - \pi\beta}{\beta}. \quad (G14)$$

Analogous relations hold for the counteroffer scenario.

G.2 Analytical results in the extended model

Again, we start with auxiliary derivations, applying $\varepsilon \sim U[\underline{\varepsilon}, \bar{\varepsilon}]$. First, Lemma 1 enables us to simplify expressions that contain reservation dividends and probabilities of sale.

Lemma 1. *The buyer reservation dividends in the counteroffer scenario and the no-counteroffer scenario relate as $\varepsilon_c^*(d) = 2\varepsilon_n^*(d) - \bar{\varepsilon}$. The probabilities of sale in these two scenarios relate as $\gamma_c(d) = 2\gamma_n(d)$.*

Proof. Using the buyer indifference conditions (G8) and (G9) together with the linear expression of the buyer value function (10), we have that

$$\varepsilon_n^*(d) = \frac{1 - \pi\beta}{\beta} p(d) + \tau(d) - (1 - \pi)(\Pi(d) + W) + (1 - \pi\beta)W \quad (\text{G15})$$

and

$$\varepsilon_c^*(d) = \frac{1 - \pi\beta}{\beta} r(d) + \tau(d) - (1 - \pi)(\Pi(d) + W) + (1 - \pi\beta)W. \quad (\text{G16})$$

With the seller optimality condition (G6), the equilibrium relation between probabilities of sale and reservation dividends in the no-counteroffer scenario (G10), and the value of the derivative in (G14), we get

$$\varepsilon_n^*(d) - \varepsilon_c^*(d) = \frac{1 - \pi\beta}{\beta} (p(d) - r(d)) = \frac{1 - \pi\beta}{\beta} \left(-\frac{\gamma_n(d)}{\partial \gamma_n / \partial p(d)|_d} \right) \quad (\text{G17})$$

$$= \frac{1 - \pi\beta}{\beta} \left(-\frac{\frac{\bar{\varepsilon} - \varepsilon_n^*(d)}{\bar{\varepsilon} - \varepsilon}}{-\frac{1 - \pi\beta}{\beta} \frac{1}{\bar{\varepsilon} - \underline{\varepsilon}}} \right) \quad (\text{G18})$$

which means that

$$\varepsilon_c^*(d) = 2\varepsilon_n^*(d) - \bar{\varepsilon}. \quad (\text{G19})$$

Translating the reservation dividends back into probabilities of sale, we have that

$$\bar{\varepsilon} - (\bar{\varepsilon} - \underline{\varepsilon})\gamma_c(d) = 2(\bar{\varepsilon} - (\bar{\varepsilon} - \underline{\varepsilon})\gamma_n(d)) - \bar{\varepsilon} \quad (\text{G20})$$

and hence $\gamma_c(d) = 2\gamma_n(d)$. □

Lemma 2. *The reservation dividends in the no-counteroffer scenario $\varepsilon_n^*(d)$ and in the counteroffer scenario $\varepsilon_c^*(d)$ increase with distance to the city center d .*

Proof. We know from (G13) that

$$\varepsilon_n^*(d) = \frac{1 - \pi\beta}{\beta} p(d) + \tau(d) - (1 - \pi)\Pi(d) + (\pi - \pi\beta)W.$$

Analogously to the main derivations, we reformulate the asking price $p(d)$ and the expected profit from reselling the property $\Pi(d)$ in terms of the reservation dividend $\varepsilon_n^*(d)$.

First, we combine the seller optimality conditions (G6) and (G7) and get

$$p(d) = -\frac{(1 - \beta)\gamma_n(d) + \beta\theta\gamma_n^2(d)}{(1 - \beta)(\partial\gamma_n/\partial p(d)|_d)}. \quad (\text{G21})$$

Expressing the probability of sale $\gamma_n(d)$ and the derivative $\partial\gamma_n/\partial p(d)|_d$ in terms of the reservation dividend $\varepsilon_n^*(d)$ using the equilibrium relations (G10) and (G14), we have

that

$$p(d) = \frac{\beta(\bar{\varepsilon} - \varepsilon_n^*(d))}{1 - \pi\beta} + \frac{\beta^2\theta(\bar{\varepsilon} - \varepsilon_n^*(d))^2}{(1 - \beta)(1 - \pi\beta)(\bar{\varepsilon} - \underline{\varepsilon})}. \quad (\text{G22})$$

Next, using the seller's conditions (G5) and (G6), we get

$$\Pi(d) = p(d) + \frac{\gamma_n(d) - \theta\gamma_n^2(d)}{\partial\gamma_n/\partial p(d)|_d}, \quad (\text{G23})$$

which, using (G22) and again expressing the probability of sale and the derivative in terms of the reservation dividend via (G10) and (G14), amounts to

$$\Pi(d) = \frac{\beta\theta(\bar{\varepsilon} - \varepsilon_n^*(d))^2}{(1 - \beta)(1 - \pi\beta)(\bar{\varepsilon} - \underline{\varepsilon})}. \quad (\text{G24})$$

Plugging these results into the linear reservation dividend expression (G13) and taking the derivative with respect to the distance to the city center d on both sides yields

$$\frac{\partial\varepsilon_n^*}{\partial d} \underbrace{\left(2 + 2\frac{\pi\beta\theta}{1 - \pi\beta} \frac{\bar{\varepsilon} - \varepsilon_n^*(d)}{\bar{\varepsilon} - \underline{\varepsilon}}\right)}_{>0} = \frac{\partial\tau}{\partial d} > 0 \quad (\text{G25})$$

and therefore $\partial\varepsilon_n^*/\partial d > 0$. Via Lemma 1, also $\partial\varepsilon_c^*/\partial d > 0$. \square

Corollary 1. *The expected profit $\Pi(d)$, the asking price $p(d)$, the seller reservation value $r(d)$, and $\mathbb{E}[\text{Sales price}(d)] = \theta p(d) + (1 - \theta)r(d)$ decrease with distance to the city center d .*

Proof. Using (G24), we have that

$$\frac{\partial\Pi}{\partial d} = -\frac{\partial\varepsilon_n^*}{\partial d} \frac{2\beta\theta(\bar{\varepsilon} - \varepsilon_n^*(d))}{(1 - \beta)(1 - \pi\beta)(\bar{\varepsilon} - \underline{\varepsilon})} < 0, \quad (\text{G26})$$

where $\partial \varepsilon_n^* / \partial d > 0$ via Lemma 2. Next, using (G22), we get

$$\frac{\partial p}{\partial d} = -\frac{\partial \varepsilon_n^*}{\partial d} \left(\frac{\beta}{1 - \pi\beta} + \frac{2\beta^2\theta(\bar{\varepsilon} - \varepsilon_n^*(d))}{(1 - \beta)(1 - \pi\beta)(\bar{\varepsilon} - \underline{\varepsilon})} \right) < 0. \quad (\text{G27})$$

Proceeding as in the proof of Lemma 1, we have that

$$r(d) = p(d) - \frac{\beta(\bar{\varepsilon} - \varepsilon_n^*(d))}{1 - \pi\beta} = \frac{\beta^2\theta(\bar{\varepsilon} - \varepsilon_n^*(d))^2}{(1 - \beta)(1 - \pi\beta)(\bar{\varepsilon} - \underline{\varepsilon})}. \quad (\text{G28})$$

Then,

$$\frac{\partial r}{\partial d} = -\frac{\partial \varepsilon_n^*}{\partial d} \frac{2\beta^2\theta(\bar{\varepsilon} - \varepsilon_n^*(d))}{(1 - \pi\beta)(1 - \beta)(\bar{\varepsilon} - \underline{\varepsilon})} < 0. \quad (\text{G29})$$

$\mathbb{E}[\text{Sales price}(d)] = \theta p(d) + (1 - \theta)r(d)$ decreases with distance to the city center, as both the asking price $p(d)$ and the seller reservation value $r(d)$ decrease with distance to the city center. \square

Time on the market. The probability $\gamma_{nc}(d)$ that a housing unit sells in a period is given via the probabilities for the two bargaining scenarios and the corresponding probabilities of sale:

$$\gamma_{nc}(d) = \theta\gamma_n(d) + (1 - \theta)\gamma_c(d). \quad (\text{G30})$$

The expected time on the market at a given distance to the city center is

$$\mathbb{E}[\text{TOM}(d)] = \frac{1}{\gamma_{nc}(d)}. \quad (\text{G31})$$

Proposition 1. *The expected time on the market $\mathbb{E}[\text{TOM}(d)]$ increases with distance to the*

city center d in the extended model with bargaining.

Proof. Using Lemma 1 and the equilibrium relations between the reservation dividends and the probabilities of sale (G10) and (G11), we can express the expected time on the market in terms of the reservation dividend in the no-counteroffer scenario:

$$\mathbb{E}[TOM(d)] = \frac{1}{(2-\theta)\gamma_n(d)} = \frac{\bar{\varepsilon} - \underline{\varepsilon}}{(2-\theta)(\bar{\varepsilon} - \varepsilon_n^*(d))}. \quad (G32)$$

The derivative of the expected time on the market with respect to the distance to the city center amounts to

$$\frac{\partial \mathbb{E}[TOM]}{\partial d} = \frac{\partial \varepsilon_n^*}{\partial d} \underbrace{\frac{\bar{\varepsilon} - \underline{\varepsilon}}{2-\theta} (\bar{\varepsilon} - \varepsilon_n^*(d))^{-2}}_{>0} > 0. \quad (G33)$$

□

Intuition. See main text.

Asking price discount. The expected asking price discount at a given distance to the city center is

$$\mathbb{E}[APD(d)] = \theta \times APD_n(d) + (1-\theta) \times APD_c(d) = (1-\theta) \times APD_c(d), \quad (G34)$$

where the asking price discount in the no-counteroffer scenario $APD_n(d) = 0$. We define the asking price discount in the counteroffer scenario analogously to our empirical measure as

$$APD_c(d) = \frac{r(d) - p(d)}{p(d)}. \quad (G35)$$

Proposition 2. *Given that the probability of no counteroffer $\theta \in (0, 1)$, the expected asking price discount $\mathbb{E}[APD(d)] < 0$ becomes more negative with distance to the city center d .*

Proof. If $\theta = 1$, then the asking price discount is always equal to zero, as the probability of being in the no-counteroffer scenario is equal to one, and hence the asking price is the same as the sales price at all distances to the city center. This corresponds to the setup in the main model. In the following, we consider $\theta < 1$. Using the expression for the optimal reservation value $r(d)$ of a seller (G7), we have that

$$APD_c(d) = \frac{\frac{\beta\theta\gamma_n(d)p(d)}{1-\beta(1-\theta\gamma_n(d))} - p(d)}{p(d)} = \underbrace{\frac{1}{1-\beta + \beta\theta\frac{\bar{\varepsilon}-\varepsilon_n^*(d)}{\bar{\varepsilon}-\varepsilon}}}_{>0} \underbrace{(\beta-1)}_{<0} < 0. \quad (\text{G36})$$

Hence, the expected asking price discount $\mathbb{E}[APD(d)] = (1-\theta)APD_c(d) < 0$. The derivative of $\mathbb{E}[APD(d)]$ with respect to the distance to the city center amounts to

$$\frac{\partial \mathbb{E}[APD]}{\partial d} = \frac{\partial \mathbb{E}[APD_c]}{\partial d} = \underbrace{\left(1-\beta + \beta\theta\frac{\bar{\varepsilon}-\varepsilon_n^*(d)}{\bar{\varepsilon}-\varepsilon}\right)^{-2}}_{>0} \underbrace{\frac{\beta\theta}{\bar{\varepsilon}-\varepsilon} \frac{\partial \varepsilon_n^*}{\partial d} (\beta-1)}_{<0} < 0, \quad (\text{G37})$$

provided that $\theta > 0$. □

Intuition. As for the time on the market, the relevant condition for liquidity in the form of the asking price discount to decrease with distance to the city center is that reservation dividends increase with distance to the city center. In principle, both the asking price and the seller reservation value decrease with distance to the city center (see Corollary 1). For the expected asking price discount to become more negative with distance to the city center, we need that the seller reservation value decreases more steeply with distance to

the city center than the asking price.²⁸ Why is this condition fulfilled? Recall from the seller optimization that the reservation value is equal to the discounted profit of the next period in equilibrium, as otherwise, the seller would always reject the buyer's optimal counteroffer. For the asking price discount to become more negative with distance to the city center, we, therefore, need that the expected profit decreases more steeply than the asking price.²⁹ A formal proof of this statement follows shortly. Intuitively, we can express the expected profit in terms of the probability of sale and the asking price. Since both the probability of sale and the asking price decrease with distance to the city center and the expected profit is composed of the two, the expected profit decreases more steeply than the asking price alone. *Proof: the expected profit decreases more steeply with distance to the city center than the asking price.* Via (G5), we can express the expected profit as

$$\Pi(d) = \theta \gamma_n(d) p(d) + (1 - \theta \gamma_n(d)) \beta \Pi(d),$$

²⁸Formally,

$$\frac{\partial \mathbb{E}[APD]}{\partial d} = (1 - \theta) \frac{\partial \left(\frac{r-p}{p} \right)}{\partial d} = (1 - \theta) \left(\frac{\partial r}{\partial d} \frac{1}{p(d)} - \frac{\partial p}{\partial d} \frac{r}{(p(d))^2} \right), \quad (G38)$$

such that for the expected asking price discount to decrease with distance to the city center, we need

$$\underbrace{\frac{\partial r / \partial d}{r(d)}}_{<0} < \underbrace{\frac{\partial p / \partial d}{p(d)}}_{<0}, \quad (G39)$$

where both sides of the expression are < 0 due to Corollary 1.

²⁹Formally,

$$\frac{\partial r / \partial d}{r(d)} = \frac{\partial (\beta \Pi) / \partial d}{\beta \Pi(d)} = \frac{\partial \Pi / \partial d}{\Pi(d)} < \frac{\partial p / \partial d}{p(d)}. \quad (G40)$$

since the seller's reservation value $r(d) = \beta \Pi(d)$ via the optimal counteroffer of the buyer.

Then,

$$\Pi(d) = \frac{\theta \gamma_n(d) p(d)}{1 - \beta + \theta \beta \gamma_n(d)} \quad (\text{G41})$$

and

$$\frac{\partial \Pi}{\partial d} = \frac{(1 - \beta + \theta \beta \gamma_n(d)) \left(\theta \frac{\partial \gamma_n}{\partial d} p(d) + \theta \gamma_n(d) \frac{\partial p}{\partial d} \right) - \theta^2 \beta \frac{\partial \gamma_n}{\partial d} \gamma_n(d) p(d)}{(1 - \beta + \theta \beta \gamma_n(d))^2}. \quad (\text{G42})$$

The proportional derivative of $\Pi(d)$ with respect to d is then

$$\frac{\partial \Pi / \partial d}{\Pi(d)} = \underbrace{\frac{\partial \gamma_n / \partial d}{\gamma_n(d)}_{<0}} + \underbrace{\frac{\partial p / \partial d}{p(d)}_{<0}} - \underbrace{\frac{(\theta \beta)(\partial \gamma_n / \partial d)}{1 - \beta + \theta \beta \gamma_n(d)}_{<0}}. \quad (\text{G43})$$

Statement (G40) says that

$$\frac{\partial \Pi / \partial d}{\Pi(d)} < \frac{\partial p / \partial d}{p(d)}, \quad (\text{G44})$$

for which to hold we need that

$$\frac{\partial \gamma_n / \partial d}{\gamma_n(d)} < \frac{(\theta \beta)(\partial \gamma_n / \partial d)}{1 - \beta + \theta \beta \gamma_n(d)}. \quad (\text{G45})$$

As $\partial \gamma_n / \partial d < 0$, this expression simplifies to

$$\frac{1}{\gamma_n(d)} > \frac{\theta \beta}{1 - \beta + \theta \beta \gamma_n(d)}, \quad (\text{G46})$$

or equivalently

$$1 - \beta > 0, \quad (\text{G47})$$

which is true, since $\beta \in (0, 1)$. Therefore, $\frac{\partial \Pi / \partial d}{\Pi(d)} < \frac{\partial p / \partial d}{p(d)}$, as required. \square

Relation between time on the market and asking price discount. Via the proofs of Propositions 1 and 2, we can directly derive that housing units that spend more time on the market also sell at more negative discounts. Thus, lower liquidity in one measure corresponds to lower liquidity in the other measure.

Corollary 2. *Given that the probability of no counteroffer $\theta \in (0, 1)$, the model correlation between the expected asking price discount $\mathbb{E}[APD(d)]$ and the expected time on the market $\mathbb{E}[TOM(d)]$ is negative.*

Proof. We start by expressing the asking price discount in terms of the time on the market. From the proofs of Propositions 1 and 2 we have that

$$\mathbb{E}[APD(d)] = \frac{\beta - 1}{1 - \beta + \frac{\beta \theta}{(2 - \theta)\mathbb{E}[TOM(d)]}} \quad (\text{G48})$$

Provided that $\theta \in (0, 1)$, the derivative of the expected time on the market with respect to the expected asking price discount, given a distance to the city center d is then

$$\frac{\partial \mathbb{E}[APD]}{\partial \mathbb{E}[TOM(d)]|_d} = \underbrace{\left(1 - \beta + \frac{\beta \theta}{(2 - \theta)\mathbb{E}[TOM(d)]}\right)^{-2}}_{>0} \frac{\beta \theta}{2 - \theta} \underbrace{\left(\mathbb{E}[TOM(d)]\right)^{-2}}_{<0} \underbrace{(\beta - 1)}_{<0} < 0. \quad (\text{G49})$$

\square

H Equilibrium existence and uniqueness

We show existence and uniqueness of an equilibrium in the extended model. The main model is obtained by setting the probability of the no-counteroffer scenario $\theta = 1$.

H.1 Equilibrium existence

First, we show the existence of a solution. Evidently, we find a solution numerically, nevertheless, we prove its existence formally, following Krainer (2001). As in (10), we can express the buyer's value in the extended model as

$$V(d, \varepsilon) = \frac{\beta}{1 - \pi\beta} \left(\varepsilon - \tau(d) + (1 - \pi) (\Pi(d) + W) \right). \quad (\text{H1})$$

Hence, $V(d, \varepsilon)$ is linear in ε and there exist reservation dividends as defined in the buyer indifference conditions (G8) and (G9). In what follows, we express the other endogenous variables in terms of the buyer's reservation dividends, the model parameters, and the travel cost function to prove uniqueness of the solution. The fact that reservation dividends exist then implies that a solution also exists, as the remaining objects listed in the previous sentence are exogenous.

H.2 Equilibrium uniqueness

To show uniqueness, we follow Vanhapelto and Magnac (2024), showing that two possible ways of expressing the value of search allow for only one pair of the buyer reservation dividends $\{\varepsilon_n^*(d), \varepsilon_c^*(d)\}$ at every distance to the city center such that both of these expressions hold. The first expression decreases in the buyer reservation dividends, whereas the second expression increases. Hence, given a set of parameters and a travel

cost function, the model's solution is unique, as we express all endogenous variables in terms of parameters, the exogenous travel cost, and the endogenous buyer reservation dividends.

Expression 1. We set up the first expression for the value of search in terms of the buyer reservation dividends via the definitions (G2), (G3), and (G4):

$$W = \mathbb{E}_{d,\varepsilon} [\theta \max [V(d, \varepsilon) - p(d), \beta W] + (1 - \theta) \max [V(d, \varepsilon) - r(d), \beta W]], \quad (H2)$$

and hence

$$W = \frac{1}{1 - \beta} \mathbb{E}_{d,\varepsilon} [\theta \max [V(d, \varepsilon) - p(d) - \beta W, 0] + (1 - \theta) \max [V(d, \varepsilon) - r(d) - \beta W, 0]]. \quad (H3)$$

Next, we express the relations within the max operators in terms of the buyer reservation dividends. Note that when the buyer indifference conditions (G8) and (G9) hold, we have that

$$\beta W = V(d, \varepsilon_n^*(d)) - p(d) = V(d, \varepsilon_c^*(d)) - r(d). \quad (H4)$$

Inserting the linear buyer value (H1), we get

$$\beta W = \frac{\beta}{1 - \pi \beta} (\varepsilon_n^*(d) - \tau(d) + (1 - \pi)(\Pi(d) + W)) - p(d) \quad (H5)$$

and

$$\beta W = \frac{\beta}{1 - \pi\beta} \left(\varepsilon_c^*(d) - \tau(d) + (1 - \pi) (\Pi(d) + W) \right) - r(d). \quad (\text{H6})$$

Hence,

$$\frac{\beta}{1 - \pi\beta} \varepsilon_n^*(d) = \frac{\beta}{1 - \pi\beta} \tau(d) - \frac{\beta(1 - \pi)}{1 - \pi\beta} \Pi(d) + \frac{\pi\beta(1 - \beta)}{1 - \pi\beta} W + p(d) \quad (\text{H7})$$

and

$$\frac{\beta}{1 - \pi\beta} \varepsilon_c^*(d) = \frac{\beta}{1 - \pi\beta} \tau(d) - \frac{\beta(1 - \pi)}{1 - \pi\beta} \Pi(d) + \frac{\pi\beta(1 - \beta)}{1 - \pi\beta} W + r(d). \quad (\text{H8})$$

Again using (H1), we can express the sum within the first max operator from (H3) as

$$V(d, \varepsilon) - p(d) - \beta W = \frac{\beta}{1 - \pi\beta} \varepsilon + - \frac{\beta}{1 - \pi\beta} \tau(d) + \frac{\beta(1 - \pi)}{1 - \pi\beta} \Pi(d) - p(d) - \frac{\pi\beta(1 - \beta)}{1 - \pi\beta} W.$$

Then, via (H7), we get

$$V(d, \varepsilon) - p(d) - \beta W = \frac{\beta}{1 - \pi\beta} \varepsilon - \frac{\beta}{1 - \pi\beta} \varepsilon_n^*(d) = \frac{\beta}{1 - \pi\beta} (\varepsilon - \varepsilon_n^*(d)). \quad (\text{H9})$$

Analogously, using (H8), we have that

$$V(d, \varepsilon) - r(d) - \beta W = \frac{\beta}{1 - \pi\beta} (\varepsilon - \varepsilon_c^*(d)). \quad (\text{H10})$$

We can then express the value of search from (H3) as

$$W = \frac{1}{1-\beta} \mathbb{E}_{d,\varepsilon} \left[\theta \max \left[\frac{\beta}{1-\pi\beta} (\varepsilon - \varepsilon_n^*(d)), 0 \right] + (1-\theta) \max \left[\frac{\beta}{1-\pi\beta} (\varepsilon - \varepsilon_c^*(d)), 0 \right] \right] \quad (\text{H11})$$

which decreases in $\varepsilon_n^*(d)$ and $\varepsilon_c^*(d)$.

Expression 2. We set up the second expression via the buyer indifference conditions. First, using the linear form of the buyer value (H1), we can express the indifference condition for the no-counteroffer scenario (G8) as

$$W = \frac{1}{\pi - \pi\beta} \left(\varepsilon_n^*(d) - \tau(d) + (1-\pi)\Pi(d) - \frac{1-\pi\beta}{\beta} p(d) \right). \quad (\text{H12})$$

We can express the price and the profit in terms of the reservation dividend in the no-counteroffer scenario via (G22) and (G24), such that

$$W = \frac{1}{\pi - \pi\beta} \left(2\varepsilon_n^*(d) - \bar{\varepsilon} - \tau(d) - \frac{(\pi - \pi\beta)\beta\theta(\bar{\varepsilon} - \varepsilon_n^*(d))^2}{(1-\beta)(1-\pi\beta)(\bar{\varepsilon} - \underline{\varepsilon})} \right). \quad (\text{H13})$$

Hence,

$$\frac{\partial W}{\partial \varepsilon_n^*(d)|_d} = \frac{2}{\pi - \pi\beta} + \frac{2\beta\theta(\bar{\varepsilon} - \varepsilon_n^*(d))}{(1-\beta)(1-\pi\beta)(\bar{\varepsilon} - \underline{\varepsilon})} > 0. \quad (\text{H14})$$

Via Lemma 1, also $\partial W / \partial \varepsilon_c^*(d)|_d > 0$. Since Expression 1 for the value of search decreases in both reservation dividends and Expression 2 increases in both reservation dividends, there can only be a single pair of reservation dividends $\{\varepsilon_n^*(d), \varepsilon_c^*(d)\}$ at a given distance to the city center such that Expression 1 and Expression 2 hold simultaneously. With W being constant across space, it immediately follows that this holds for all distances.

I Model solution method

The equilibrium condition (4), which describes the value of search W as an expectation over distances to the city center and idiosyncratic dividends, and the equilibrium conditions (2), (6), (8), and (9), which have to hold for all distances to the city center $d^\Delta \in \mathcal{D}^\Delta$, constitute the relevant system of $1+z \times 4$ equations. Solving the system as it is via standard solvers brings up problems of numerical instability due to the high degree of non-linearity involved. Hence, we instead iterate over the value of search to find a value that is consistent with (2), (6), (8), and (9) at each $d^\Delta \in \mathcal{D}^\Delta$.

We implement the iteration as follows. First, we initialize an arbitrary guess for the value of search. Given this guess, we solve (2), (6), (8), and (9) for all $d^\Delta \in \mathcal{D}^\Delta$. We update the guess via

$$\tilde{W} = \frac{1}{z} \sum_{d^\Delta \in \mathcal{D}^\Delta} \gamma(d^\Delta) \left(V(d^\Delta, \frac{\varepsilon^*(d^\Delta) + \bar{\varepsilon}}{2}) - p(d^\Delta) \right) + (1 - \gamma(d^\Delta)) (\beta W), \quad (\text{I1})$$

using that a buyer purchases a housing unit at d^Δ with probability of sale $\gamma(d^\Delta)$ and continues to search with probability $1 - \gamma(d^\Delta)$, which follows the alternative definition of the value of search in Krainer and LeRoy (2002) and is simply a rewritten version of the expectation in (4). This expression only requires information from (2), (6), (8), and (9). The new guess for the value of search is then set to \tilde{W} , and the whole process is repeated until $W = \tilde{W}$ up to a fixed iteration tolerance. In principle, convergence is not necessarily guaranteed by the standard contraction mapping theorem, even though $(1 - \gamma(d^\Delta))\beta < 1$, as the entire right-hand side of (I1) depends on W . In practice, convergence is not a problem and we obtain fast and reliable solutions, which allows us to estimate the model's structural parameters without problems.

J Additional model results

J.1 Variance of time on the market across space

An additional prediction of our model mentioned in Section 4.3 is that the variance of time on the market increases with distance to the city center. To see this, consider the variance of the geometric distribution that results from the multiplication of sale probabilities over time, together with the equilibrium relation (9) between probabilities of sale and reservation dividends:

$$\text{Var}[TOM(d)] = \frac{1 - \gamma(d)}{(\gamma(d))^2} = \frac{\frac{\varepsilon^*(d) - \underline{\varepsilon}}{\bar{\varepsilon} - \underline{\varepsilon}}}{\left(\frac{\bar{\varepsilon} - \varepsilon^*(d)}{\bar{\varepsilon} - \underline{\varepsilon}}\right)^2} = (\bar{\varepsilon} - \underline{\varepsilon}) \frac{\varepsilon^*(d) - \underline{\varepsilon}}{(\bar{\varepsilon} - \varepsilon^*(d))^2}. \quad (\text{J1})$$

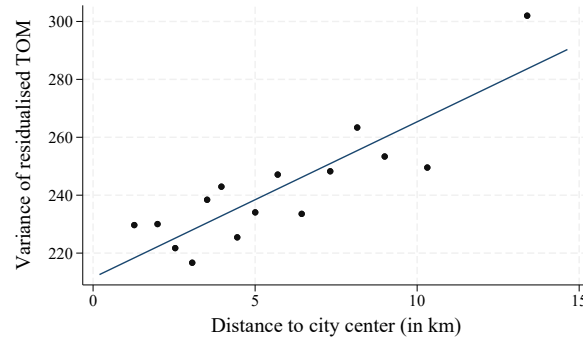
Taking the derivative with respect to the distance to the city center yields

$$\frac{\partial \text{Var}[TOM(d)]}{\partial d} = \frac{\partial \varepsilon^*}{\partial d} (\bar{\varepsilon} - \underline{\varepsilon}) \underbrace{\frac{(\bar{\varepsilon} - \varepsilon^*(d))^2 + 2(\bar{\varepsilon} - \varepsilon^*(d))(\varepsilon^*(d) - \underline{\varepsilon})}{(\bar{\varepsilon} - \varepsilon^*(d))^4}}_{>0} > 0 \quad (\text{J2})$$

with auxiliary result (16) that the reservation dividend $\varepsilon^*(d)$ increases with distance to the city center. Intuitively, with a lower probability of a successful sale in the outskirts, a higher variability in success rates can realize, and therefore also a higher variability in time on the market.

We test this prediction of the model using transaction-level data from Germany. To focus on the relationship between distance to the city center and the variance of time on the market we estimate Regression (1) with time on the market as the dependent variable. We then use the squared residuals as our measure of time on the market variance, having accounted for differences in property characteristics. Finally, in Figure J1, we plot the

Figure J1: Variance of time on the market and distance to the city center, Germany (2012–2024)



Notes: This binned scatter plot shows the relation between the variance of the residualized time on the market and distance to the city center, using 15 equally-sized distance bins. The data points are calculated using the main specification of Regression (1). The binned scatter plot is produced following Cattaneo et al. (2024).

squared residuals against distance to the city center. The Figure shows that the variance increases with distance to the city center, thereby confirming the model's prediction.

J.2 Magnitude of price vs. liquidity gradient

Another prediction of our model mentioned in Section 4.3. is that the price gradient is larger than the liquidity gradient. For this comparison, we express both gradients in absolute values and in relative terms for immediate comparison. For the expected time on the market, this gradient is

$$\left| \frac{\partial \mathbb{E}[TOM]/\partial d}{\mathbb{E}[TOM(d)]} \right| = \left| \frac{\partial \gamma/\partial d}{\gamma(d)} \right|, \quad (J3)$$

by definition of the time on the market. Using the probability of sale $\gamma(d)$ here instead of the reservation dividend $\varepsilon^*(d)$ simplifies the comparison to the expression for the relative price gradient. Using (12) and (F1), the relative price gradient amounts to

$$\left| \frac{(\partial \gamma/\partial d) \left(1 + 2 \left(\beta/(1-\beta) \right) \gamma(d) \right)}{\gamma(d) + \left(\beta/(1-\beta) \right) (\gamma(d))^2} \right| > \left| \frac{\partial \gamma/\partial d}{\gamma(d)} \right|. \quad (J4)$$

This is due to the factor 2 in front of $(\beta/(1 - \beta))$, which results from the expression for expected profit in which the seller obtains a value of selling the property in the next period with probability $(\gamma(d))^2$. This option of selling the property in the future is priced in today. For a given increase in the expected time on the market when going further away from the city center, the corresponding price decreases more. The demand-driven level of liquidity, given a stationary equilibrium, will also determine market conditions in the following period in case the seller is not able to sell their housing unit in this period. With a successful sale in the next period, the seller then obtains the discounted profit.

Table J1: Standardized TOM and price gradients, Germany and U.S.

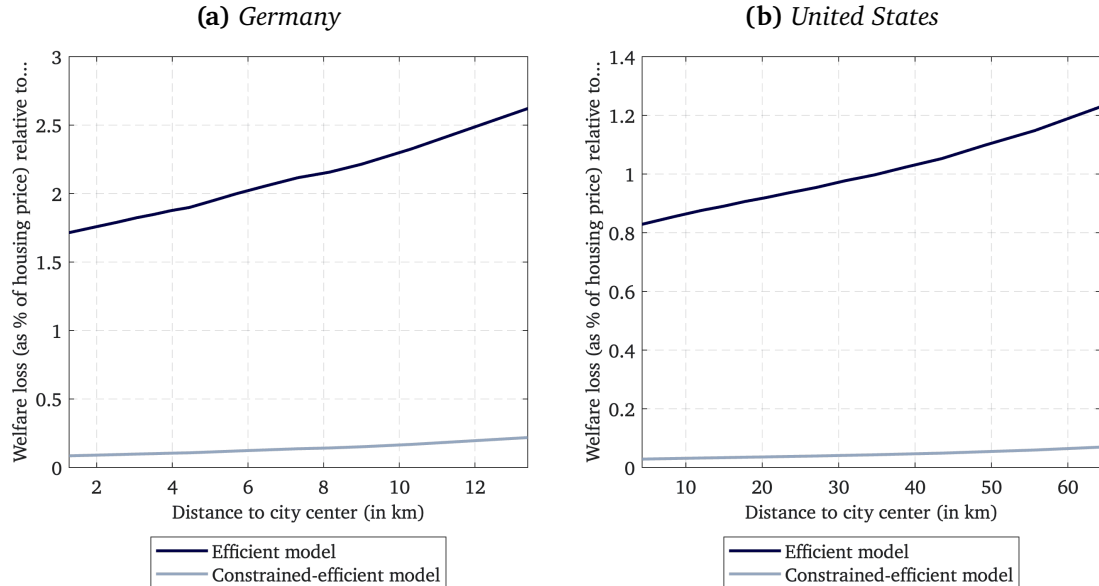
Country	Dataset	TOM gradient	Price gradient
Germany	Condos full sample	0.048	-0.202
U.S.	Single-family FUA (full sample)	0.029	-0.146
U.S.	Single-family MSA (50km radius)	0.048	-0.276
U.S.	Single-family MSA (full sample)	0.134	-0.074

Note: This table presents regression coefficients of time on the market (TOM) and log sales price on property characteristics with time and location fixed effects based on Regression (1). The coefficients are standardized by the sample standard deviation of the respective variable. For Germany, the fixed effects are at the year-quarter-city level. For the U.S., the fixed effects are at the year-month-MSA or year-month-FUA level. More information on data sources is provided in the main text.

Table J1 provides empirical comparisons of the price and liquidity gradients for Germany and the United States. The theoretical prediction that the price gradient is larger than the liquidity gradient holds empirically, except in the U.S. at the MSA level across the full sample. This is likely due to the spatial boundaries of some MSAs reaching very far out, which makes the estimates noisier. With functional urban area boundaries, the result holds, as well as when restricting the U.S.-MSA sample to a 50km radius around the MSA center.

J.3 Welfare comparison in terms of housing prices

Figure J2: Spatial welfare loss distributions in terms of housing prices

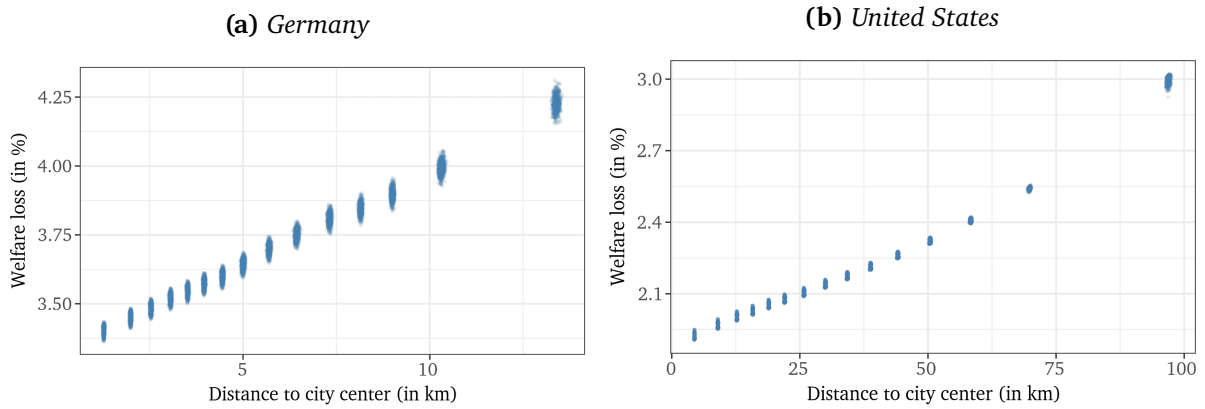


Notes: These plots show the welfare loss in the baseline model compared to the counterfactual model versions by distance to the city center. Welfare is calculated as defined in (20) and scaled up to an expected lifetime value with factor $\beta/(1-\pi\beta)$. The percentages refer to the absolute loss in welfare in the baseline model compared to a counterfactual as a fraction of the housing price at every distance to the city center.

J.4 Model sensitivity analysis

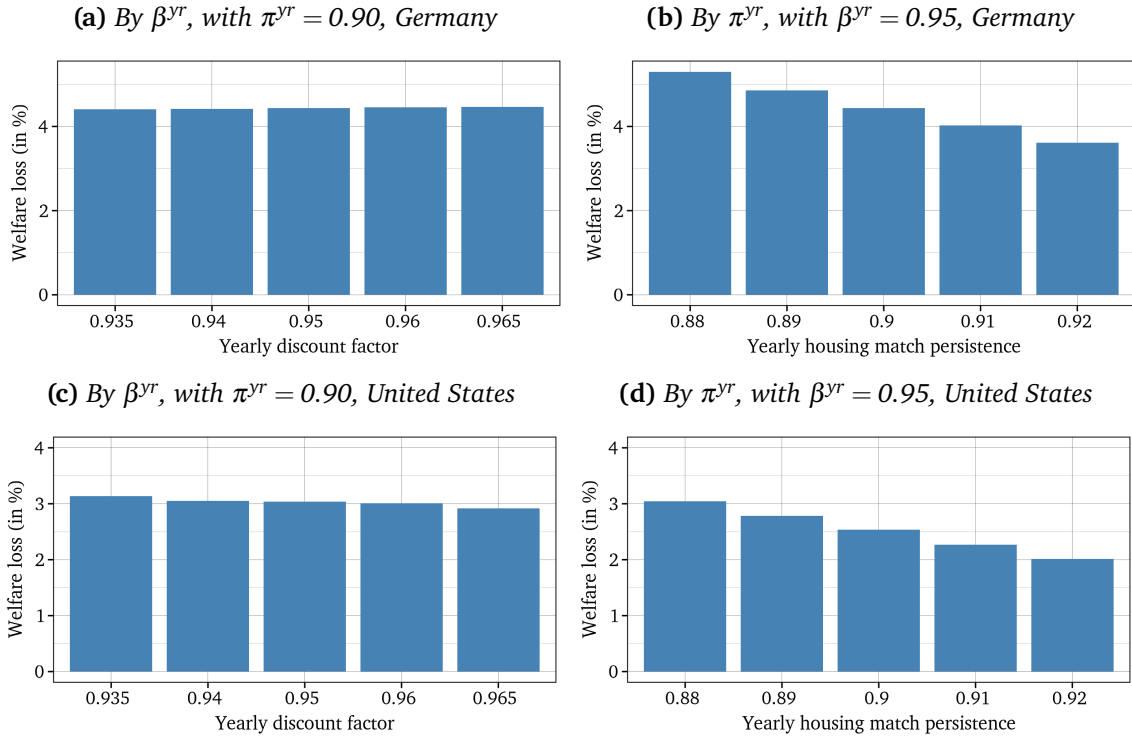
In this subsection, we provide a sensitivity analysis for our welfare estimates. First, in Figure J3, we plot the welfare loss in the baseline model relative to the efficient model with bootstrapped confidence bounds. As described in the main text, the confidence intervals are narrow, which leaves us confident about our estimates. Moreover, in Figure J4, we plot the welfare loss in the outskirts, varying the yearly discount factor β^{yr} between 0.935 and 0.965 and the yearly housing match persistence π^{yr} between 0.88 and 0.92. Each bar represents a recalibration of the model. As explained in the main text, the choice of the discount factor leaves the welfare loss estimates unaffected, while a lower match persistence increases the welfare loss.

Figure J3: Bootstrapped welfare loss estimates



Notes: These plots show the welfare loss in the baseline model compared to the efficient model version by distance to the city center. Welfare is calculated as defined in (20). The percentages refer to the loss in welfare in the baseline model relative to the efficient model at every individual distance. The individual dots depict the 1,000 bootstrapped replication draws.

Figure J4: Sensitivity analysis for outskirt welfare loss



Notes: These plots show the welfare loss in the baseline model compared to the efficient model version at the outermost distance to the city center, with varying yearly discount factors and housing match persistence probabilities. Welfare is calculated as defined in (20). The percentages refer to the loss in welfare in the baseline model relative to the efficient model at every distance to the city center.

J.5 Alternative travel cost calculation

In the main model, we think of a physical cost of car travel when estimating the parameter μ , consistent with the canonical monocentric city model. μ then reflects a conversion of travel time in minutes, fed into the model from our travel time estimates, to the associated travel cost in model units. Alternatively, we can think of the travel cost in the model as an opportunity cost which results from lost time due to traveling to the city center. We also conceptualize this opportunity cost as translating travel time to the city center in minutes linearly into a monetary cost. To do so, we must specify what a minute of travel time is worth to agents in the model. We do this using the average hourly wage in Germany and the United States. For Germany, we retrieve wage statistics via the German Statistical Office (GENESIS database, variable code: 81000-090³⁰). For the United States, we retrieve wage statistics via FRED (variable code: CES0500000003, primary source: U.S. Bureau of Labor Statistics (2025)). We keep the wage rates nominal on purpose for a direct comparison to the nominal travel cost estimates in the main calibration. We obtain a gross hourly wage in Germany from 2012 to 2024 of €28.33 and in the United States from 2012 to 2023 of \$27.49.

Then, we calculate the average travel time in our sample, multiplied by 2, to get a measure of daily travel time. In our model, agents travel to and from the city center for 34 minutes per day on average in Germany and for 74 minutes per day in the United States. Measured in terms of an opportunity cost, if we assume that the value of time lost can be expressed in terms of wages, agents in Germany lose $(34/60) \times €28.33 = €16.05$ per day, while agents in the United States lose \$33.90 per day. The actual losses should

³⁰ <https://www.destatis.de/DE/Themen/Wirtschaft/Volkswirtschaftliche-Gesamtrechnungen-Inlandsprodukt/Publikationen/Downloads-Inlandsprodukt/statistischer-bericht-2180120.html>

be somewhat lower, since these are gross wages, and net wages are typically considerably below gross wages. Moreover, the same words of caution as for the travel cost estimates apply: these calculations are at the country level and likely vary to a considerable degree at the city level, and it is not clear to what extent wages capture the opportunity cost experienced when commuting. Hence, we conclude that, roughly speaking, opportunity costs can serve as an alternative interpretation of travel costs.

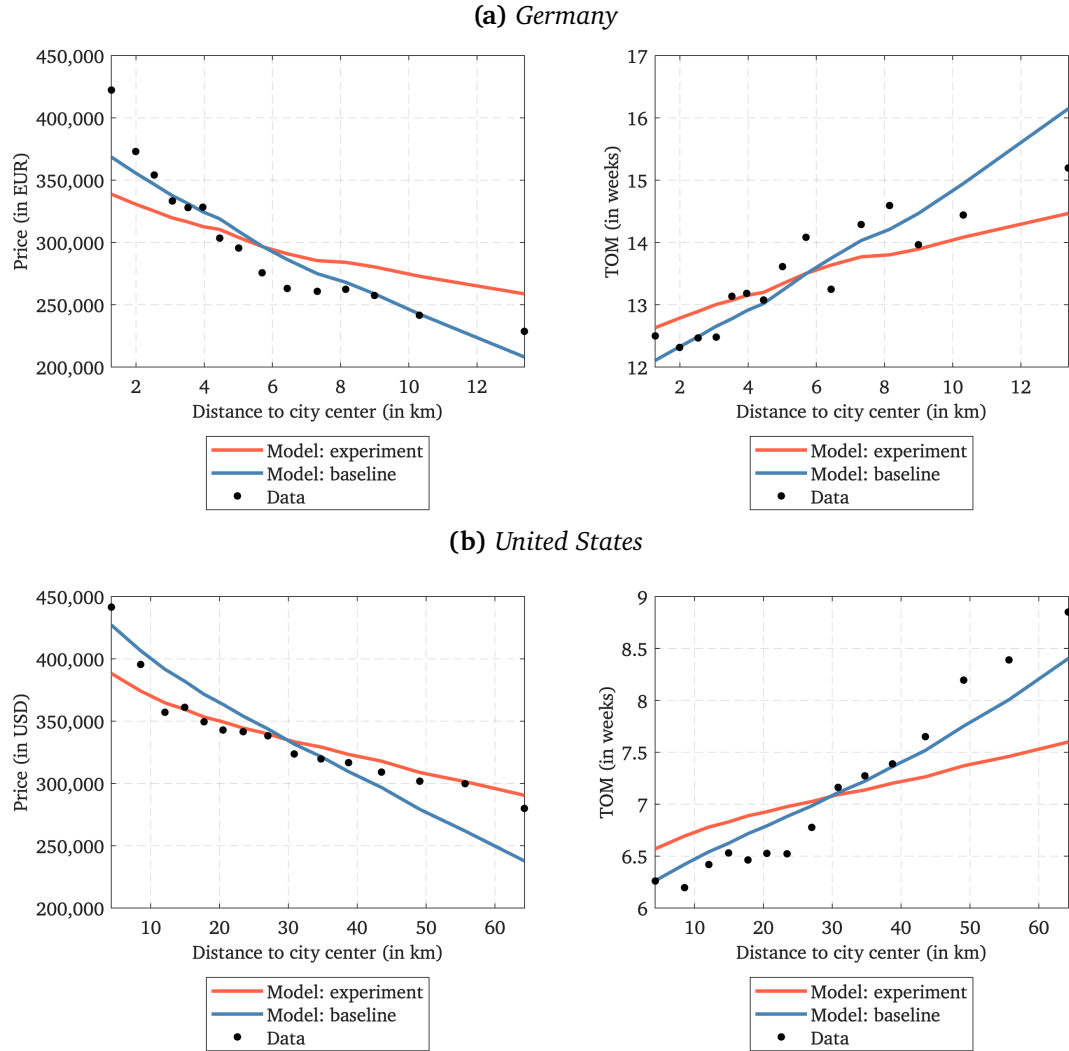
J.6 COVID experiment in the model

We test whether our baseline model can replicate the flattening of the price gradient as documented in Gupta et al. (2022) and produce a flattened liquidity gradient as we document in our empirical results. The COVID-19 pandemic induced a shift to working from home. The experiment consists of varying the travel time input, which generates a travel cost curve within the model, such that it reflects the shift in commuting patterns induced by working from home.

Per se, we have no information available on the change in time traveled to the city center across space within cities. Hence, we impose restrictions on the changes that we make by using the results from Gupta et al. (2022). To get the result that prices decrease in the city center and increase in the outskirts compared to before, the travel cost within our model must increase in the city center and decrease in the outskirts compared to before. A straightforward way to implement this is to let the average travel cost stay the same while changing its spatial distribution. Then, we must only specify one number which changes in the experiment. We impose that, keeping the average travel time constant, the slope of the linearly approximated travel time input curve is multiplied by some factor between 0 and 1. We add back the residuals between the original travel

time input curve and its linear approximation to the new tilted curve. With a factor of 1/2, we approximately replicate the price decrease of 5-10% in the city center and the price increase of 15-20% in the outskirts estimated for New York City in Gupta et al. (2022) and our flattened liquidity gradients from Internet Appendix D.2, see Figure J5.

Figure J5: Results of COVID experiment in the model



Notes: This figure shows the main model results for individual bins of distances to the city center, for the baseline model and the COVID experiment. “TOM” refers to (expected) time on the market. The data points are calculated using the main specification of Regression (1), as displayed in Figure 1. The binned scatter plots are produced following Cattaneo et al. (2024), using 15 equally-sized distance bins.

References

Amaral, Francisco, Martin Dohmen, Moritz Schularick, and Jonas Zdrzalek (2023). “German Real Estate Index (GREIX)”. ECONtribute Discussion Paper No. 231.

Anglin, Paul M., Ronald Rutherford, and Thomas M. Springer (2003). “The trade-off between the selling price of residential properties and time-on-the-market: The impact of price setting”. In: *The Journal of Real Estate Finance and Economics* 26(1), pp. 95–111.

Burrows, Michael, Charlynn Burd, and Brian McKenzie (2021). “Commuting by public transportation in the United States: 2019”. American Community Survey Report No. ACS-48.

Carrillo, Paul E. (2012). “An empirical stationary equilibrium search model of the housing market”. In: *International Economic Review* 53(1), pp. 203–234.

Cattaneo, Matias D., Richard K. Crump, Max H. Farrell, and Yingjie Feng (2024). “On binscatter”. In: *American Economic Review* 114(5), pp. 1488–1514.

Chetty, Raj, John N. Friedman, Nathaniel Hendren, Maggie R. Jones, and Sonya R. Porter (2025). “The Opportunity Atlas: Mapping the childhood roots of social mobility”. In: *American Economic Review* 116(1), pp. 1–51.

Cirman, Andreja, Marko Pahor, and Miroslav Verbic (2015). “Determinants of time on the market in a thin real estate market”. In: *Engineering Economics* 26(1), pp. 4–11.

Delventhal, Matthew J. and Andrii Parkhomenko (2024). “Spatial implications of telecommuting”. Working paper.

Dijkstra, Lewis, Hugo Poelman, and Paolo Veneri (2019). “The EU-OECD definition of a functional urban area”. OECD Regional Development Working Paper No. 2019/11.

Genesove, David and Christopher J. Mayer (1997). “Equity and time to sale in the real estate market”. In: *American Economic Review* 87(3), pp. 255–269.

Glöwer, Michel, Donald R. Haurin, and Patric H. Hendershott (1998). “Selling time and selling price: The influence of seller motivation”. In: *Real Estate Economics* 26(4), pp. 719–740.

Gupta, Arpit, Vrinda Mittal, Jonas Peeters, and Stijn Van Nieuwerburgh (2022). “Flattening the curve: Pandemic-induced revaluation of urban real estate”. In: *Journal of Financial Economics* 146(2), pp. 594–636.

Guren, Adam M. and Timothy J. McQuade (2020). "How do foreclosures exacerbate housing downturns?" In: *The Review of Economic Studies* 87(3), pp. 1331–1364.

Han, Lu and William C. Strange (2016). "What is the role of the asking price for a house?" In: *Journal of Urban Economics* 93, pp. 115–130.

Haurin, Donald R., Jessica L. Haurin, Taylor Nadauld, and Anthony Sanders (2010). "List prices, sale prices and marketing time: An application to US housing markets". In: *Real Estate Economics* 38(4), pp. 659–685.

Knight, John R. (2002). "Listing price, time on market, and ultimate selling price: Causes and effects of listing price changes". In: *Real Estate Economics* 30(2), pp. 213–237.

Krainer, John (2001). "A theory of liquidity in residential real estate markets". In: *Journal of Urban Economics* 49(1), pp. 32–53.

Krainer, John and Stephen F. LeRoy (2002). "Equilibrium valuation of illiquid assets". In: *Economic Theory* 19(2), pp. 223–242.

Moreno-Monroy, Ana I., Marcello Schiavina, and Paolo Veneri (2021). "Metropolitan areas in the world. Delineation and population trends". In: *Journal of Urban Economics* 125:103242.

Pesaresi, Martino and Panagiotis Politis (2023). "GHS-BUILT-V R2023A". GHS built-up volume grids derived from joint assessment of Sentinel2, Landsat, and global DEM data, multitemporal (1975-2030). European Commission, Joint Research Centre (JRC).

Pesaresi, Martino et al. (2024). "Advances on the Global Human Settlement Layer by joint assessment of Earth Observation and population survey data". In: *International Journal of Digital Earth* 17(1):2390454.

RWI - Leibniz-Institut für Wirtschaftsforschung and ImmobilienScout24 (2024). "RWI Real Estate Data - Hauskauf - SUF". RWI-GEO-RED.

Schiavina, Marcello, Ana I. Moreno-Monroy, Luca Maffenini, and Paolo Veneri (2019). "GHS-FUA R2019A". GHS functional urban areas, derived from GHS-UCDB R2019A, (2015), R2019A. European Commission, Joint Research Centre (JRC).

Sirmans, G. Stacy, Lynn MacDonald, and David Macpherson (2010). "A meta-analysis of selling price and time-on-the-market". In: *Journal of Housing Research* 19(2), pp. 139–152.

Smith, Brent (2009). “Spatial heterogeneity in listing duration: The influence of relative location to marketability”. In: *Journal of Housing Research* 18(2), pp. 151–171.

U.S. Bureau of Labor Statistics (2025). “Average hourly earnings of all employees, total private [CES0500000003]”. U.S. Bureau of Labor Statistics. Retrieved from FRED, Federal Reserve Bank of St. Louis.

Vanhapelto, Tuuli and Thierry Magnac (2024). “Housing search and liquidity in spatial equilibrium”. TSE Working Paper No. 24-1596.